THE UNIVERSITY OF MICHIGAN

INDUSTRY PROGRAM OF THE COLLEGE OF ENGINEERING

AN EXPERIMENTAL STUDY OF MAGNETOHYDRODYNAMIC FLOWS INDUCED BY APPLIED ELECTRIC AND MAGNETIC FIELDS

Robert M. Caddell

A dissertation submitted in partial fulfillment
of the requirements for the degree of
Doctor of Philosophy in the
University of Michigan
Department of Mechanical Engineering
1963

October, 1963

IP-637

Doctoral Committee:

Professor Arthur G. Hansen, Co-Chairman
Professor Mahinder S. Uberoi, Co-Chairman, University of Colorado
Associate Professor Vedat S. Arpaci
Professor Lee O. Case
Professor Arthur D. Moore
Assistant Professor Dale C. Ray

ACKNOWLEDGEMENTS

To acknowledge everyone who in some way contributed to the completion of this study is a difficult task. However, the following persons and organizations must be mentioned directly.

My deepest thanks go to my Co-Chairman, Professors A. G. Hansen and M. S. Uberoi whose suggestions, counsel and encouragement not only provided the impetus to start the problem but helped throughout the entire program.

To the other members of my doctoral committee goes my sincere appreciation for the time they have given to provide the counsel and aid so necessary in any thesis problem. I must pay special thanks to Professor A. D. Moore whose intuition and years of experience enabled him to make several key suggestions at certain critical stages when the writer was confronted with a degree of uncertainty.

I should also like to express my appreciation to the National Science Foundation for awarding me a Science Faculty Fellowship, the Department of Mechanical Engineering for a grant-in-aid supplied by the DuPont Corporation, and the Ford Foundation who supplied a loan through the Engineering College Faculty Development Program. This financial support permitted me to devote my full efforts to my doctoral studies for one and one-half years.

For the preparation of the final manuscript I am indebted to the Industry Program of the University of Michigan.

Last, and most important of all, I must pay tribute to my wife whose love, patience, urging, and understanding were indispensable during this entire program of study. May she now begin to reap her just rewards.

TABLE OF CONTENTS

		Page
ACKNOWLEDGEMENT		ii
LIST OF TABLES		iv
LIST OF FIGURES		v
NOMENCLATURE		viii
PREFACE		xi
I INTRODUCTION		1
	1.1 Opening Remarks	1
	1.2 Literature Survey	3
	1.3 Origin of the Problem	5
	1.4 Purpose of the Problem	7
II EXPERIMENTAL INVESTIGATION		8
	2.1 Exploratory Model	8
	2.2 Results of the Exploratory Tests	10
	2.3 Order of Magnitude Analysis of Electromagnetic and Convective Effects	12
	2.4 Initial Version of the Experimental Model	16
	2.5 Selection of the Test Fluid	20
	2.6 Results with the Initial Test Model	21
	2.7 First Revision of the Experimental Model	24
	2.8 Second and Final Revision of the Experimental Model	38
III COMPARISON OF ANALYTICAL AND EXPERIMENTAL RESULTS		74
	3.1 Explanatory Remarks	74
	3.2 Variations Between Analysis and Experiment	74
	3.3 Procedure for Obtaining Velocity Measurements	76
	3.4 Predicted Versus Measured Results	80
IV CONCLUSIONS		91
	4.1 Induced Motion Due to Fluid Current Only	91
	4.2 Motion Induced Between Concentric Tubes	91
	4.3 Test Fluid and Photographic Technique	92
	4.4 Theoretical and Experimental Comparisons of MHD Flow Between Concentric Tubes	92
	4.5 Suggestions for Further Study	93
APPENDIX		94
BIBLIOGRAPHY		109

LIST OF TABLES

Table		Page
A.1	Constants Resulting from Model Geometry.....	103
A.2	Constants resulting from Model Geometry and Current Densities.....	104
A.3	Constants for Equation (A-25) as a Function of the Ratio of Current Densities.....	105

LIST OF FIGURES

Figure		Page
1	Assembly of the Initial Experimental Unit	19
2	Fluid Motion in the Top and Bottom Sections of the Unit	19
3	Fluid Motion Around the Top of the Hole in the Separator Plate	22
4	Fluid Motion Around the Bottom of the Hole in the Separator Plate	22
5	Assembly of the First Revision of the Experimental Model	27
6	Electrical Accessories and Temperature Recording Components	27
7	Setup of Photographic Accessories	30
8a	Fluid Patterns after 5 Seconds of Current Flow with the Unit in a Vertical Position	32
8b	Fluid Patterns 25 Seconds After Figure 8a	32
9	Fluid Patterns After 30 Seconds of Current Flow with the Unit in a Vertical Position and No Rod Current	33
10	Sequence of Fluid Patterns After Various Time Intervals of Current Flow with the Unit in a Vertical Position	34
11	Fluid Patterns After 2 Minutes of Current Flow with the Unit Horizontal	37
12	Fluid Patterns After 3 Minutes of Current Flow with the Initial Version of the Unit Horizontal	37
13	Schematic Drawing of the Unit After the Second Revision	40
14	Assembly of the Second Revision of the Unit in a Vertical Position	42
15	Assembly of the Second Revision of the Unit in a Vertical Position	42
16	Assembly of the Second Revision of the Unit in a Horizontal Position	43

LIST OF FIGURES (CONT'D)

Figure		Page
17	Assembly of the Second Revision of the Unit with the Blackout Hood in Place	43
18	Sequence of Fluid Patterns After Various Time Intervals of Current Flow with the Unit Horizontal and a Fluid Current of 10 Amps	45
19	Velocity Measurements Versus Time	49
20	Repeat of Figure 18 but with Current in the Rod Reversed.	50
21	Sequence of Fluid Patterns After Various Time Intervals of Current Flow with the Unit Horizontal and a Fluid Current of 5 Amps	54
22	Sequence of Fluid Patterns After Various Time Intervals of Current Flow with the Unit Horizontal and a Fluid Current of 2 1/2 Amps	56
23	Sequence of Fluid Patterns After Various Time Intervals of Current Flow with the Unit Vertical and a Fluid Current of 5 Amps	58
24	Fluid Patterns After 15 Minutes of Current Flow with the Unit Horizontal and with Various Fluid Currents	62
25	Fluid Patterns After 15 Minutes of Current Flow with the Unit Horizontal, the Rod Current Turned off, and Fluid Currents of 15 and 30 Amps Respectively	66
26	Sequence of Fluid Patterns After Various Time Intervals of Current Flow with the Unit Horizontal and Shimmed at One End, and a Fluid Current of 30 Amps	68
27	Sequence of Fluid Patterns After Various Time Intervals of Current Flow with the Unit Vertical and a Fluid Current of 25 Amps	72
28	Grid Pattern for Correction of Measurements	78
29	Enlargement of One Quadrant of Figure 18f	79
30	Analytical Versus Experimental Values of Velocity Versus Fluid Current for Three Different Coordinate Points	81

LIST OF FIGURES (CONT'D)

Figure		Page
31	Analytical Versus Experimental Values of the Stagnation Point Coordinates.....	83
32a,b	Three Dimensional Field Maps For the Geometric Shapes of the Analytical and the Experimental Models.....	84
32c,d	Field of Force Vectors, Due to Electromagnetic Effects, Positioned on the Field Map for the Analytical and the Experimental Models.....	87
33	Field Maps for the Analytical and Experimental Models Superimposed to Indicate the Differences.....	90

NOMENCLATURE

$\vec{B}$	Magnetic flux density vector
B	Magnetic flux density
b	Maximum amplitude of wall variation around the mean radius "R"
$C_{1,2,3,4}$	Non-dimensional constants
C_p	Specific heat
$\vec{E}$	Electric field vector
F_b	Thermal Buoyant body force
F_m	Electromagnetic body force
g	Acceleration due to gravity
$\vec{H}$	Magnetic intensity vector
i	$\sqrt{-1}$
i_f	Current flowing through an elemental volume of fluid
I	Current flowing through the fluid enclosed by radius "r"
I_f	Total current flowing through the fluid
I_R	Total current flowing through the center rod
I_n	Modified Bessel function of the first kind of order n
I_*	Function of the non-dimensional radius "x"
I'_*	Derivative of I_*
$\vec{J}$	Current density vector
J	Average current density of the fluid
J_R	Average current density of the center rod
K_n	Modified Bessel function of the second kind of order n
K_*	Function of the non-dimensional radius "x"

K_*'	Derivative of K_*
k	Wave number
L	Length of an elemental volume of fluid parallel to the direction of current flow
p	Pressure
q'''	Internal heat generation
R	Mean radius of the inner surface of the outside cylinder
R_e	Electrical resistance of the fluid
R_m	Magnetic Reynolds Number
R_o	Outer radius of inner cylinder
r	Radial spatial coordinate
ΔT	Temperature rise
U_r	Radial velocity component
U_z	Axial velocity component
U	Total velocity
$\vec{U}$	Velocity vector
x	Non-dimensional radial coordinate
y	Non-dimensional axial coordinate
z	Axial spatial coordinate
α	Non-dimensional constant
β	Volumetric coefficient of thermal expansion
γ	Non-dimensional constant
λ	Wave length of the period of the outer tube
μ	Viscosity of the fluid
μ_e	Magnetic permeability
σ	Electrical conductivity of the fluid

ρ	Density of the fluid
$\psi(x)$	Component part of the stream function
Ψ	Function of $\psi(x)$ and z

PREFACE

Interest in the field of magnetohydrodynamics has become widely manifest in the last two decades, the various aspects and potential applications being numerous. With all of this interest, relatively little work has been devoted to experimentation, the vast majority of publications being analytical in nature. In many instances adequate experimental models would be extremely expensive or nearly impossible to construct, and it would seem that these restrictions account primarily for the lack of experimental endeavor. Of the experimentation presented in the literature, most involved the use of liquid metals since their electrical conductivities are extremely large and they possess constant properties for all practical purposes.

When this present study was undertaken, it was the intent to devote the major effort towards an experimental study of a class of MHD flows. Numerous alterations were required as the work progressed and in final summation it would appear that several avenues of extension have been opened up from the experiences gained in this present work. One of the major conclusions reached regards the use of reasonably simple models to demonstrate certain phenomena. Unless highly adequate financial support is available, studies should be restricted to problems that can be attacked with the aid of simple geometric forms.

I. INTRODUCTION

1.1 Opening Remarks

Magnetohydrodynamics, often shortened to MHD for simplicity, may be defined as the study of the motion of electrically conducting fluids in the presence of applied magnetic and/or electric fields. From a macroscopic viewpoint, which is of sole concern in this thesis problem, the analysis of such motion requires coupling the laws of hydrodynamics and electromagnetics. Thus, the pertinent equations of fluid mechanics, based upon the concept of a continuum, and the relations known as Maxwell's equations are utilized.

In addition to the forces due to viscosity, gravity, and pressure gradients normally present in hydrodynamic problems, the aforementioned fields create an electromagnetic body force which must be included in the equations of motion. It is the presence of this force and its influence on the motion of the fluid that serves to distinguish MHD from ordinary hydrodynamics. Coupling of the laws, as mentioned previously, comes about through the inclusion of this body force in the equations of motion.

From a mathematical viewpoint, the introduction of electromagnetic forces into the already non linear equations of hydrodynamics brings about no simplifications. In fact, non linearity becomes further aggravated with the consequence that mathematical difficulties are intensified. This inevitably leads one to seek solutions that approximate a specific physical problem under consideration by linearizing the pertinent equations. Another method of attack on such a problem is to employ experimental models which duplicate the problem of interest to a reasonable

degree. Either, and preferably both of these techniques can convey meaningful information. Since numerous approximations are made in a purely analytical approach, it would be highly desirable to supplement analysis with experiment to determine how reasonable such approximations are.

During the last twenty years, many publications have been devoted to various aspects of MHD, the vast majority having been analytical. For some of these studies, the construction of experimental models would be next to impossible. Others would demand highly elaborate and expensive models. It would seem, therefore, that the direction of experimentation should be towards the type of problems that can be described by reasonably simple and practical models which, if possible, are amenable to analysis. It is certainly plausible that such experiments would help to evince the phenomena that are typical of particular MHD flows, especially where the assumption of a continuum is considered adequate.

Although much of the present emphasis in MHD is being devoted to problems involving ionized gases or very low density fluids, most of the original investigations employed mercury as the conducting fluid. In fact, at this time there seem to be only two actual working applications of MHD and both involve liquids as the fluid medium. These are the pumping of liquid metals and the flow measuring of certain electrically conducting liquids.

For those individuals concerned primarily with a continuum viewpoint of MHD, experimental studies which employ liquids should be of interest in helping to demonstrate the phenomena that are predicted analytically or, perhaps, expected intuitively.

1.2 Literature Survey

Major efforts in this survey were devoted to those publications wherein the concept of a continuum was employed, special emphasis being placed upon those studies involving experimental work.

Although the diverse interests in MHD have been evident in relatively recent times, investigations which utilized the same basic concepts can be traced back long before the name MHD appeared in the literature. Northrup[1] conducted several interesting experiments from which the term "pinch phenomenon" seems to have originated. In one of these studies it was shown that by passing current through mercury, a pressure of sufficient magnitude to pump the mercury could be developed. Another experiment indicated that the passage of current flow through a conductor, an ionized salt solution was employed, created a force field that acted radially inward. No fluid motion was observed, undoubtedly due to the use of a tube whose cross-sectional area was constant.

Williams,[2] studied the effects of an applied magnetic field on the flow of copper sulphate in straight and curved tubes. Similar studies[3] followed with mercury. From the results, Williams suggested the possibility of using such techniques for flow measurement. Probably, this was the initial conception of a MHD flowmeter.

The works of Hartmann and Lazarus,[4,5] are usually considered to be the true origination of MHD. Regardless of one's point of view on the historical accuracy of this attitude, it does seem that these works provided the impetus which led to the diversity of interest in MHD that is now so evident. In the original work, Hartmann[4] developed the equations which described the flow of mercury in a rectangular channel as it

was subjected to a magnetic field. In the experimental continuation [5] reasonable correlation between theory and actuality was obtained. The predictions regarding the magnetic effects on the velocity profile were certainly verified. One of the remarkable findings that developed, was that an applied magnetic field could suppress the transition from laminar to turbulent flow up to Reynolds numbers far beyond those at which this result would occur in a purely hydrodynamic situation. Some fifteen years later, Murgatroyd[6] extended Hartmann's work well into the turbulent region of hydrodynamics and verified that MHD channel flows could be maintained as laminar up to Reynolds numbers of 10^5. Recent investigations employing channel flows,[7,8] have been concerned with free surface studies of liquid metals in order to analyze surface wave motions.

A major conceptual breakthrough occurred when Alfvén[9] conceived the idea that with a fluid of infinite electrical conductivity, the field lines and fluid motion would be "frozen" together. Based upon this premise he predicted that a wave motion would exist along the direction of the magnetic field which, in essence, presented a new type of energy propagation. Subsequent experimental studies[10,11,12] were conducted with liquid metals possessing high electrical conductivity, and these works first verified the predictions of Alfvén.

The influence of a magnetic field on the convective instability of a fluid heated from below was studied by Lehnert and Little[13] and Nakagawa.[14] In their experiments, mercury was employed and it was shown that convective effects could be inhibited by an applied magnetic field.

Although it had been thought that field effects always tended to stabilize fluid motion, Lehnert[15] showed that this was not so for certain geometries. Others,[16,17,18] also investigated instabilities by employing various geometric configurations.

In the area of MHD pumps, Rossow, et al.,[19] investigated the influence of the shape of applied fields on the velocity profile and pressure head of a copper sulphate solution as it was pumped in a closed loop. A recent translation of a work by Okhremenko[20] pertains to the pumping of liquid metals.

References (21), (22), and (23) are included to indicate the diversity of topics and interest currently involved in MHD.

It is of interest to note that in those few experimental studies where the fluid employed was not a liquid metal, a solution of copper sulphate was used.

1.3 Origin of the Problem

Since it had been decided to concentrate on some experimental study in MHD, it seemed both natural and desirable to consider a problem that had been solved analytically. It could then be determined how reasonable it would be to construct a model which described that problem or one similar to it. The major restriction imposed was that the model should possess a reasonably simple geometry as far as actual construction was concerned. Rather than viewing it as a drawback, this restriction could prove advantageous since revisions of simple geometries would be easier to accomplish compared with more elaborate ones. During the search for a problem, discussions were held with the author of the published

analytical solutions to a class of MHD flows.[24] One phase of this analysis seemed to pose a problem that would lend itself to the type of work being sought. This involved the motion induced by the passage of an electric current through an originally static fluid which was incompressible, viscous, and electrically conducting. The fluid was contained in an insulated, axisymmetric tube of nearly constant cross sectional area, the variation in cross section arising from a small wall perturbation about the mean radius. In the analysis this variation is a cosine wave superimposed upon the mean radius. One of the assumptions was that the maximum wave amplitude was much less than the mean radius. The sketch shown below is a schematic of the analytical model used.

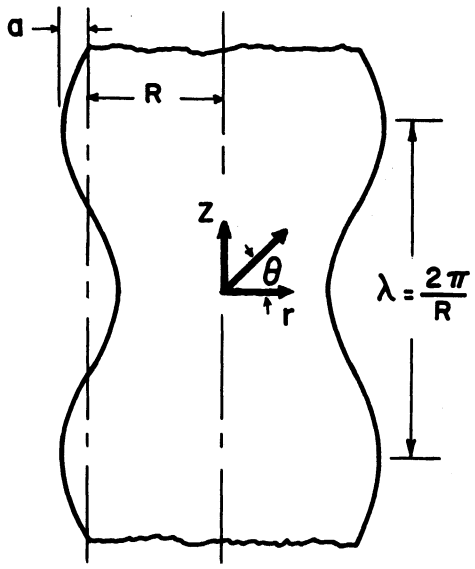

An applied electric field created a potential drop between electrodes which were located at the ends of the tube. End effects were ignored by assuming a tube of infinite length. In the class of flows studied the assumption of a small magnetic Reynolds numbers was made, thus,

convection of the magnetic field was neglected. With this approximation, the electric current and electromagnetic field intensity would not depend upon the fluid motion and the magnetic field intensity would result solely from the current flow in the fluid. It was further assumed that the fluid possessed constant properties and approximate solutions were obtained by satisfying boundary conditions at the mean radius rather than at the tube wall itself. From this analysis it was concluded that the electromagnetic rotational forces would not be balanced by potential pressure forces, so motion must follow. Theoretically, no motion would occur only if the tube had a straight wall.

A decision was reached to proceed with a general study of the problem outlined above, but with certain modifications and guide lines. From a practical viewpoint, the production of a physical model identical to the analytical one was ruled out as being too complicated. Also, since it could not be foreseen what further alterations might be necessitated as the study progressed, it was concluded that the type of problem, rather than a specific problem, should be the target of investigation.

1.4 Purpose of the Problem

The purpose of this study was to design, construct, and experiment with a model in order to investigate a type of MHD flow. One of the principal requirements would be to develop a method whereby the internal motion of the fluid could be detected and photographed. Since the experimental model would probably possess characteristics that differed from the analytical model which generated this study, major comparisons would probably be qualitative in nature. Quantitative comparisons would be made if feasible.

II. EXPERIMENTAL INVESTIGATION

2.1 Exploratory Model

It was apparent that a certain amount of preliminary work would have to be completed before any consideration could be given to the design of the model that would be used for the major experimental study. A later section is devoted to a detailed discussion of the test fluid (hereafter simply called fluid), so it will suffice here to state that a solution of copper sulphate was used. The magnitudes of current and voltage requirements, a reasonable concept of physical dimensions to be encountered, and the effects of variation in fluid concentration had to be investigated during this exploratory phase.

An inexpensive model of simple geometry which would cause non-uniform current densities was desired, and its size had to be determined first. Although it would lead only to a rough approximation, but since nothing else was available, initial attention was directed to Uberoi's[24] analysis. In his solution for the steady state centerline velocity of the fluid, the mean radius "R", and maximum wall amplitude "a" were the parameters of immediate interest. As the ratio a/R approaches zero, the cross sectional area of the tube approaches a constant value and the current density required to produce a finite motion approaches infinity. Physically then, this would require an applied voltage approaching infinity. At the other extreme as a/R approaches unity, the minimum cross sectional area of the tube approaches zero with the consequence that the fluid resistance approaches infinity in that region. Again, the applied voltage, needed to produce a current that would cause finite motion,

approached infinity. These considerations led to the conclusion that voltage needs should be investigated first since they might pose the most severe restriction regarding practical limitations. In addition, the concept of small wall perturbations was abandoned temporarily.

Following the calculations of approximate voltage requirements for different combinations of fluid resistance and current flow, an exploratory model was produced from a large commercial glass funnel. The funnel was altered to yield a frustum of a right cone, its approximate physical size being 7 inches high with top and bottom diameters of 4 and 12 inches respectively. The average wall thickness was 1/8 inch. Solid copper plates, to serve as electrodes, were fitted to the ends of this glass unit. These plates were 1/2 inch thick and were fabricated from electrolytic copper. Sealing between the glass and larger electrode was accomplished with a clear epoxy which produced a permanent leakproof joint. This formed the base of the unit in reference to a vertical position. To accommodate fluid expansion, an overflow tube was adapted to the top electrode and this joint was also sealed with epoxy. Upon filling the unit with fluid, the top electrode was placed in position with a rubber "O" ring arrangement preventing leakage at this joint. The electrodes were connected in series with a commercial power source that provided a stabilized D.C. current up to 25 amperes at 35 volts. Polarity reversal was obtained by changing two connections at the power source.

Several concentrations of the copper sulphate solution were used, ranging from specific gravities of 1.05 to 1.14. Currents up to 25 amperes were employed and based upon the area of the top electrode, this led to average current densities as high as 2 amperes per square

inch. A few tests were conducted with small amounts, about 1/2 per cent by volume, of sulphuric acid added to the fluid, the purpose being to increase the electrical conductivity of the fluid. Although no rotational motion was observed during any of these tests, (as would be theoretically expected) it appeared in view of later developments that the means for detecting such motion were not adequately developed at that time.

2.2 Results of the Exploratory Tests

Several observations and conclusions resulted from these tests and proved helpful in later studies. These major findings are listed as follows:

1. After several minutes of continuous current flow, the increase in fluid temperature caused the top electrode to become heated. Although actual temperatures were not obtained, touching this electrode verified that a definite increase in temperature had occurred. Fluid motion due to thermal causes was observed in the vicinity of the top electrode but nowhere else.
2. Depending upon the fluid concentration, a certain combination of time and current density (based upon the smaller area of the top electrode) caused noticeable chemical activity at the top electrode. Gas bubbles and the separation of copper colored particles from the electrode were observed. This particle separation was especially severe when the top electrode was anodic. A drop in current followed, which is

probably what Rossow[19] refers to as breakdown current density. Values of current density which led to this result for a given fluid concentration were almost identical with those reported by that author.

3. Even the addition of small amounts of acid to the fluid caused a decided increase in gas emission. This occurred regardless of polarity at the electrodes.

Several conclusions drawn from the above observations are listed as follows:

1. Both electrodes should be the same size because the smaller one always governs the limiting allowable current density. (Different sized electrodes were used in the exploratory model in order to reduce the over-all height of the unit and thus, the fluid resistance. It had been hoped that by so doing, available D.C. power sources would supply sufficient current.)
2. The physical size of the electrodes should be on the order of the larger one employed in the exploratory testing since currents in excess of 25 amperes might be encountered and current densities at the electrodes must be held below levels that would cause some of the adverse effects noted previously.
3. No acid would be added to the test fluid in the future since undesirable reactions would result.

4. From an electrochemical viewpoint, the top electrode should be the cathode. As the anode loses metal, a thin layer adjacent to this electrode would, if anything, possess a higher concentration of heavier copper ions than would the remainder of the solution. Therefore, this higher density layer should be kept at the bottom of the unit to avoid motion due to density differences.
5. Convective motion due to thermal buoyancy might create a serious problem.

This last point was of great concern. Any conceivable test model must possess some variation in cross sectional area if the type of rotational motion predicted theoretically was to occur. Thus, non-uniform internal heat generation would result and cause a buoyancy effect. If both the electromagnetic and convective effects were proportional to the square of the fluid current, the relative order of magnitude of these effects was critical. Obviously, if forces due to thermal sources predominated, it would be fruitless to study electromagnetic effects since they could easily be masked out. Of course, if an order of magnitude study indicated the reverse condition, the problem would be considerably eased. It was decided to conduct such an analysis of relative effects before considering the design of a new model.

2.3 Order of Magnitude Analysis of Electromagnetic and Convective Effects

To gain an approximate idea of the relative magnitudes of the forces involved, a model consisting of two frustums of cones, identical in size to the exploratory model, was assumed. By inverting one section,

the smaller diameters would contact at the horizontal centerline of the over-all unit. The diameter at this centerline would be 4 inches and as current flowed from an electrode at one of the 12 inch end diameters to the opposite end, it would be forced to converge through this narrow section. Non-uniform current densities would result and both the internal heat generation and magnetic flux density would reach maximum values at this constriction.

Current density was assumed to be directly proportional to area and an elemental cube of fluid whose sides were (dr) inches long was considered. The element was located at the mid-radius, r, of the cross sectional area of the central plane mentioned above. Electromagnetic effects would produce a force on this element that acted radially inward as shown in the sketch below.

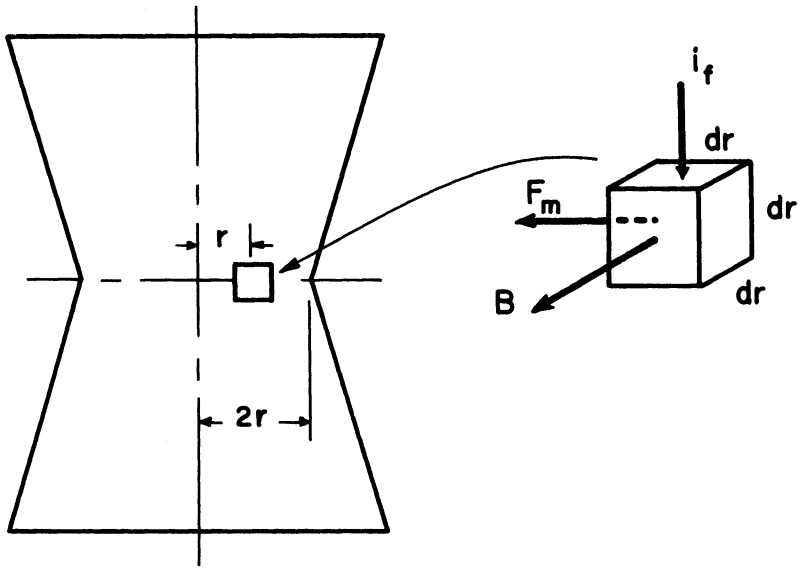

This force was determined as follows:

$$F_m = Bi_f L(8.85 \times 10^{-8}) \qquad (2.1)$$

$$B = 3.2I/2\pi r \text{ (for one ampere- turn)} \qquad (2.2)$$

where:

F_m = force on element, in pounds force

B = magnetic flux density at the element, in lines/inch^2

i_f = current flowing through the element, in amperes

L = length of the conductor (element), in inches

I = current flowing inside the fluid of radius "r", in amperes

r = radius from axial centerline to the element, in inches

I_f = total current flowing through the fluid, in amperes

now,

In Equation (2.2) $\qquad I = I_f \dfrac{(\pi r^2)}{\pi(2r)^2} = \dfrac{If}{4}$

The current i_f, flowing through an element of area $(dr)^2$ becomes:

$$i_f = \frac{I_f\,(dr)^2}{\pi(2r)^2} = \frac{I_f\,(dr)^2}{4\pi r^2}$$

while the length of the conductor, L is simply dr. Thus, the force caused electromagnetically would be:

$$F_m \approx \frac{0.885\, I_f^2\,(dr)^3\,(10^{-8})}{\pi^2 r^3} \text{ lbf} . \qquad (2.3)$$

To approximate the bouyant force caused by thermal effects, certain assumptions were enforced. For the first second of current flow it was assumed that all of the heat generated in the element merely heats the element, none being conducted away. Next, it was assumed that the

properties of the regions above the element remained undisturbed during this short time interval. The element of copper sulphate was assumed to have the following properties:

$$\sigma(\text{electrical conductivity}) = 1/20 \ \frac{\text{mhos}}{\text{inch}}$$

$$C_p(\text{specific heat}) = 1.0 \text{ BTU/lbm } ^\circ\text{F}$$

$$\rho(\text{density}) = 1.1\ (62.4)/1728 = .04 \text{ lbm/inch}^3$$

The electrical resistance of the element would be:

$$Re = \frac{L}{A\ \sigma} = \frac{dr}{(dr)^2(1/20)} = \frac{20}{dr} \text{ ohms}$$

Thus, the internal heat generation in the element, q''' would be:

$$q''' = i_f^2 Re = \frac{1.25\ I_f^2 (dr)^3}{\pi^2 r^4} \text{ watts}$$

Appropriate conversion factors give:

$$q''' = \frac{1.2\ I_f^2 (dr)^3\ (10^{-3})}{\pi^2 r^4} \quad \frac{\text{BTU}}{\text{sec}}$$

The temperature rise may be found from:

$$\Delta T = q'''/(C_p)\ (\text{Specific Weight}), \text{ therefore,}$$

$$\Delta T = \frac{3(10^{-2})\ I_f^2 (dr)^3}{\pi^2 r^4} \quad \frac{\text{in.}^3\ ^\circ\text{F}}{\text{sec}}$$

The buoyant force caused by this thermal rise would be:

$$F_B = \rho Bg \Delta T$$

where the quantity ρBg for water at 80°F was obtained from Kreith[25] as:

$$\rho Bg = 5 \times 10^{-6} \text{ lbf./}^\circ\text{F in.}^3 \quad \text{thus,}$$

$$F_B = 15 \times 10^{-8}\ I_f^2 (dr)^3/\pi^2 r^4 \text{ lbf} \qquad (2.4)$$

Dividing Equation (2.4) by (2.3) gives:

$$\frac{F_B}{F_m} = \frac{15}{.885\,r} \approx 16 \qquad \text{where} \quad r = 1 \text{ inch}$$

Thus, the buoyant force apparently would be larger than the electromagnetic force. Admittedly, this analysis may be questioned as to accuracy, however, since magnetic effects are independent of time whereas convective effects increase with time, it did seem that the convective influence would pose a serious problem.

2.4 Initial Version of the Experimental Model

It appeared probable that revisions of any experimental model would be demanded if the forces of electromagnetic origin were solely dependent upon current flowing through the fluid. Attempting to remove, or at best reduce, the forces caused by thermal buoyancy seemed highly impractical if not impossible. Therefore, in planning an initial model, consideration was given to an alternative device which would utilize this first model, entail minor revision, and stray as little as possible from the original problem. It was felt that this initial model should be completed and used, if only to ascertain that convective effects would truly predominate.

As first constructed, the model as shown in Figure 1 consisted of two right circular cylinders of clear acrylic plastic. Each cylinder was six inches high, twelve inches outside diameter, and had a wall thickness of about 3/8 inch. All end faces were machined perpendicular to the axial centerline. These cylinders were adapted to a 1/2 inch thick plastic plate which contained machined shoulders to accommodate the inside diameters of the two cylinders. Through the center of this

separator plate, a one inch hole was bored. Two pieces of 1/2 inch thick electrolytic copper, used as end electrodes, were individually fitted to the large cylinders by turning appropriate shoulders. Assembling these individual components as one unit led to four interface joints. Each joint contained a proper sized rubber "O" ring. The application of clamping pressure on the ends of the assembly forced the "O" rings to provide a satisfactory seal. This was found necessary even at the low fluid pressures encountered. Clamping was accomplished by machining holes in the four corners of the electrodes and separator plate and inserting brass rods, threaded on each end, through each group of aligned holes. Nuts were adapted to the ends of each rod and could be tightened to provide the clamping desired. Plastic plugs, pressed into the corner holes in the electrodes, electrically insulated the brass rods from the copper plates. Plastic legs were adapted to the lower ends of the four brass rods, their purpose being to provide adjustments for leveling the unit as it stood in a vertical position. A plastic overflow tube was adapted as an integral part of the top cylinder while another tube, connected to the bottom cylinder, provided a means for filling or emptying the assembled unit with fluid. Threaded brass studs were located on the axial centerlines of the electrodes and connecting cables from the D.C. power source were attached to these terminals. A small hole was drilled radially through the separator plate to permit the injection of dye into the one inch hole. The actual opening through which the dye would emit, was 1/64 inch diameter. Figure 1 shows the unit as assembled. One large circuit cable may be seen connected to the

top electrode, while the unseen lower cable passed down through a hole in the overflow tray. Both cables were kept perpendicular to the electrodes for a distance of at least 3 feet to avoid possible effects from the magnetic fields resulting from current flow through the cables. The two smaller wires in the photograph were connected to a voltmeter that measured the potential drop between the electrodes. A Hobart D.C. Arc Welding Generator served as the power source and its continuous output rating was 300 amps at 40 volts. A check for current ripple, made with an oscilloscope, indicated that the current output was almost perfectly constant up to levels that far exceeded 300 amps.

After some experimentation it was concluded that the most acceptable method of dye injection was a gravity feed. Of the several techniques attempted with squeeze bulbs and small positive displacement pistons, none were satisfactory since the dye surged into the fluid with a noticeable velocity. The gravity feed system consisted of a funnel, rubber connecting tube, and a pinch clamp. Figure 1 shows the funnel, containing dye, as it was adapted to the test unit. Care had to be exercised even with this system to prevent dye from gushing into the fluid as the clamp was opened.

The dye was a commercial jet black ink ordinarily used in fountain pens. Crystals of copper sulphate were dissolved in the ink until its specific gravity was close to the solution being used. This was determined by injecting small drops of ink into a sample of the test solution. It was found that no matter how closely the specific gravities were matched the droplet of ink tended to break up. Portions would slowly

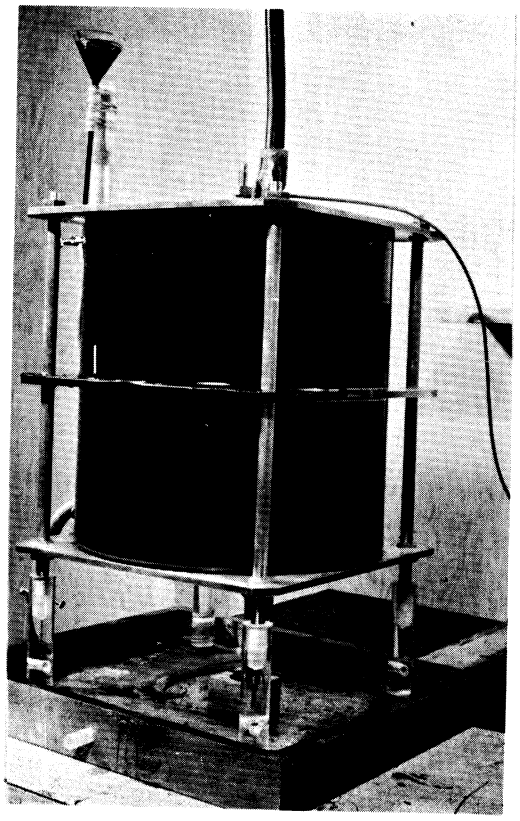

Figure 1. Assembly of the Initial Experimental Unit.

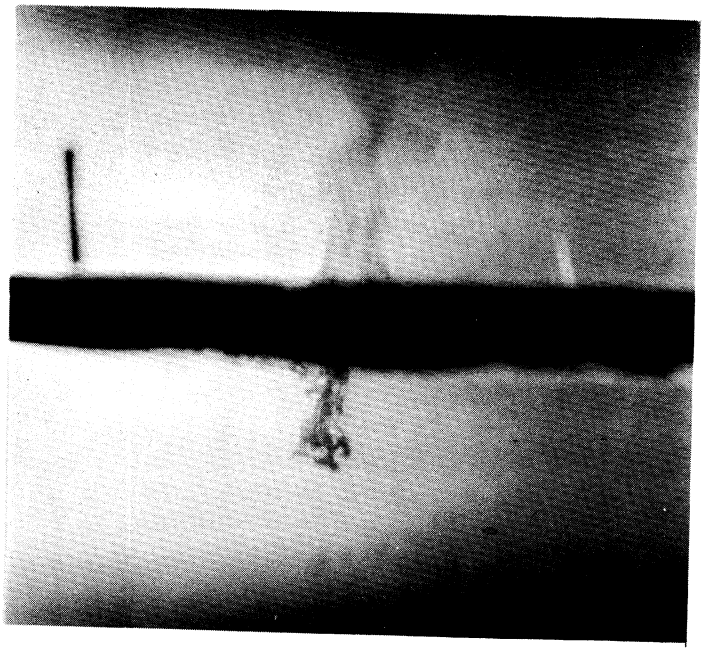

Figure 2. Fluid Motion in the Top and Bottom Sections of the Unit.

diffuse both upward and downward while the major mass of ink remained in suspension. When this condition was reached, the specific gravities were considered identical. This point of discussion finds some importance when viewing certain photographs.

2.5 Selection of the Test Fluid

Since one of the principal goals of this study was to photograph internal fluid motion, a transparent medium was demanded. Although liquid metals possess certain desirable properties, being opaque they must be abandoned. One must then turn to the numerous salt solutions in which ions act as current carriers. In seeking a best solution certain characteristics are desired. It should not be toxic, its electrical conductivity and density should be uniform, and gas emission and property variations should be negligible when it is subjected to a current flow. Unfortunately, no liquid salt solution completely fulfills these requirements, but of those available, copper sulphate seemed to be the best choice. As mentioned at the conclusion of the literature survey, in those experiments where liquid metals were not employed, a copper sulphate solution was used. This would seem to imply that previous investigators judged such a solution to be most acceptable.

The principal purpose of the fluid was to conduct current and it seemed reasonable at first that solutions of high concentration would be desired to lessen voltage requirements. Findings with the exploratory model pointed out that certain adverse reactions occurred more readily with stronger solutions. It was decided therefore that once a particular concentration was found acceptable, further adjustments would not be made.

Compared with the results reported by Rossow,[19] the findings obtained with the exploratory model were substantially the same, thus, it was concluded that information in that publication, pertaining to copper sulphate solutions, was quite reliable. Additional data regarding properties were obtained from Lange[26] and it was deemed unnecessary to conduct a detailed investigation of fluid properties and characteristics.

The major disadvantage in using any salt solution at the level of current densities required was the susceptibility of these water based fluids towards non-uniform density in the presence of non-uniform heat generation. This tendency proved to be most troublesome as work progressed, but a later section will demonstrate how such effects were handled. A second limiting factor with such a solution pertains to the upper limit of current density that may be used. Exceeding such a limit causes adverse chemical reactions at the electrodes, consequently, one must stay below such an extreme.

2.6 Results with the Initial Test Model

As the current was turned on, the pinch clamp on the gravity feed system was slowly adjusted until a small stream of dye seeped into the center hole in the separator plate. Figure 2 shows the results when the camera was on line with the plate. Upward motion of the dye in the top section was extremely pronounced whereas the dye seen in suspension in the lower section was almost motionless. As mentioned at the end of section 2.4, some portions of the dye tended to be slightly heavier than the main mass and this caused some dye to settle downward as it was admitted into the fluid. Figure 3 was obtained by placing the

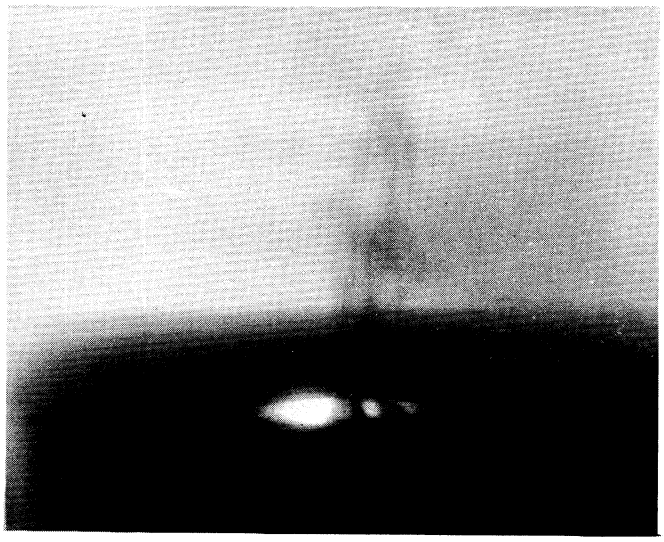

Figure 3. Fluid Motion Around the Top of the Hole in the Separator Plate.

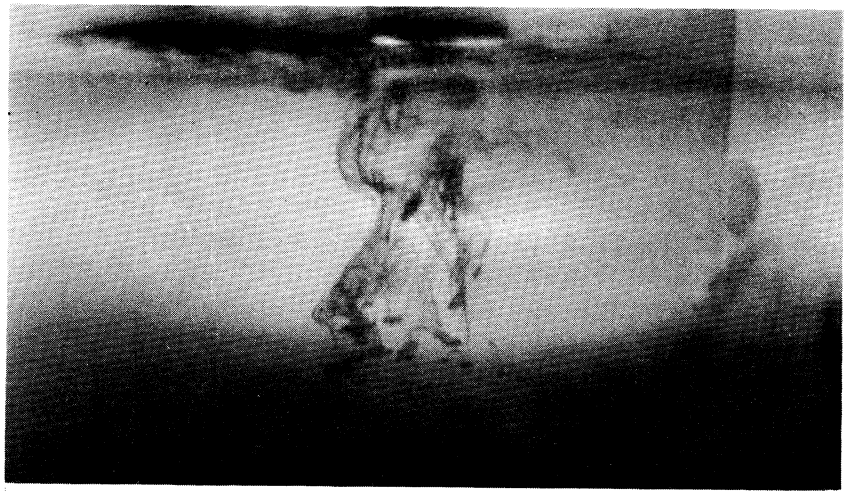

Figure 4. Fluid Motion Around the Bottom of the Hole in the Separator Plate.

camera above the separator plate and focusing downward on the hole whereas Figure 4 illustrates a shot aimed upward at the bottom of the hole. Although the majority of dye can be seen hanging in suspension in this latter figure, some agitation may be noted at the under side of the plate immediately adjacent to the hole.

Several combinations of fluid concentration and current were used and Figures 2 through 4 are typical of the findings. These figures resulted when a current of 5.6 amps passed through a solution whose specific gravity was 1.08. The voltage drop between the electrodes was 97 volts, the top electrode being cathodic. The current had been applied for about 15 seconds when these photographs were taken.

Regardless of the magnitude of current employed, this being varied from about 1/2 to 8 amps, convective motion inevitably originated at the hole and in most instances occurred almost immediately after the current was applied. As expected, this motion was more pronounced with increased currents and in a matter of minutes the top section of the tank would receive so much dye that further photography was impossible. Although visual contrast between the darker dye and the fluid was quite pronounced, no circulatory motion was observed. Fresh batches of fluid were prepared as needed and since the unit held about 5 gallons, this proved to be a time consuming problem.

These tests verified the predictions of the order of magnitude study in section 2.3, certainly in a qualitative sense. Two conclusions were drawn. First, since both electromagnetic and convective effects were proportional to the square of the fluid current, further adjustments

of the hole size or current levels would be useless as the convective influence would always remain predominant. Further testing with this unit was pointless. The second conclusion related to the dye system. Restricting dye emission to the hole only was inadvisable if motion elsewhere were to be viewed. A number of dye outlets at the top and bottom faces of the separator plate was contemplated, with each outlet flow to be controlled independently of any other.

2.7 First Revision of the Experimental Model

The basic problem to be solved was to create forces of electromagnetic origin that were not solely dependent upon the fluid current. Large solenoids, concentric with the outer diameter of the unit, were considered as a means of creating the major magnetic field, but this would lead to fluid motions far different than those sought at the outset since the magnetic field would no longer be concentric with the axis of the unit. Consequently, this was ruled out at an earlier stage of study. A relatively minor alteration could be made which, if effective, should cause motion similar to that expected with the original model. It was decided to proceed with this change.

A solid copper rod, about 3/4 inch diameter, was mounted inside of a clear plastic tube of 1 inch outside diameter and held concentric with the plastic tube by small plugs. This assembly was located along the axis of the test unit by extending through and beyond holes that were machined in the two electrodes. The copper rod was connected in series with the D.C. generator, while proper connections permitted the electrodes to be connected in series with D.C. wet storage batteries.

This latter circuit contained a switch, variable resistor and a shunted ammeter. In essence, the two circuits were completely independent, each possessing means for adjusting and reading current flow. As the tank was filled with fluid, the plastic tube electrically insulated the copper rod from the fluid. By employing relatively large currents in the rod circuit a sufficiently strong magnetic field, concentric with the rod, would be set up in the fluid. Simultaneously, relatively small currents would be admitted through the fluid and the interaction of magnetic field and fluid current would produce an electromagnetic force that would be proportional to the first power of the fluid current. Since convective effects would still vary with the second power of the fluid current, it appeared possible to reverse the previous condition of relative force levels by continually increasing the rod current while decreasing the fluid current. It seemed probable that the magnetic field intensity caused by the fluid current would be negligible compared with the field intensity created by the rod current so for all practical purposes, current directions should influence the direction of fluid motion only.

A new separator plate, 1 1/8 inches thick, was used to more readily accommodate dye holes and thermocouples. Except for enlargement of the center hole to 3 inches, this plate was identical in most aspects to the one used previously. Copper-constantan thermocouples, of 30 gage wire, were located in the hole of the separator plate, at the fluid-copper interface of the top electrode, and at several fluid-plastic interfaces in the top section of the unit. All thermocouples were

introduced from the outside of the unit to reduce extraneous effects on fluid motion to a minimum. Each of these temperature sensing devices projected approximately 1/4 inch into the fluid and each was insulated from the fluid with a thin coating of Miccrostop, a commercial lacquer produced by the Michigan Chrome and Chemical Company. This insulation served two purposes. First, it prevented the wires from any possible chemical reaction with the fluid, and secondly, it prevented any signal pickup by the wires when the D.C. power source was applied to the fluid. A check of response time for both a bare and insulated thermocouple indicated a negligible difference. A reference junction, maintained at 32°F, was employed throughout.

Figure 5 shows the assembled unit, the thermos which housed the reference junction in the thermocouple circuit, photographic lights, and the reservoir container used for filling or emptying the test unit. Figure 6 shows the accessories employed in the thermocouple and fluid circuits. The slide wire resistor, single pole double throw switch, and shunted ammeter were connected in series with the electrodes and batteries. The double pole switches, Leeds and Northrup Precision Potentiometer, and Honeywell Visicorder, Model 906 C, comprised the circuit for calibrating and recording the data that provided direct temperature measurements of the fluid at pertinent locations.

Although much effort was expended, no success with a dye injection system was obtained. Control of ink flow through individual orifices was obtained, but it was found that the small streamers of emitted dye simply blended in with the copper sulphate and disappeared

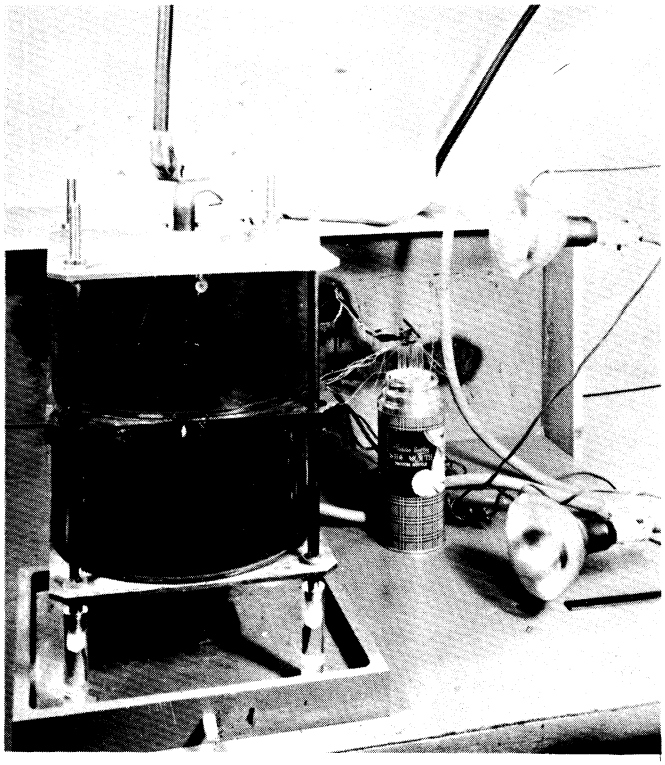

Figure 5. Assembly of the First Revision of the Experimental Model.

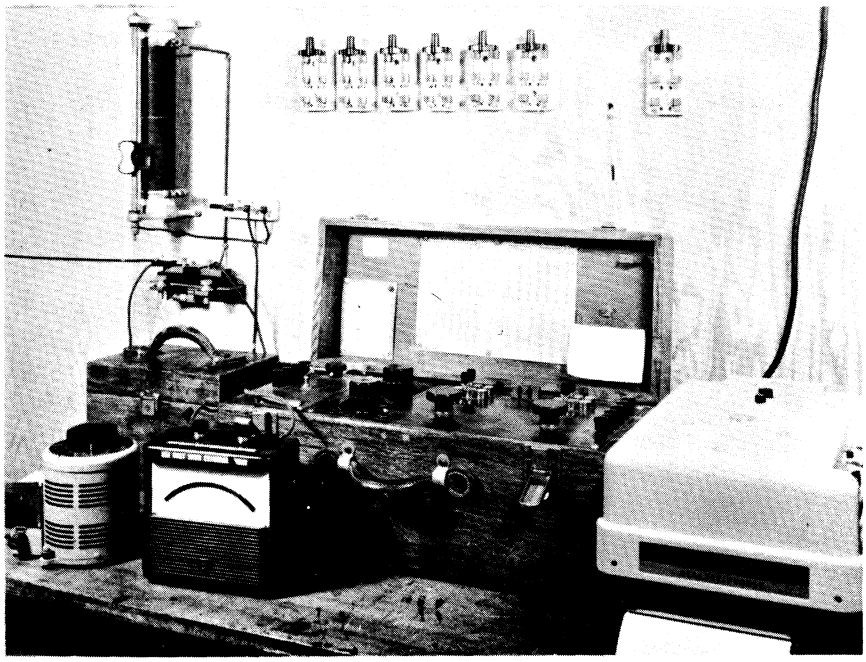

Figure 6. Electrical Accessories and Temperature Recording Components.

from view. The technique which finally proved satisfactory was to pour small quantities of aluminum pigment, produced by the Alcoa Company and classified as Standard Unpolished Powder No. 606, into the solution of copper sulphate. Prior washing of this powder with methanol removed surface contaminants and led to better suspension of the powder after it was mixed with the fluid.

Small light slits were produced on diametrically opposite sides of the test unit by applying black paint to all but the slit and viewing areas of the large plastic tubes. Large photo flood bulbs in conjunction with light boxes made of asbestos board provided a concentrated beam of light which passed through the slits and illuminated any particles that were suspended in this lighted region. The optimum width of slit for this particular situation was about 3/16 inch, so the lighted plane possessed a thickness of several sixteenths of an inch. In general, the other particles in suspension throughout the fluid caused no visual difficulties as they were not illuminated, however, if too much powder were introduced into the fluid the mixture appeared cloudy and the lighted region was dimmed to such a degree that it was impossible to obtain decent photographs. After several trials, judgement regarding an optimum amount of powder became quite accurate. It should be noted that if an insufficient quantity of powder were used, lighting was too poor to obtain clear pictures.

The general procedure followed was to pour some powder into the reservoir full of fluid, fill the unit with this mixture, and wait until an apparent state of equilibrium existed. In reality, a perfectly

static state might not result for hours and residual velocities probably were present. When the axis of the unit was vertical, this waiting period involved a matter of 30 to 45 minutes. Although some powder settled to the surfaces of the separator plate and bottom electrode, a sufficient amount remained in suspension. In time, the powder became copper colored. This was probably a result of chemical action since aluminum and copper are widely spaced in the electrochemical series. Whenever necessary, the fluid was drained, the interiors of the test unit and reservoir were cleaned, and fresh powder added. Several tests indicated that the electrical conductivity of the fluid was practically identical whether it contained powder or not.

A feature added to the photographic setup was the incorporation of an interrupter between the camera and lighted plane of fluid. This was in the form of a disc mounted to a phonograph turntable and motor, and containing a hole slightly larger than the lens opening of the camera. The disc speed was adjusted to 75 RPM by means of a variac and this was fixed during all further testing.

Figure 7 shows the components of the camera system and is illustrative of the exact setup employed for obtaining pictures. Large black curtains were draped over the entire physical setup to exclude exterior light. A standard test sequence involved starting the disc motor, applying rod and fluid currents, turning on the photo bulbs and opening the camera shutter for a certain time period. As a result of the interrupting action of the disc, actual particle traces were exposed. If gross motion patterns were desired, an ordinary time exposure would suffice. As it was hoped to obtain some velocity measurements individual particle traces appeared necessary.

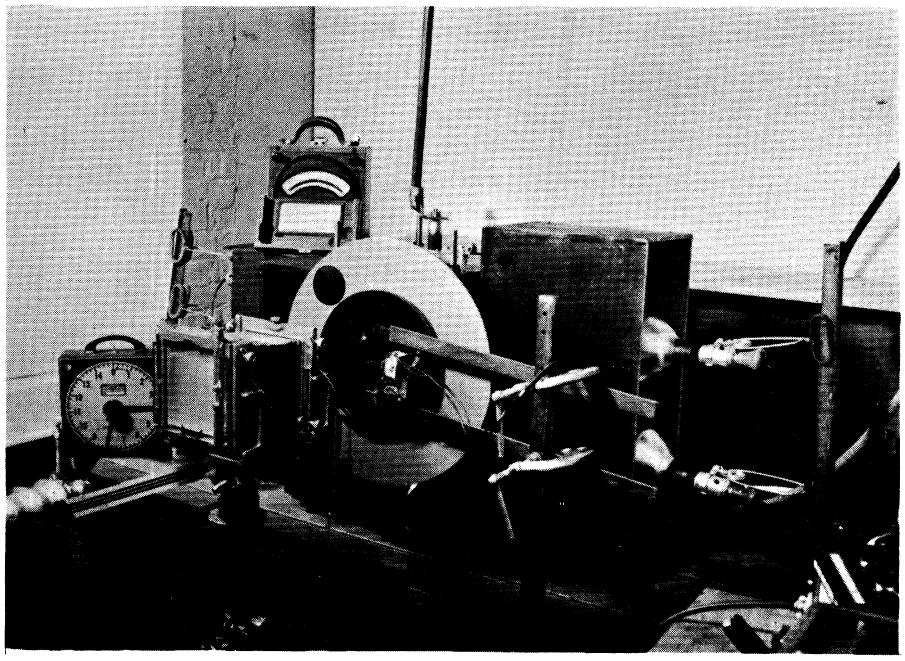

Figure 7. Setup of Photographic Accessories.

Various combinations of rod current, fluid current, and time were employed. Only a few illustrative results are shown. Figure 8a shows the results for the first 5 seconds after the currents were applied. A fluid current of 4 amps and a rod current of 400 amps were used and they flowed in opposite directions. As a result of the interrupter action, the total film exposure time was considerably less than 5 seconds. The axis of the unit was in a vertical position and the horizontal marks on the center plastic tube were spaced one inch apart to provide an idea of actual vertical distances traversed by a particle.

Test conditions which led to Figure 8b were identical to those just discussed, the only difference being that the fluid current was active for 30 seconds before this picture was taken. Figure 9 resulted when a fluid current of 2 amps was applied for 30 seconds, the rod current being zero. The maximum temperature difference recorded, between the hole in the separator plate and the top electrode, was about $3^{\circ}F$ during these tests.

Figures 10a to 10d portray a time sequence that resulted when currents of 1 and 400 amps flowed through the fluid and rod respectively. These currents were in the same direction. Figure 10a shows the equilibrium condition of the fluid and powder after the unit sat stationary for one hour upon filling. After applying the currents, pictures were taken after 10, 40, and 180 second intervals and are shown as Figures 10b, 10c, and 10d respectively. Strong convective effects are obvious in the top half of the unit, but interest should also be focused on the bottom section. In Figure 10c, symmetrical

Figure 8a. Fluid Patterns after Five Seconds of Current Flow with the Unit in a Vertical Position.

Figure 8b. Fluid Patterns 25 Seconds after Figure 8a.

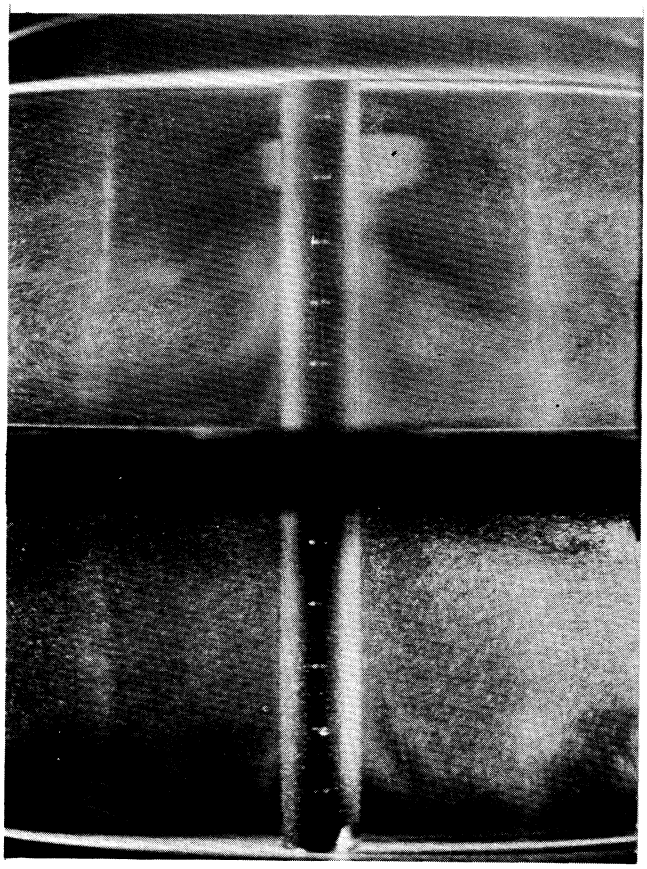

Figure 9. Fluid Patterns after 30 Seconds of Current Flow with the Unit in a Vertical Position and No Rod Current.

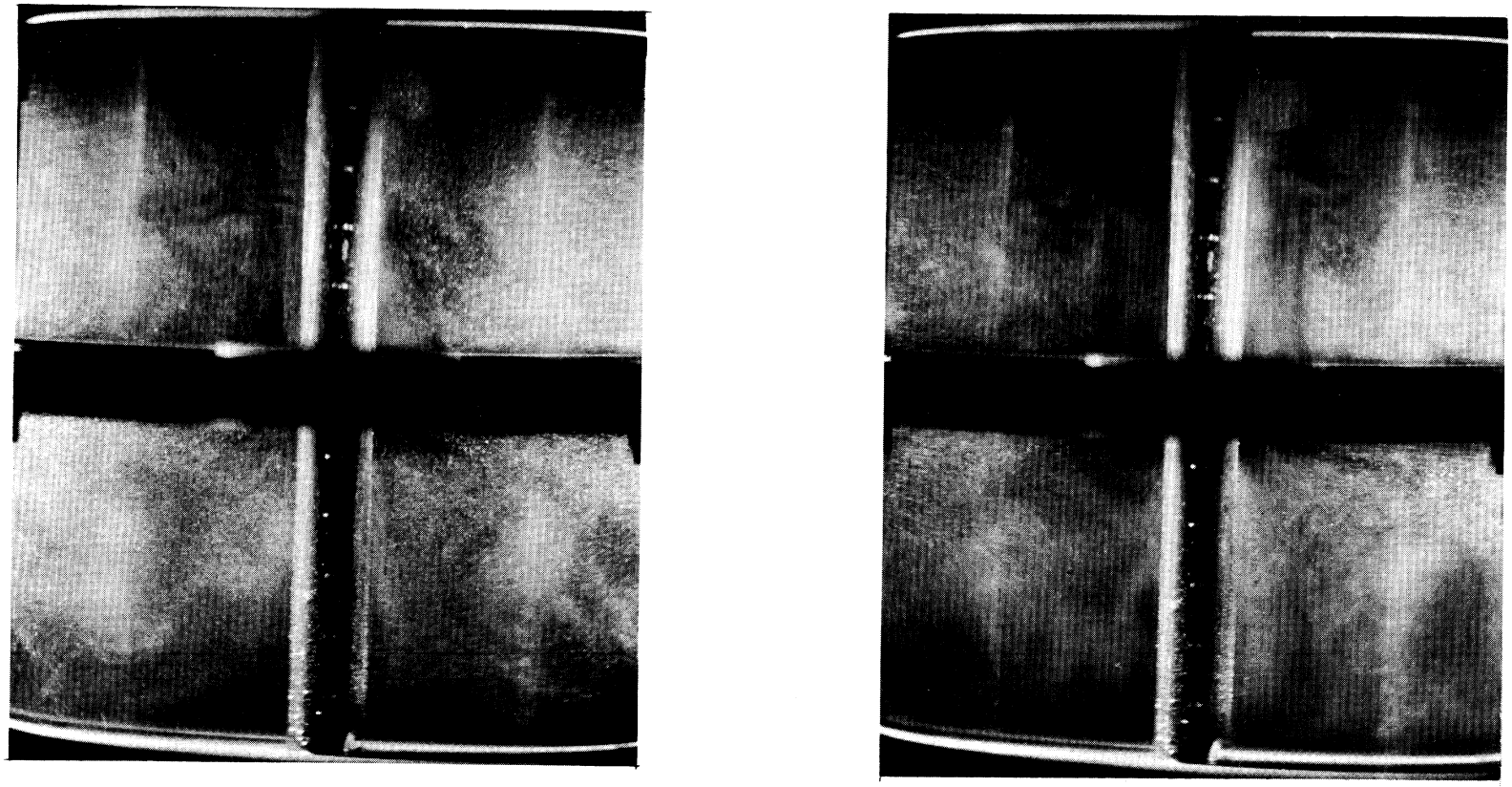

(a) (b)

Figure 10. Sequence of Fluid Patterns after Various Time Intervals of Current Flow with the Unit in a Vertical Position.

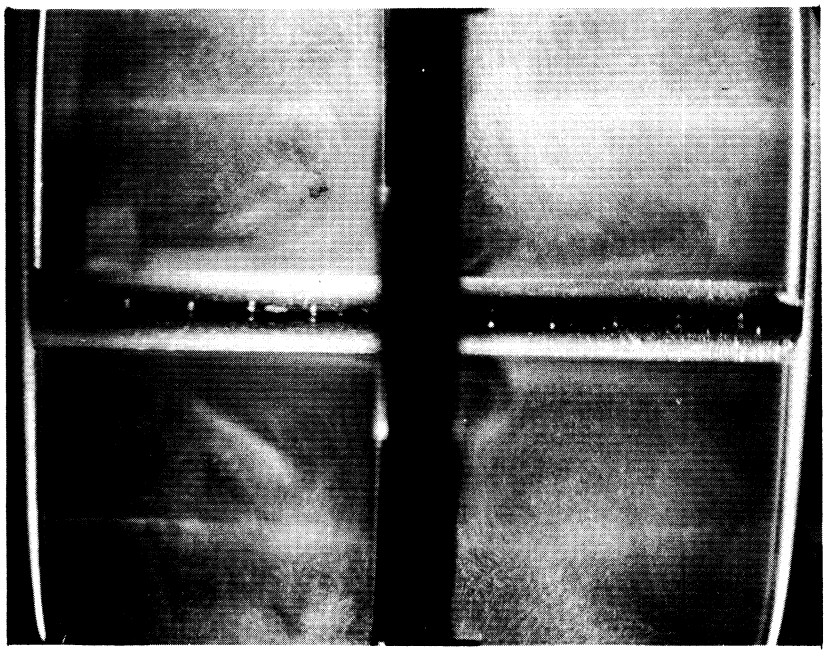

(d)

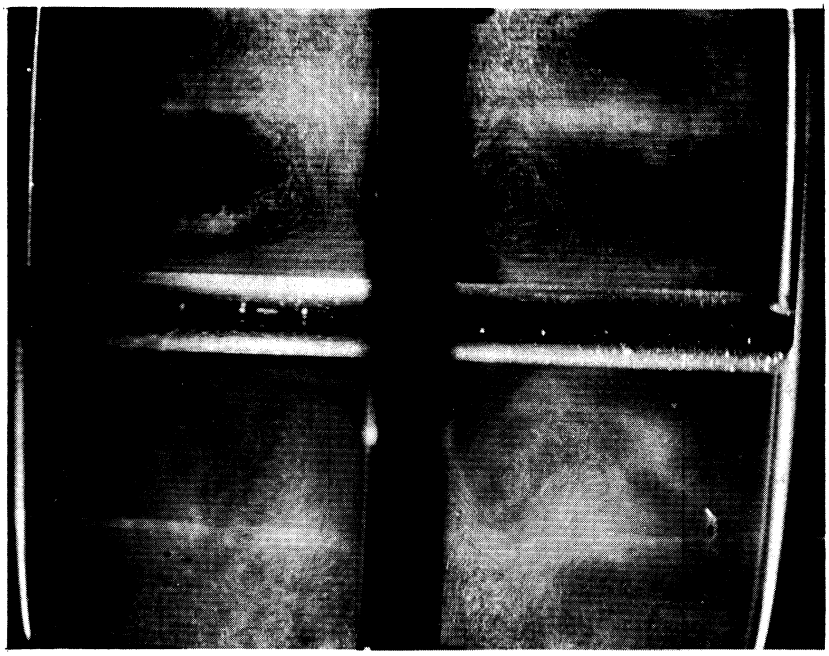

(c)

Figure 10. Cont'd.

circulatory patterns may be noted in the lower quadrants. It is quite possible that they illustrate a magnetic effect, yet in Figure 10d the flow patterns in the lower quadrants have changed completely. Whether this indicates a type of instability cannot be stated with assurance but future reference to similar results will be noted.

Conclusive evidence showed that convective effects were still predominant, but before further alterations of the unit were contemplated, one modification of the existing setup was made. The unit was rotated 90° to place the center rod in a horizontal plane and necessary changes in the light sources were completed. After a fluid current of 4 amps and rod current of 400 amps had been applied for 2 minutes, the resultant motion was photographed and is shown in Figure 11. Although an insufficient amount of powder and alignment of light bulbs did not provide a satisfactory degree of lighting, definite circulatory traces may be seen in all 4 quadrants. More important, the patterns show an almost perfect symmetry in all quadrants. Further tests confirmed these observations. This raised the question as to what would occur if the center rod were removed, thereby restoring the unit to its original condition, and the unit tested in the horizontal position. Necessary modifications were accomplished and Figure 12 shows the patterns that occurred after 8 amps had been applied for 3 minutes. Apparently the convective influence was still extremely pronounced since all semblance of circulatory motion vanished. This would appear to be a significant result, especially in considering future tests. Destruction of circulatory motion observed in a horizontal plane must be caused by convection, consequently, if

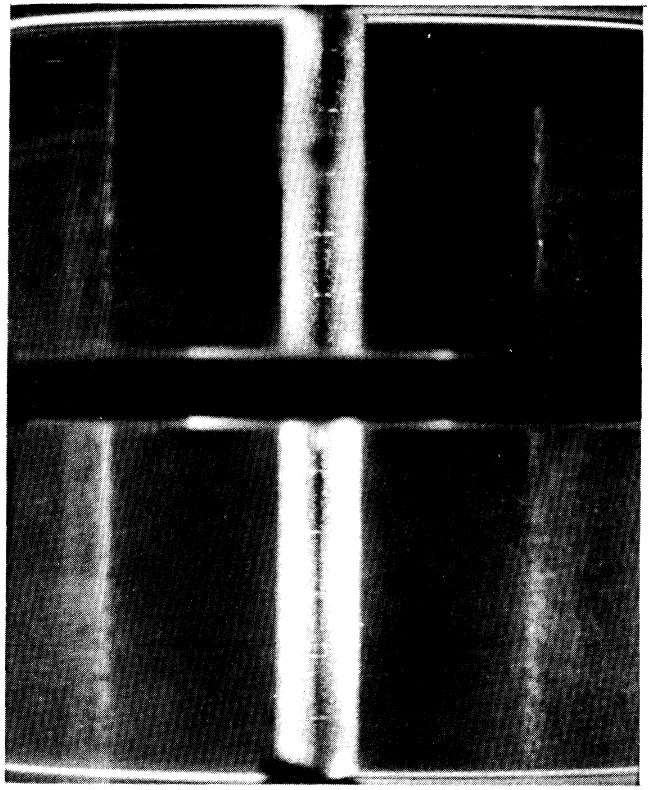

Figure 11. Fluid Patterns after Two Minutes of Current Flow with the Unit Horizontal.

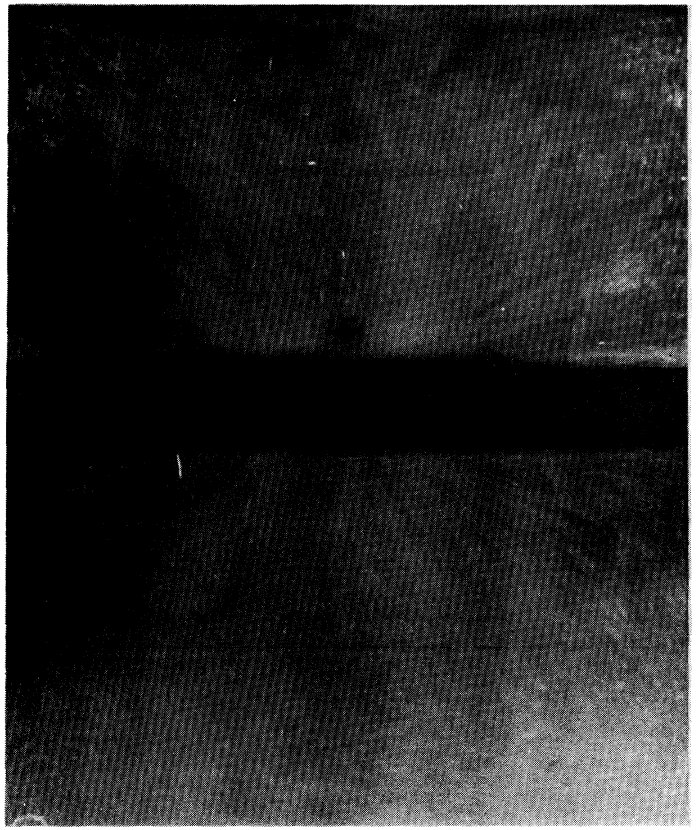

Figure 12. Fluid Patterns after Three Minutes of Current Flow with the Initial Version of the Unit Horizontal.

motion remains circulatory it would seem reasonable to assume that electromagnetic effects are being observed. This same result occurred with various fluid currents down to 2 amps, so it was concluded that a model which produced fluid motion solely because of current in the fluid must be abandoned premanently.

2.8 Second and Final Revision of the Experimental Model

Although it was contemplated that the majority of future tests would be conducted with the unit in a horizontal position, some further testing with the unit vertical was also planned. To avoid any tendency of cable sag at the electrode junctions, a new center rod of solid copper was used. It was 1 inch in diameter and extended beyond each electrode by about 1 foot. The large generator cables, when adapted to the ends of the rod, could then be held reasonably perpendicular to the electrodes regardless of the position of the assembled unit. To more readily accommodate thermocouples in the region of the axial centerline, where convective effects seemed strongest, a larger insulating tube was employed This was made of clear plastic with an outer diameter of 2 1/2 inches and an inner diameter of 2 inches. Two end plugs of plastic were press fitted into the opposite ends of the insulating tube and holes, bored concentric with the outside of the tube, were produced through these plugs. These holes served to locate the copper rod almost perfectly concentric with the tube when it was inserted in place. When this subassembly was completed an annular clearance space of 1/2 inch existed between the copper rod and inner diameter of the plastic tube. Thermocouples were positioned in this clearance space with their hot junctions

extending through the wall of the tube at selected intervals. As before, they protruded about 1/4 inch into the fluid and were coated with Miccrostop. The holes in the plastic tube, through which these hot junctions passed, were sealed to prevent any contact between the fluid and copper rod. Additional thermocouples were employed and are indicated in Figure 13 which is a schematic drawing of the assembled unit. Except for the minor changes mentioned, this was identical to the unit in Figure 5. It should be added that the hole in the separator plate was enlarged to 7 1/2 inches, and "O" ring assemblies were used to prevent leakage at the joints between the outer diameter of the plastic tube and the center holes in the electrodes.

The assembled unit was bolted to four pieces of angle iron whose ends were adapted to two end plates of plywood. Shafts, connected to these end plates, were supported in two pillow blocks, the entire structure being supported by end spacing units of sufficient height. This permitted the entire structure to be rotated 90° quite readily. New light boxes with their individual photo bulbs were adapted directly to the angle irons. A platform was secured to the angle irons at right angles to the axis of rotation. It supported the camera, disc interrupter assembly, and a covering hood. With this arrangement, all components moved as one unit as the structure was rotated to position the test section either vertically or horizontally. Two overhead bars were employed to secure the structure when it was rotated to position the axis of the test section horizontally. A simple platform, placed upon the floor, served to support the unit when the test section was vertical. An additional change was made in the interrupter disc.

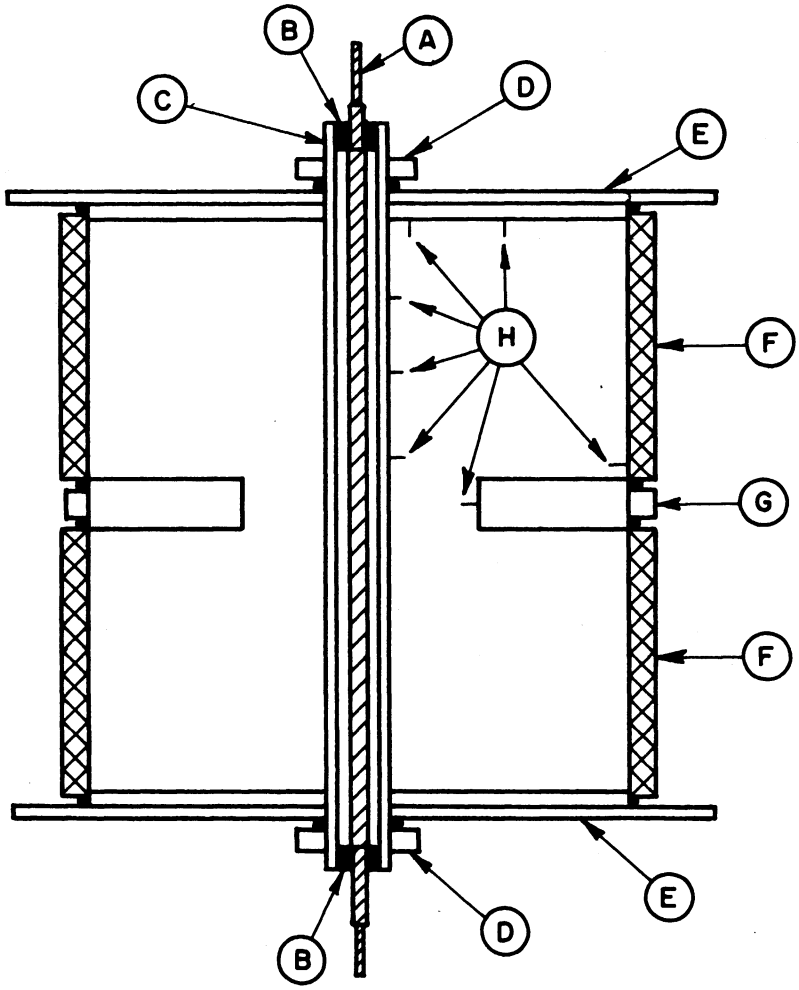

A- CENTER COPPER ROD
B- PLASTIC LOCATING PLUGS
C- PLASTIC INSULATING TUBE
D- PLASTIC "O" RING CAPS
E- COPPER ELECTRODES
F- PLASTIC CYLINDERS
G- PLASTIC SEPARATOR PLATE
H- THERMOCOUPLES
●- RUBBER "O" RINGS

Figure 13. Schematic Drawing of the Unit After the Second Revision.

Instead of a hole, a semi-circular arc was produced to increase exposure time per revolution.

Figures 14 and 15 show two views of the complete assembly with the axis of the test section in a vertical position, while Figure 16 shows the assembly when it was rotated 90° to place the test unit in a horizontal position. For most of the experimentation that followed, the unit was positioned as shown in Figure 16. Another view of the vertical position of the test section is shown in Figure 17. Here, the blackout hood, which was bolted to the platform that supported the camera and disc interrupter, may be seen. Heavy black drapes were also employed to provide additional aid in excluding exterior light.

For the remainder of the program the copper sulphate solution possessed a specific gravity of 1.10 and the rod current was always set at 300 amperes. This latter restriction was necessitated by the lengths of time involved for most of the tests. If higher currents were employed, the internal wiring and insulation of the generator became severely overheated after a few minutes of continuous operation.

Any future use of the term "horizontal" position will mean that the axis of the test section, or the center copper rod, lies in a horizontal plane. "Vertical" position follows from the previous definition. Since most of the figures that follow involve the lighted plane through the test section, the presence of 4 quadrants will serve for reference. For consistency, "upper" right or left quadrants will pertain to the two regions adjacent to the top electrode when the unit stands in a vertical position and will be positioned at the top of every photograph that displays such a pattern.

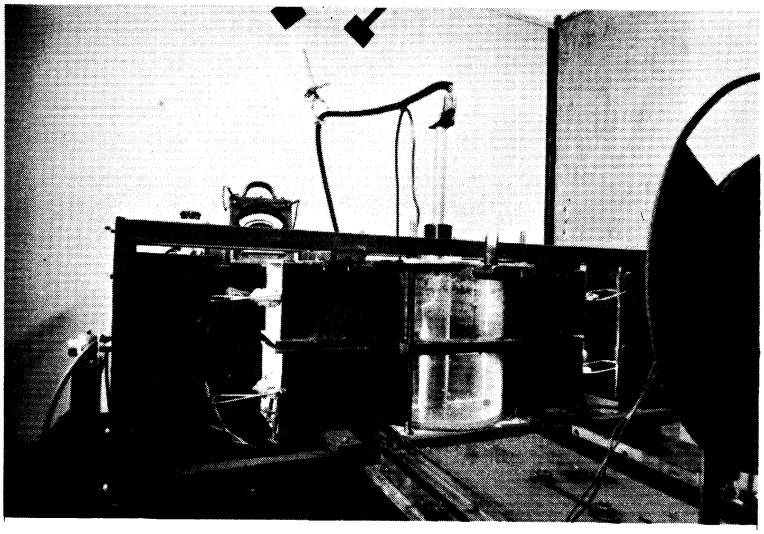

Figure 14. Assembly of the Second Revision of the Unit in a Vertical Position.

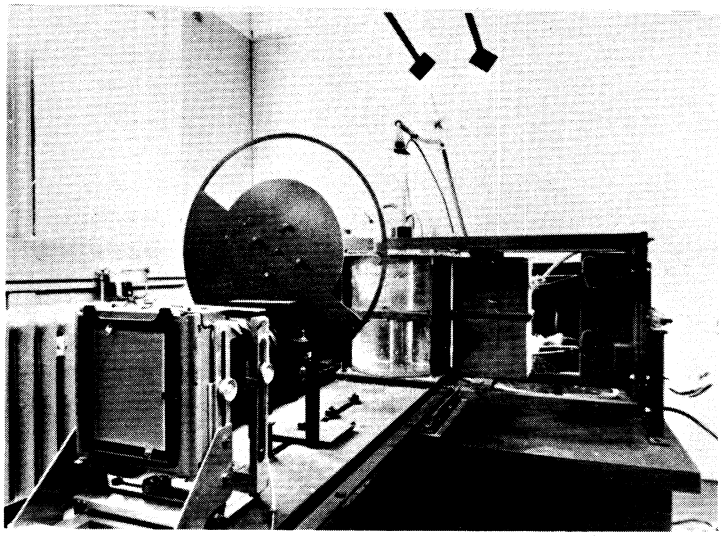

Figure 15. Assembly of the Second Revision of the Unit in a Vertical Position.

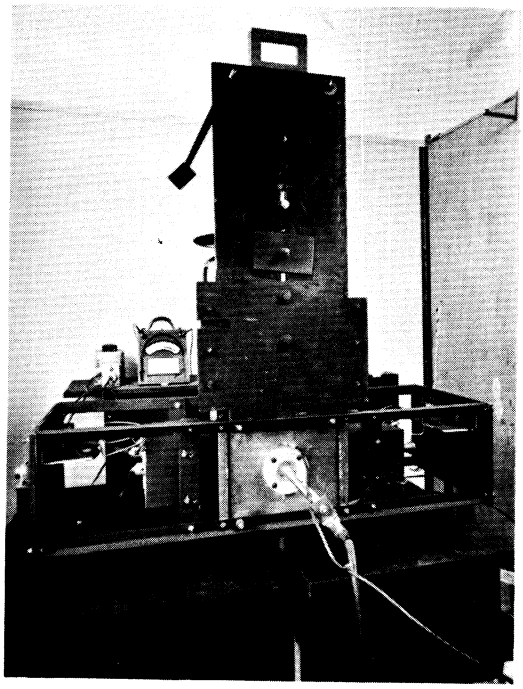

Figure 16. Assembly of the Second Revision of the Unit in a Horizontal Position.

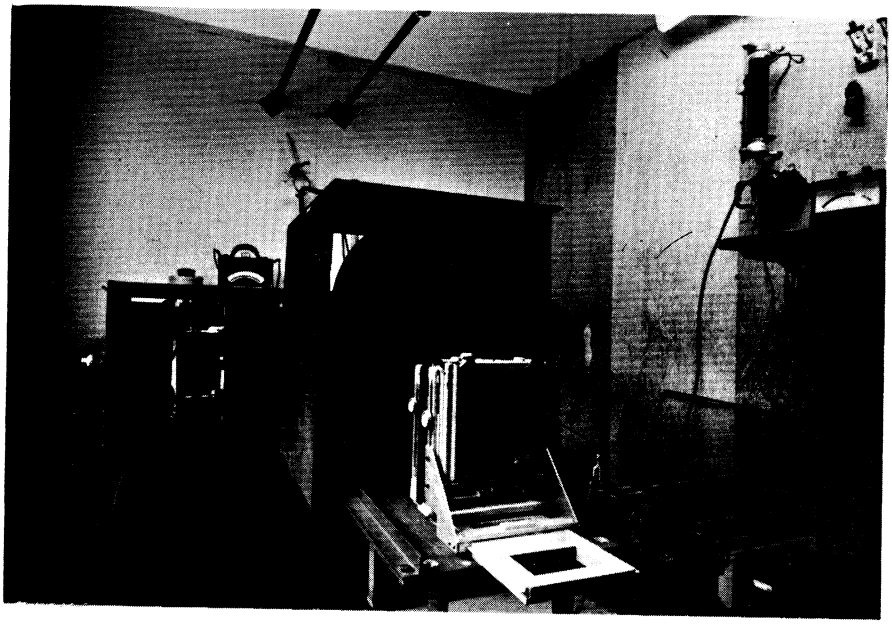

Figure 17. Assembly of the Second Revision of the Unit with the Blackout Hood in Place.

After a few preliminary tests confirmed that circulatory and symmetrical flow patterns occurred when the unit was horizontal, an investigation of steady state conditions was made. Figures 18a to 18f show the change in pattern that resulted when a fluid current of 10 amperes was applied continuously for 10 minutes. The rod current was in the same direction as the fluid current. An optimum shutter opening time had not yet been selected and both 2 and 4 second openings were utilized during this test. From these initial tests it was decided to standardize on a four second shutter opening in the future. Since the disc rotation caused exposure every 1/2 revolution, the total exposure time of the film was 2 seconds. It might be of interest to note that Super-Panchro Press, Type B, Kodak film, in the form of 4 inch by 5 inch negatives was used throughout.

Since Figures 18a to 18f show a time dependent result, velocity measurements, as a function of time, were obtained. A detailed discussion regarding the procedure used to attain these measurements follows in another section, consequently, it will suffice to state here that velocities were measured at particular coordinate points indicated in the schematic sketch below.

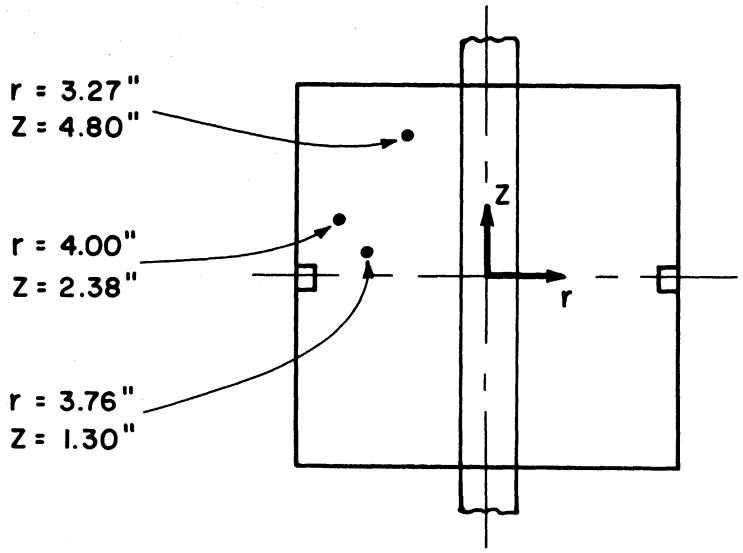

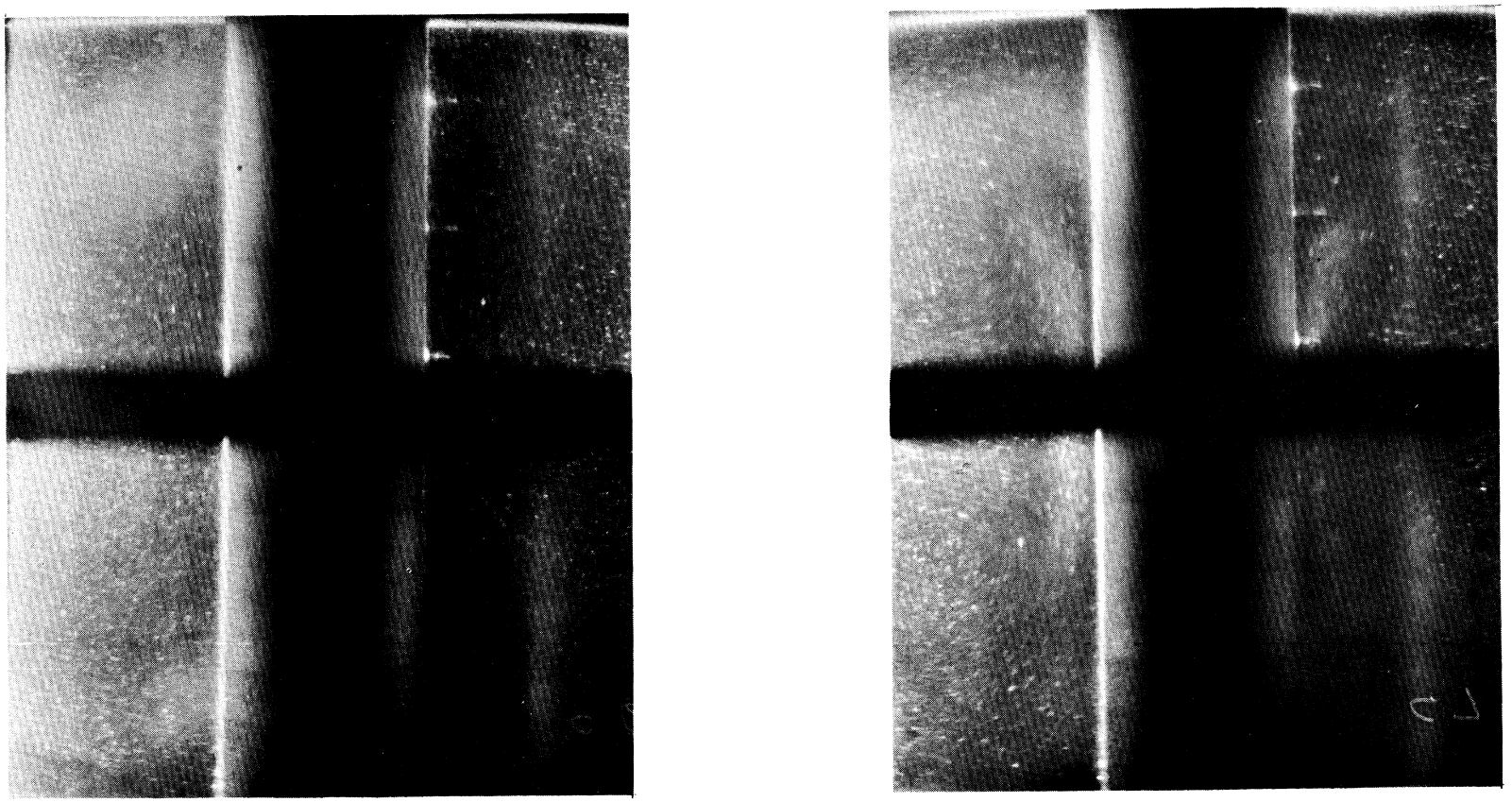

10 Seconds (a) (b) 1.5 Minutes

Figure 18. Sequence of Fluid Patterns after Various Time Intervals of Current Flow with the Unit Horizontal and a Fluid Current of 10 amps.

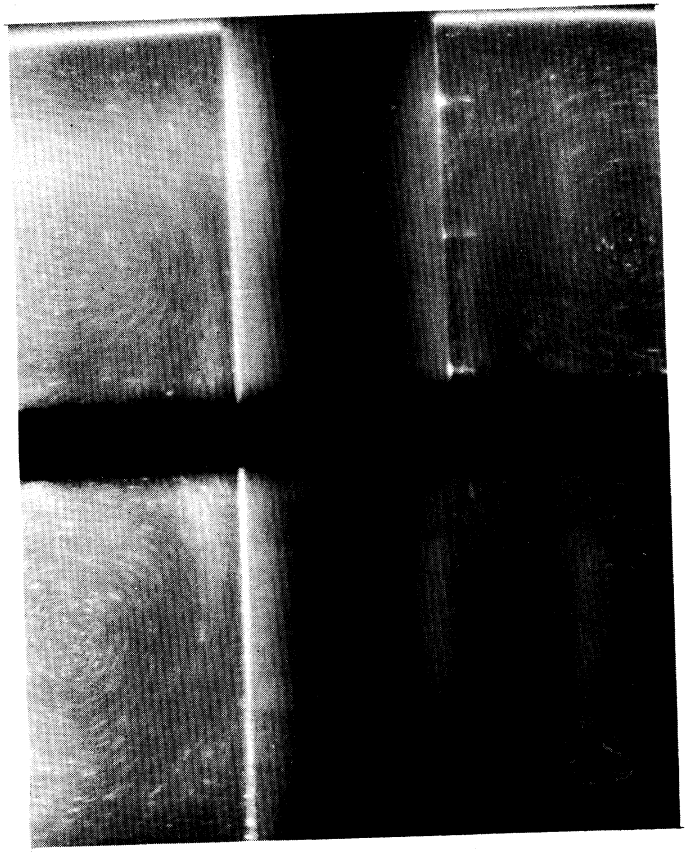

3 Minutes (c)

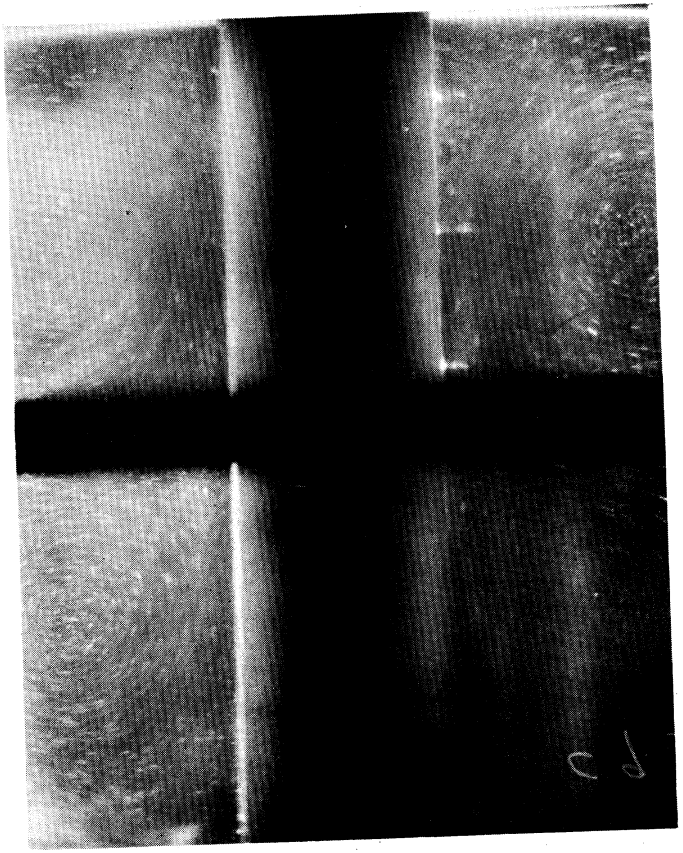

(d) 4.5 Minutes

Figure 18. Cont'd.

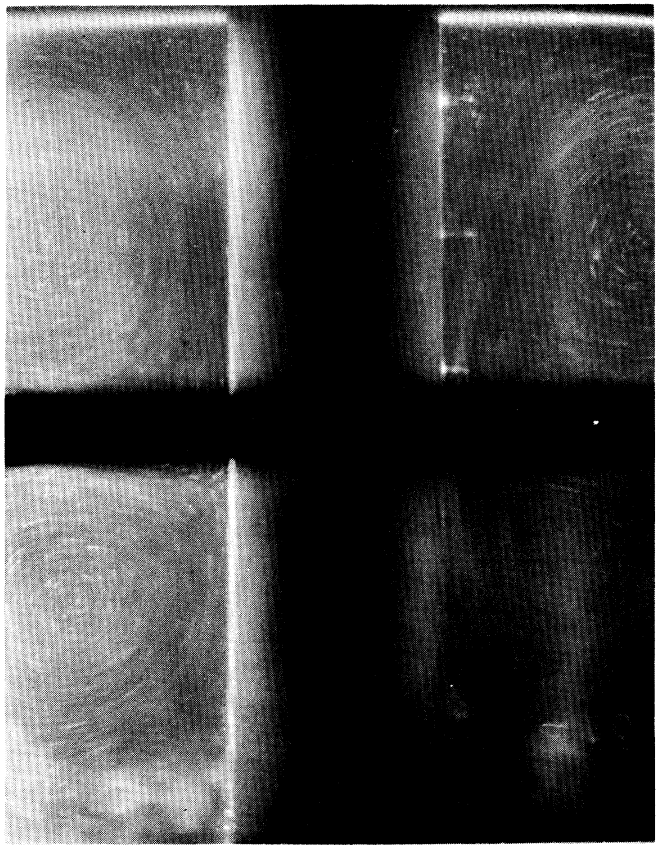

6 Minutes (e)

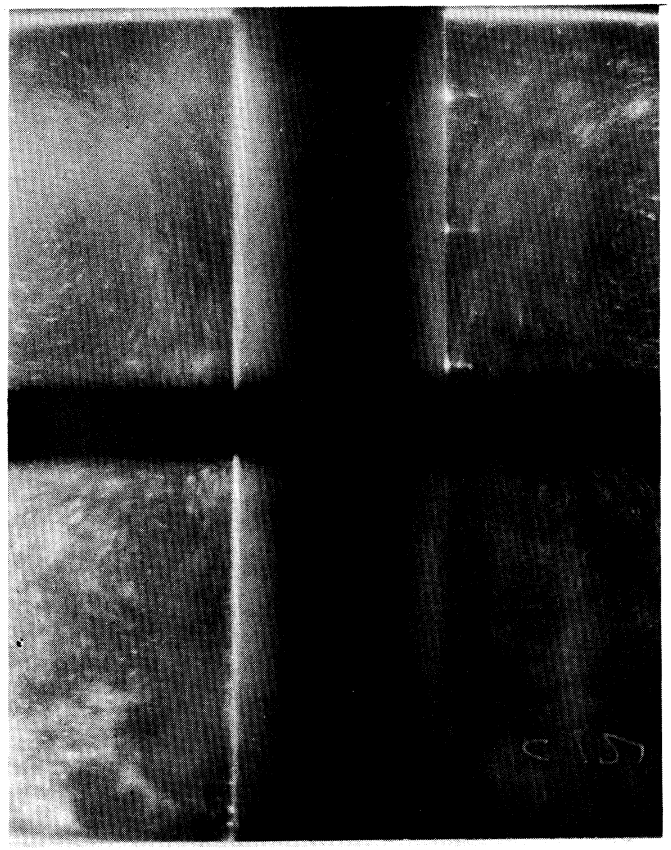

(f) 10 Minutes

Figure 18. Cont'd.

The results are plotted on Figure 19. These curves typify the trends that were found so it was not considered necessary to include all of the measured data. Of the three sets of points plotted, the groups of greatest consistency and greatest scatter are included.

An explanation regarding the selection of a particular quadrant for velocity measurements is in order. It can be seen from the photographs that symmetry in all four quadrants prevailed during the first half of the 10 minute test but in the last two Figures, 18e and 18f, some change occurred in the lower two quadrants. No complete explanation can be offered, although electrochemical effects might have been partially responsible. This apparently random and sudden loss of 4 quadrant symmetry often, but not always, occurred and remained unsolved. The possibility certainly exists that convective effects might influence this symmetry. In most cases, natural convection is notoriously unstable and a small disturbance caused by such effects could conceivably produce non-symmetrical patterns. For the purpose of velocity measurements, one of the upper quadrants was selected since it was felt they more accurately portrayed the basic motion created by the currents in the fluid and rod. The plots in Figure 19 indicate that the velocity appears to approach a steady state condition during the time interval of these tests.

Figures 20a to 20f resulted when the direction of the rod current was reversed, all other factors being identical to those used when Figures 18a to 18f were obtained. Theoretically, the only difference in the motion caused by electromagnetic effects for these two situations should be one of direction of rotation. Visual observation

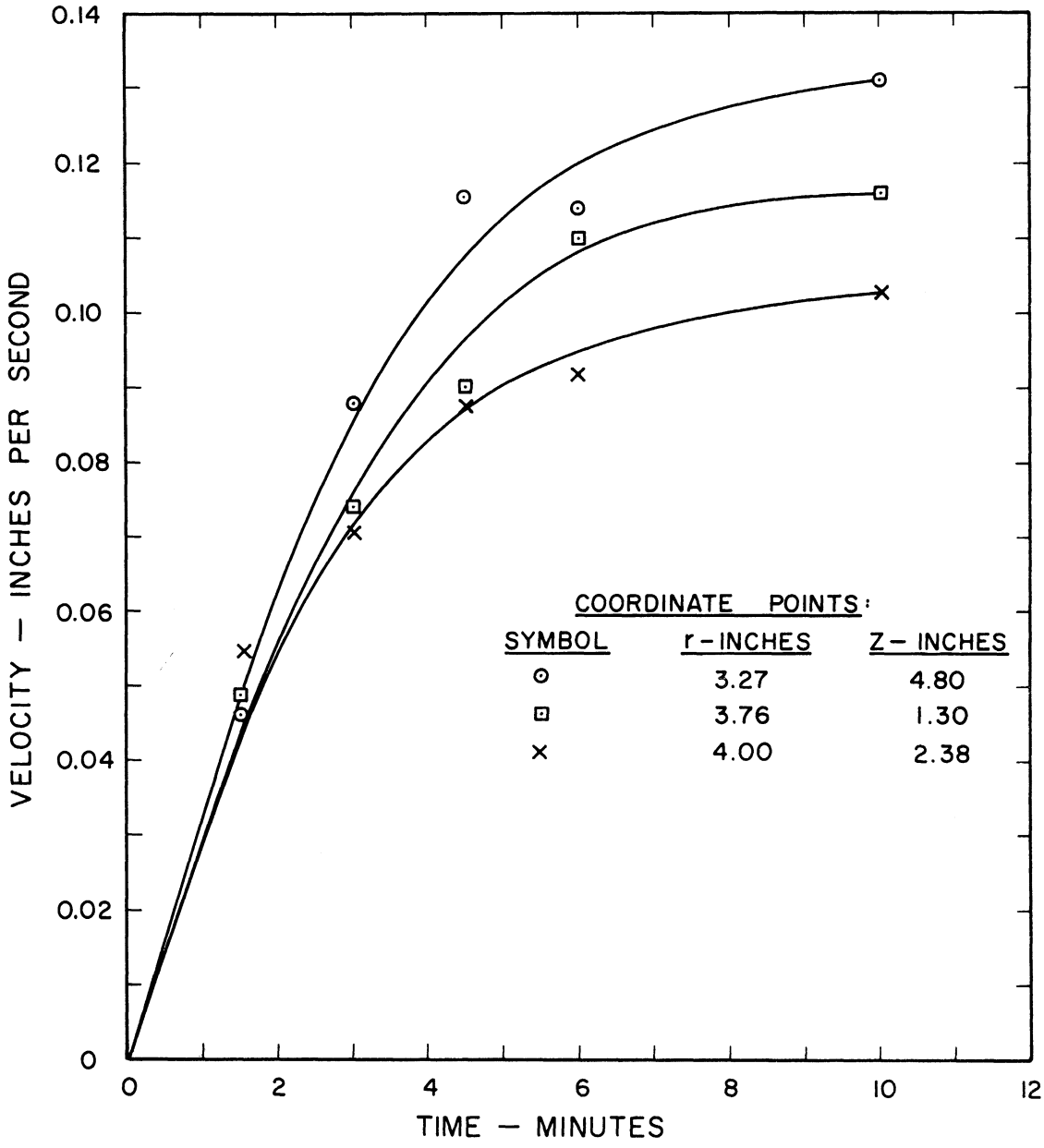

Figure 19. Velocity Measurements Versus Time.

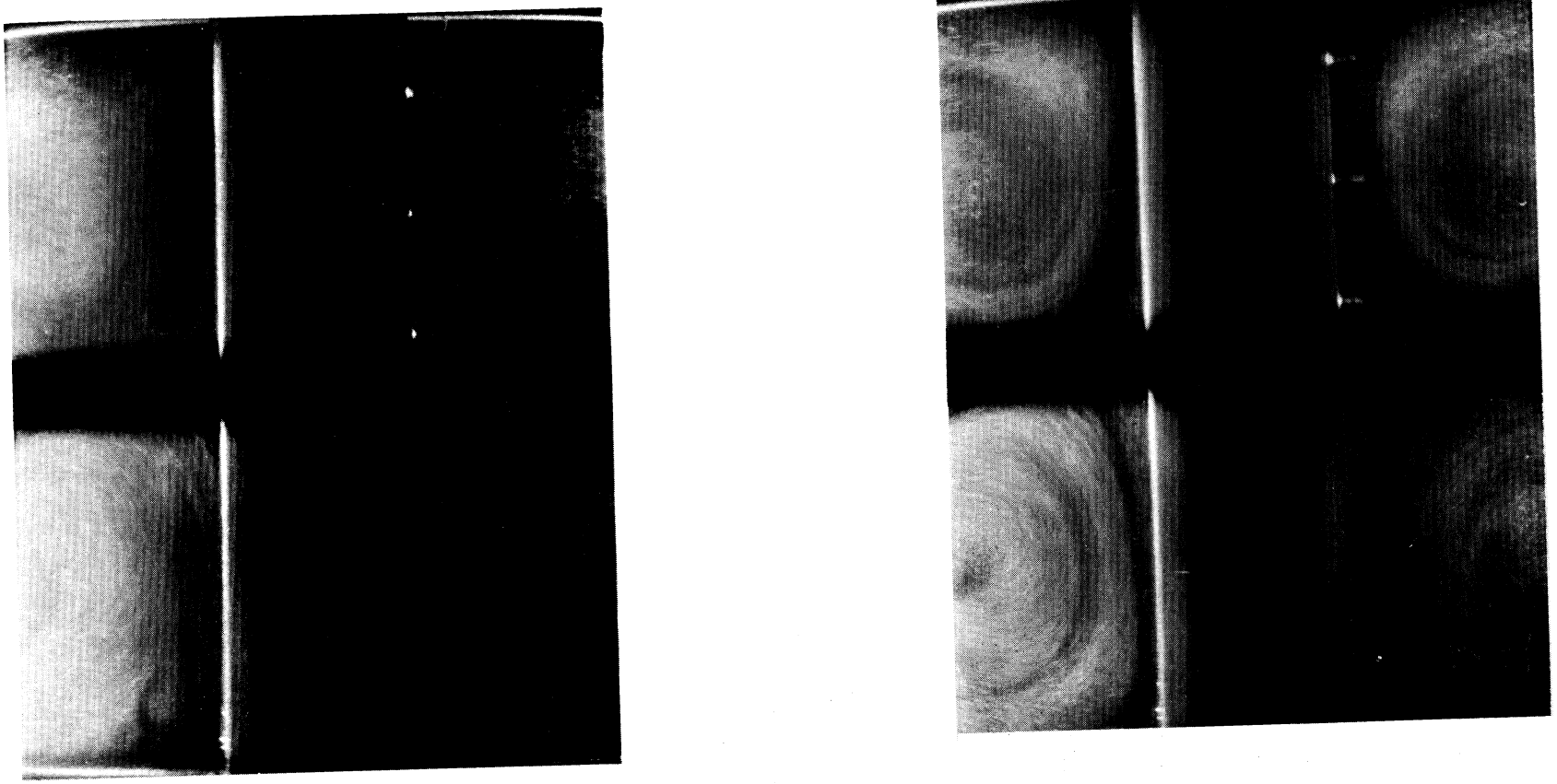

(a) (b)

Figure 20. Repeat of Figure 18 but with Current in the Rod Reversed.

(c)

(d)

Figure 20. Repeat of Figure 18 but with Current in the Rod Reversed.

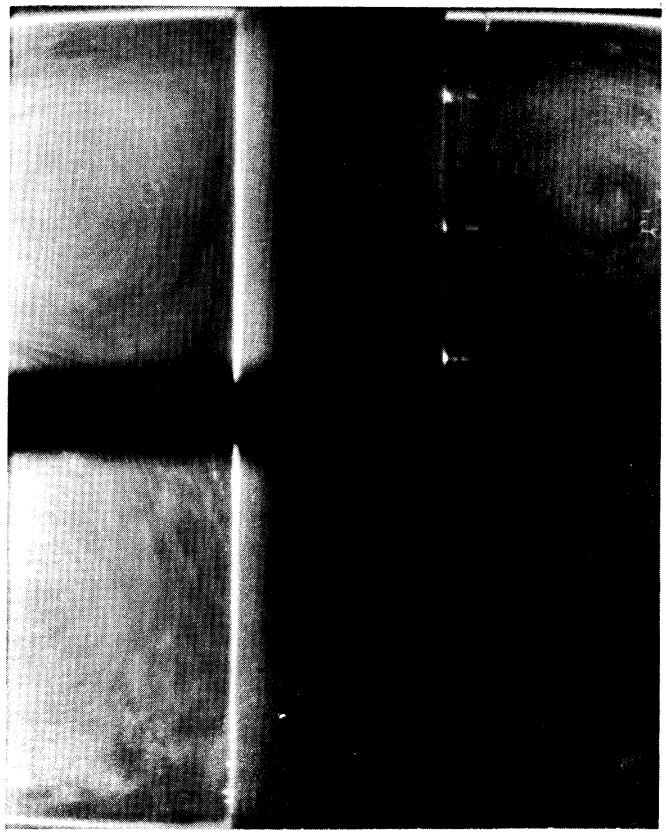

(e)

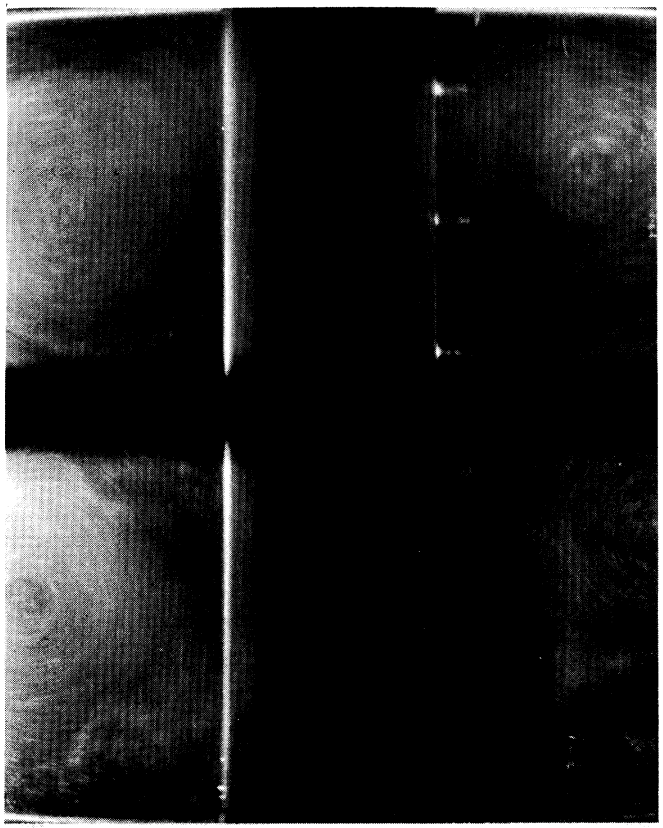

(f)

Figure 20. Repeat of Figure 18 but with Current in the Rod Reversed.

confirmed this was the case. In general, the overall patterns are quite similar. The difference in contrast between the two sets of pictures was caused by using a greater quantity of aluminum powder during the latter test. Gross motion seems to be better defined in Figures 20a to 20f, but velocity measurements were more readily obtained with the conditions of the initial set of pictures. Again, it may be noted that in the latter pictures of the set in Figure 20, symmetry has been altered in the lower quadrants.

A total test time of 15 minutes was used for most of the remaining tests when the unit was horizontal. It was felt that this would provide a margin of safety in assuring the approach to a steady state condition of velocity. Figures 21a to 21d show the results obtained with a fluid current of 5 amps. Time intervals per picture are indicated. Except that the fluid current was 2 1/2 amps, the test conditions that led to Figures 22a to 22d were identical to those used in the previous test. For both of these sets of pictures the fluid and rod currents were in the same direction. Symmetry prevailed throughout the total run for each of these tests and since both of these fluid currents were lower than the one used for Figures 18 and 19, this could support the notion that electrochemical effects were at least partially responsible for the loss of symmetry in the earlier tests.

To observe the major effects of thermal buoyancy, the assembly was rotated to the vertical position. With a fluid current of 5 amperes, Figures 23a to 23c resulted at the time intervals

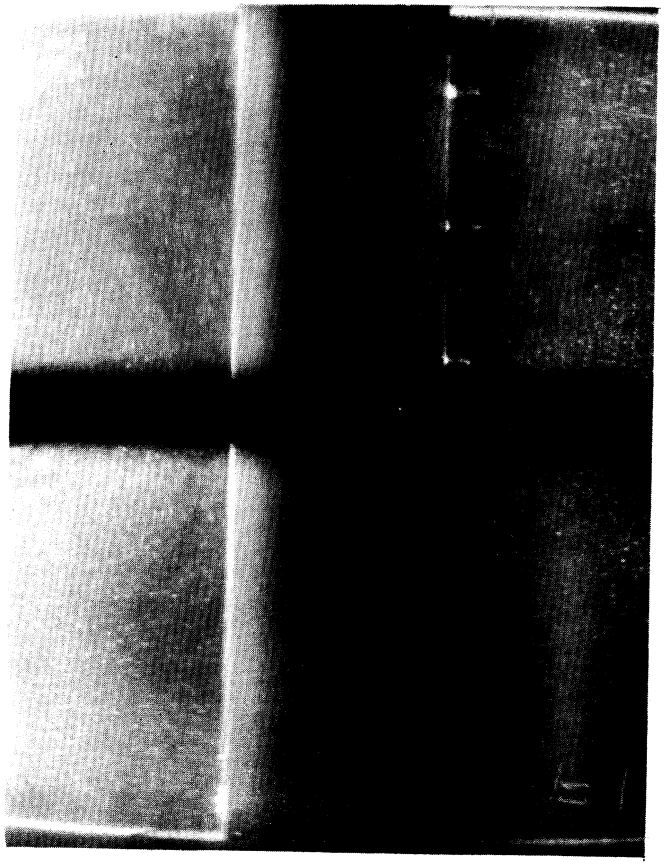

30 Seconds (a)

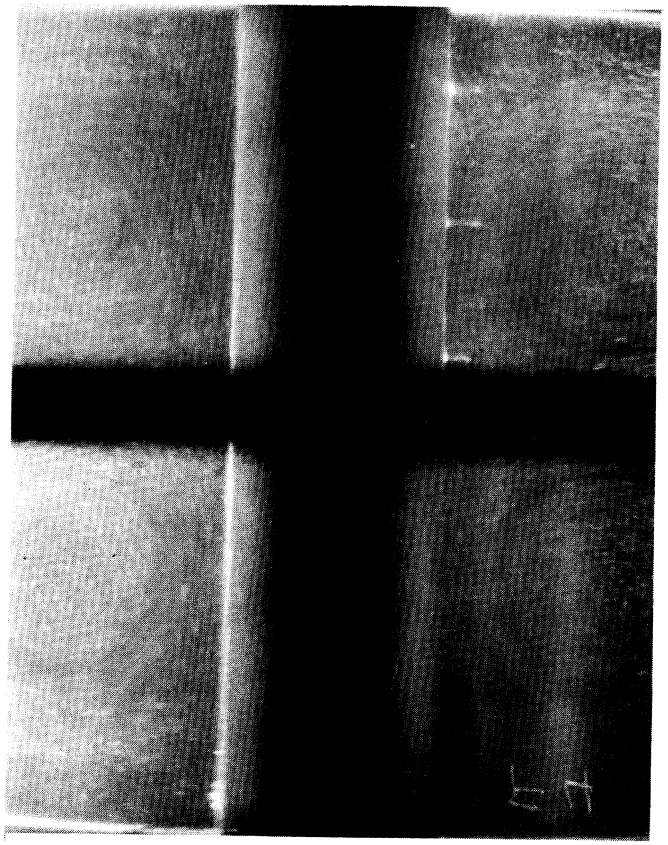

(b) 6 Minutes

Figure 21. Sequence of Fluid Patterns After Various Time Intervals of Current Flow with the Unit Horizontal and a Fluid Current of 5 Amps.

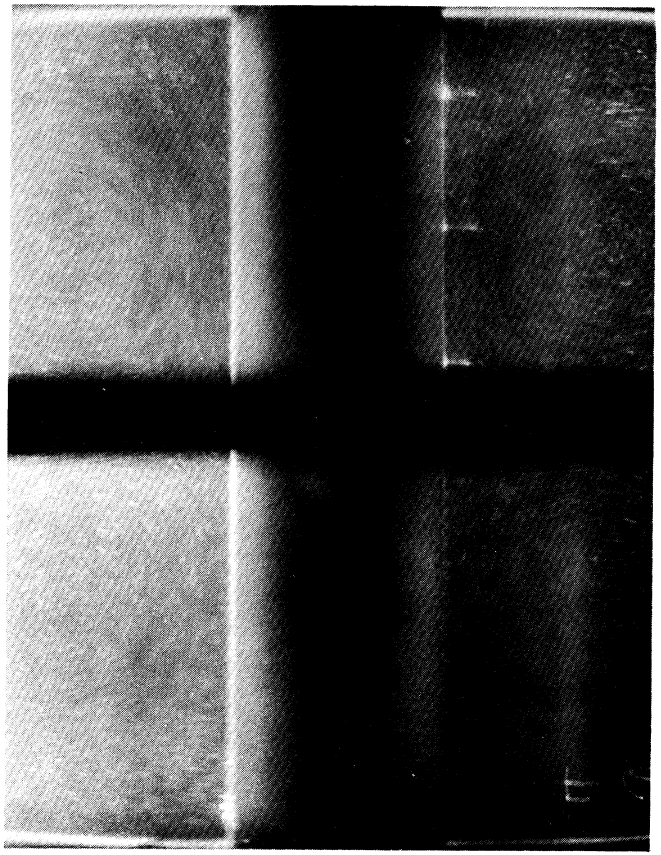

10 Minutes (c)

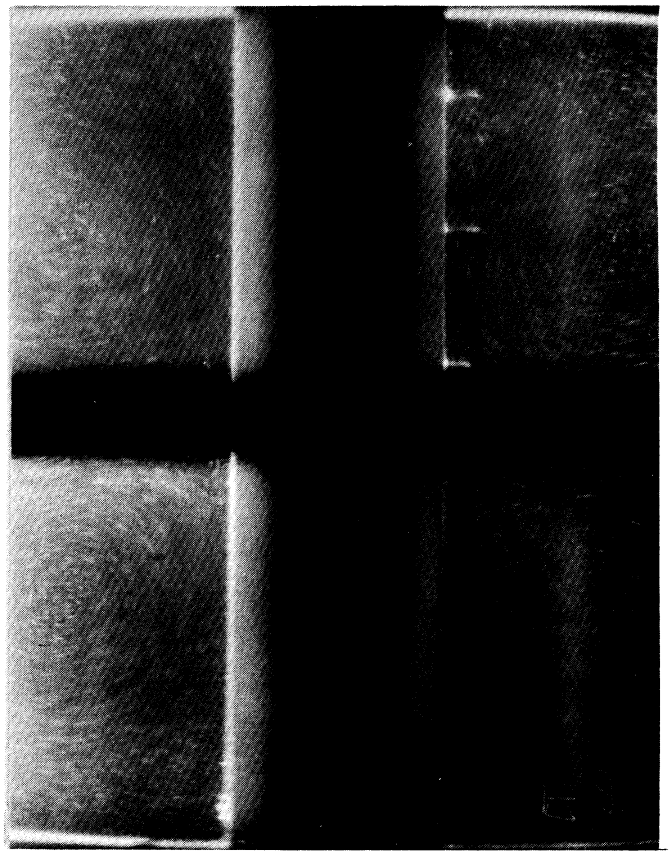

(d) 15 Minutes

Figure 21. Sequence of Fluid Patterns After Various Time Intervals of Current Flow with the Unit Horizontal and a Fluid Current of 5 Amps.

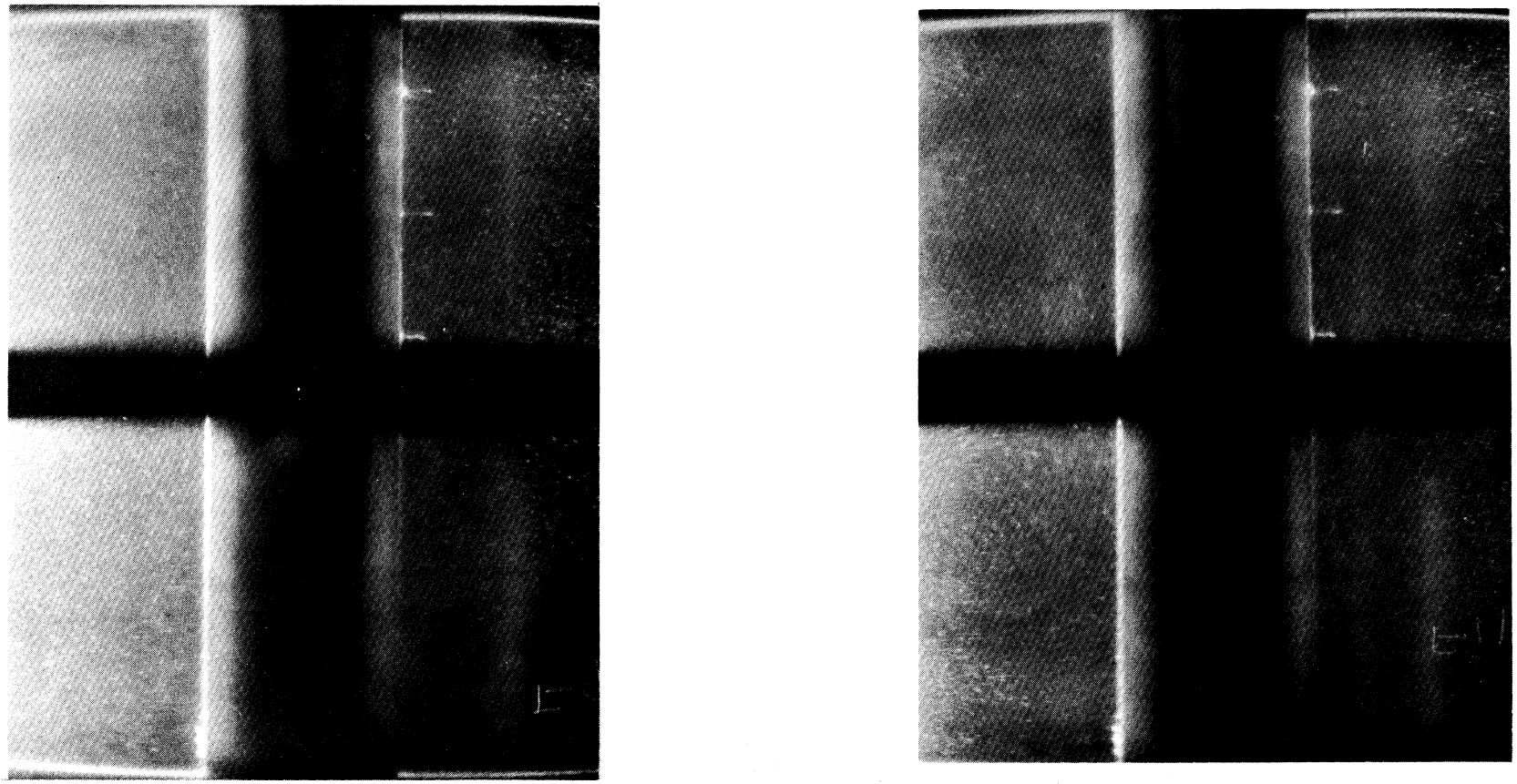

(a) (b)

Figure 22. Sequence of Fluid Patterns After Various Time Intervals of Current Flow with the Unit Horizontal and a Fluid Current of 2 1/2 Amps.

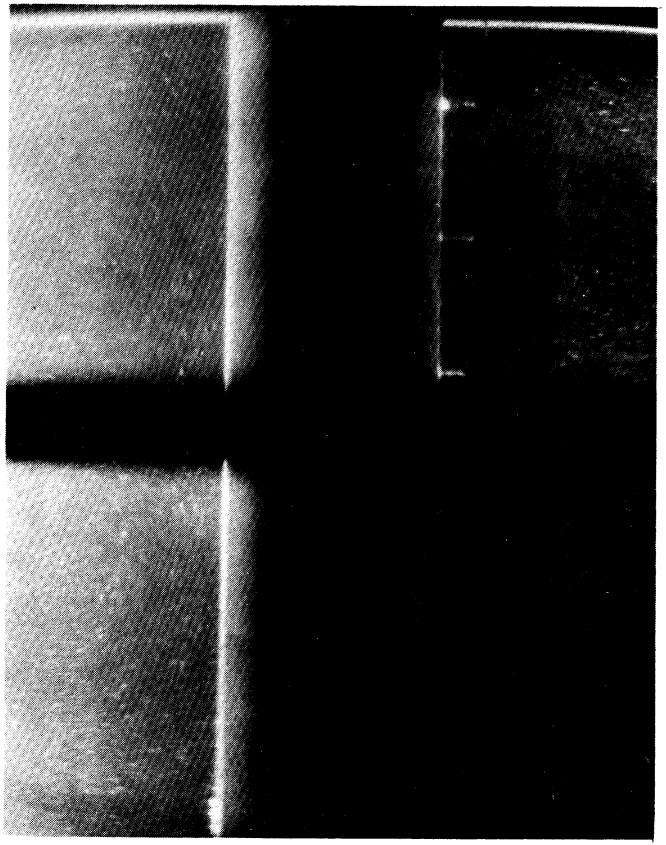

(c)

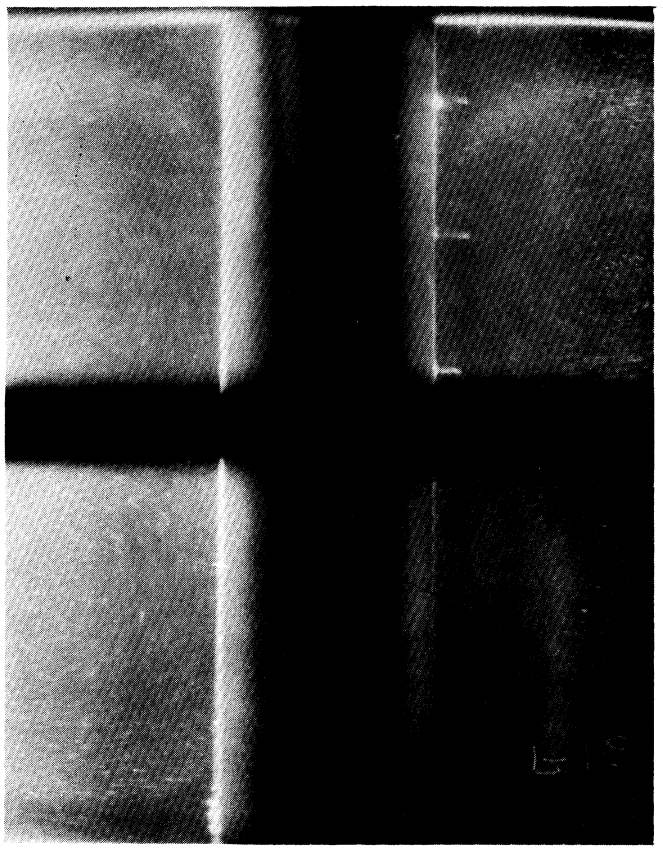

(d)

Figure 22. Sequence of Fluid Patterns After Various Time Intervals of Current Flow with the Unit Horizontal and a Fluid Current of 2 1/2 Amps.

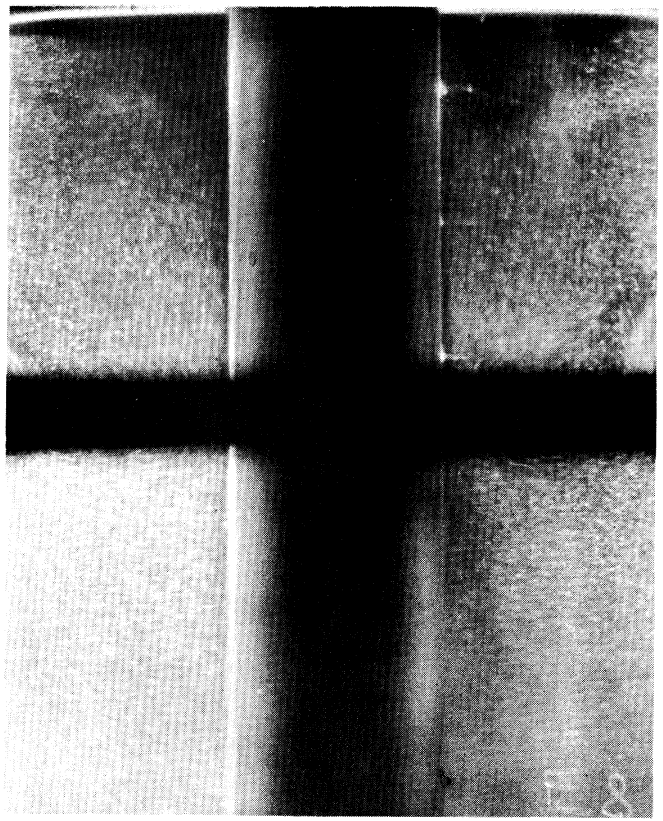

30 Seconds (a)

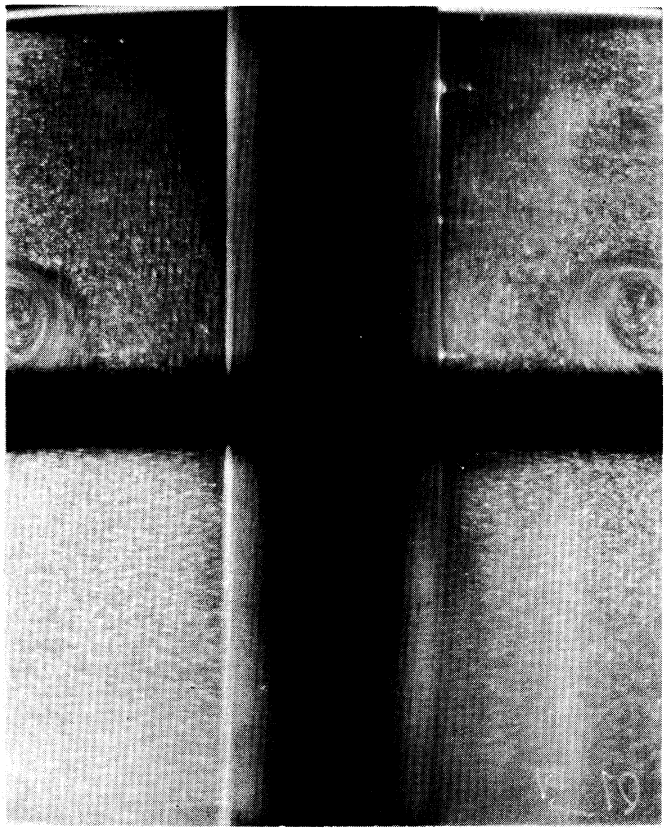

(b) 1.5 Minutes

Figure 23. Sequence of Fluid Patterns After Various Time Intervals of Current Flow with the Unit Vertical and a Fluid Current of 5 Amps.

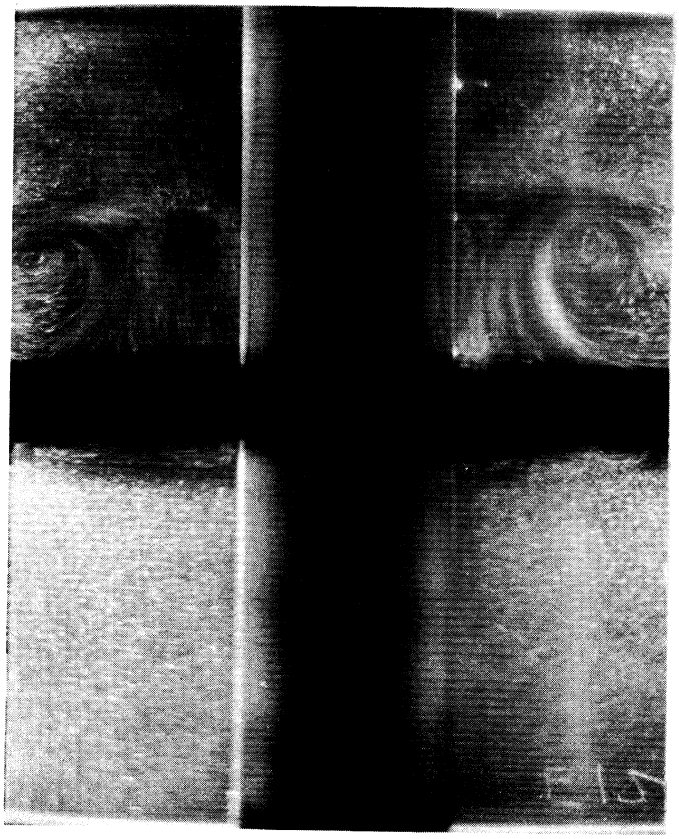

(c) 4 Minutes

Figure 23. Sequence of Fluid Patterns After Various Time Intervals of Current Flow with the Unit Vertical and a Fluid Current of 5 Amps.

indicated. It was obvious that convective effects remained predominant when the unit was vertical but these results strengthened the conviction that the motion observed when the unit was horizontal resulted primarily from electromagnetic effects.

The only temperature information that appeared meaningful pertained to the maximum differential that occurred between the hole and the furthest solid-liquid interface from the hole. In the vertical position, this would be the top copper electrode-liquid interface whereas in the horizontal position this would be the interface between the liquid and the inner wall of the large plastic outer cylinder. The maximum temperature differences found were on the order of 15°F, but as this would occur during the end of a test run it was again obvious that very small temperature differences led to convective motion since this was observed almost immediately after the fluid current was turned on. It was decided at this stage to forsake any further temperature measurements since, except for providing differential indications, they did not appear amenable to more refined analysis.

The final phase of experimentation was conducted with a test unit that somewhat approached the type possessing a small wall perturbation. This was accomplished by enlarging the center hole in the separator plate to 10 7/16 inches. It may be recalled that the inside diameter of the large plastic tubes was about 11 3/16 inches, thus a 3/8 shoulder was created at the junction of the separator plate and plastic tubes. Because larger fluid currents were anticipated, the connecting wires in the fluid current were all replaced with heavier

copper leads whose continuous current rating was 50 amps. In Figure 16 one such lead may be seen as it was connected to the bottom electrode and taped to the heavy generator cable so as to be reasonably perpendicular to the electrode.

For future reference it is here emphasized that the enlargement of the hole and replacement of leads in the fluid circuit were the only physical changes made at this time.

Fluid currents of 25, 32, 36, 40, and 50 amperes were used for 5 independent tests, each conducted for a total time of 15 minutes. The individual photographs taken after 15 minutes had elapsed are shown in sequence in Figures 24a to 24e. Four quadrant symmetry no longer prevailed, even when tests were conducted at shorter time intervals. It was observed that chemical activity at the anode was quite pronounced with currents of 36 to 50 amps in the fluid. This activity resulted in large particles, sometimes in a sheet-like form, falling from the anode. As they passed downward through the lighted region of fluid, they drastically altered the existing flow pattern. At the cathode, the formation of bubbles was noted.

Although this chemical action affected the flow patterns, it cannot completely explain the non-symmetry since on certain occasions the patterns were symmetrical on opposite sides of the separator plate but not on opposite sides of the axial tube. It was thought that perhaps convective effects might have caused such results, consequently, tests were conducted with the unit horizontal and no current in the rod. This would cause both the convective and

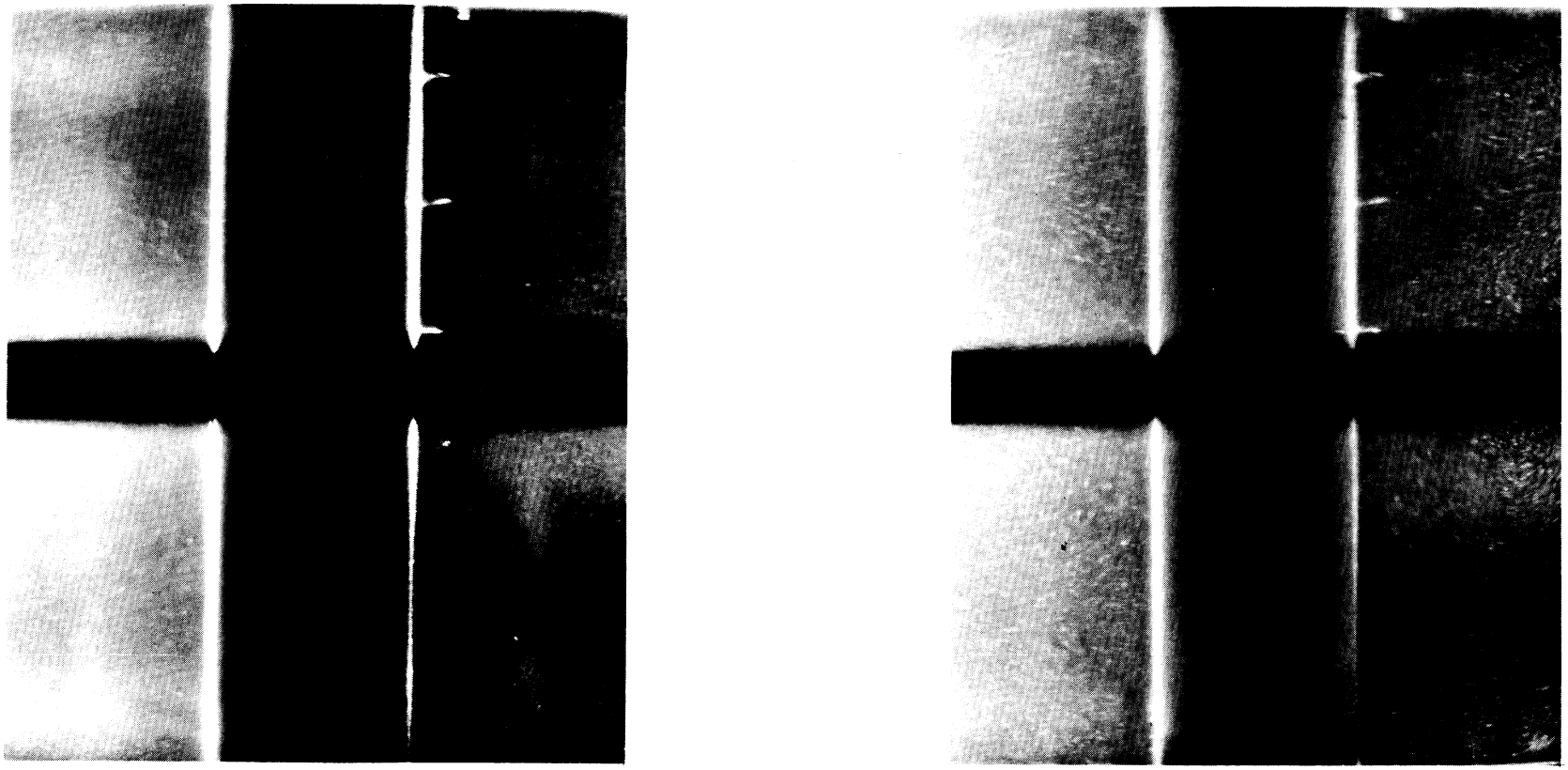

(a) (b)

Figure 24. Fluid Patterns After 15 Minutes of Current Flow with the Unit Horizontal and with Various Fluid Currents.

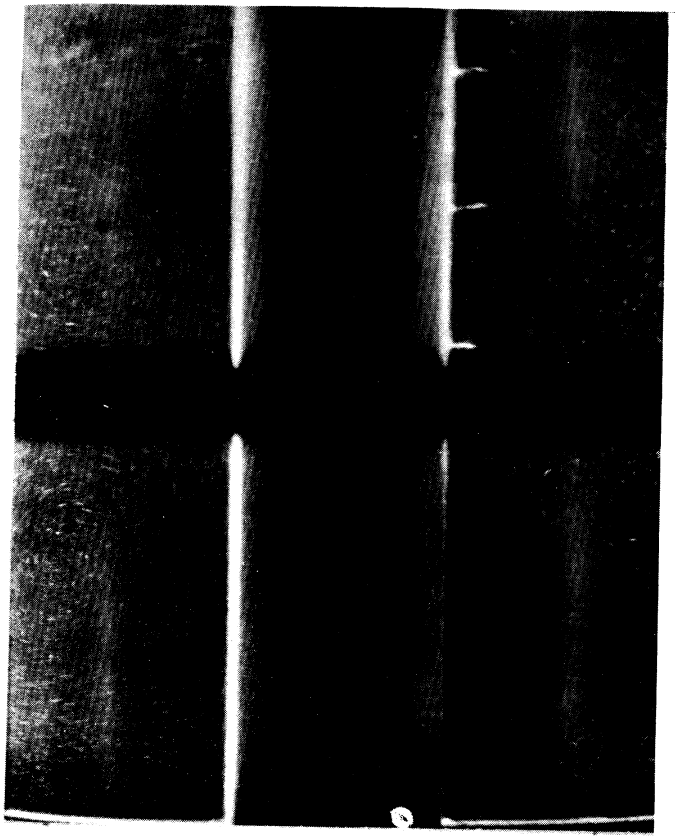

(c)

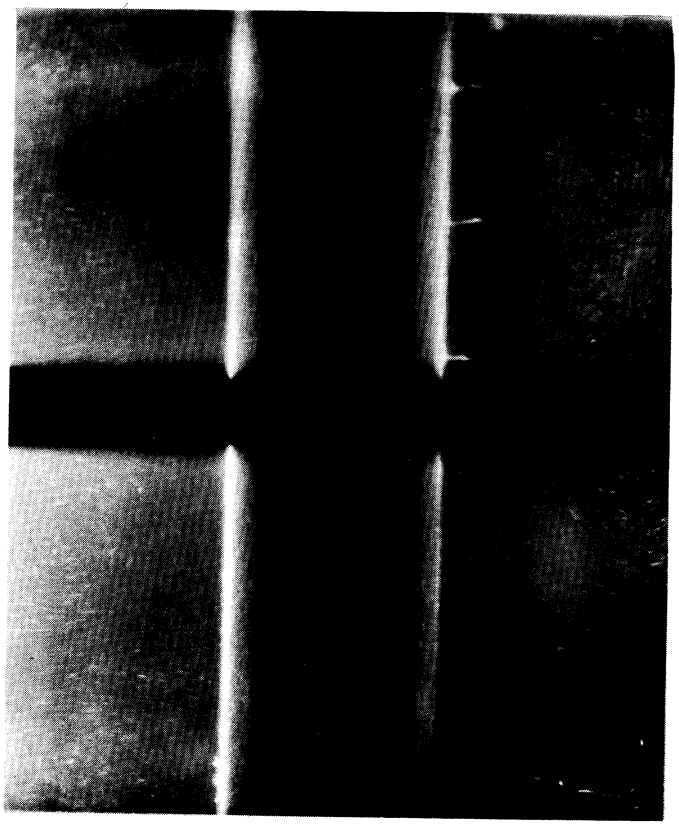

(d)

Figure 24. Fluid Patterns After 15 Minutes of Current Flow with the Unit Horizontal and with Various Fluid Currents.

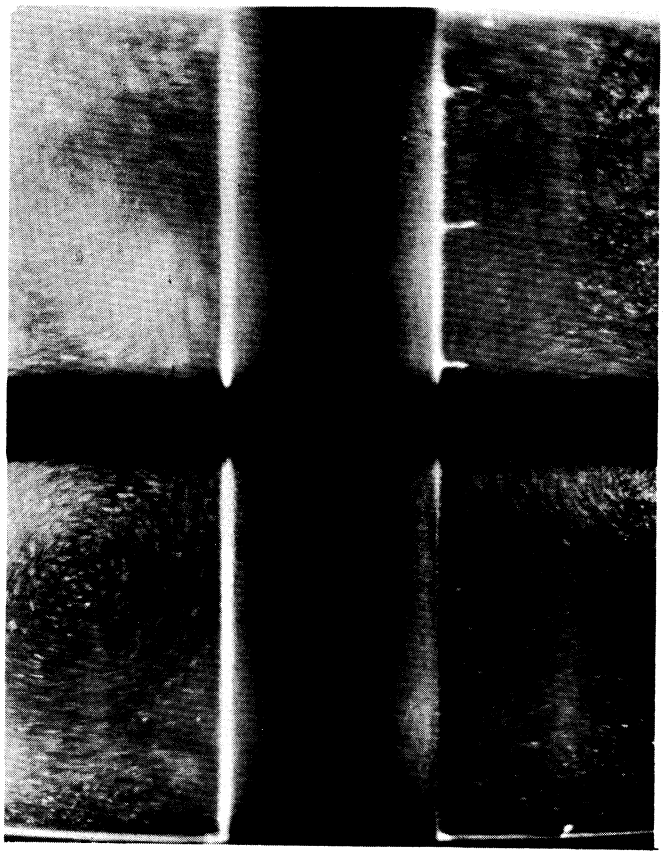

(e)

Figure 24. Fluid Patterns After 15 Minutes of Current Flow with the Unit Horizontal and with Various Fluid Currents.

electromagnetic effects to be solely dependent upon the fluid current. If anything, the relative convective influence would be stronger than in the preceeding tests since the electromagnetic effects due to the rod current would be eliminated. Figures 25a and 25b resulted after applying fluid currents of 15 and 30 amps respectively for a time of 15 minutes. These would seem to confirm that convective motion, which was observed to cause a circulation around the inner boundaries of the test unit, did not significantly contribute to the flow patterns observed in the lighted plane.

Several sources were considered in seeking the cause of non-symmetry, the first being the true physical symmetry of the unit itself. As mentioned previously, enlargement of the hole in the separator plate was one of the two changes completed since the existence of symmetry had prevailed. This hole had been machined to a concentricity within several thousandths of an inch of the previous hole, so this alteration was ruled out as a source. Since care had been exercised in machining all of the individual components accurately, including the attainment of perpendicularity between the electrodes and center rod, it seemed apparent that the structure of the model was not a contributing factor. Such a judgement appeared valid since the same unit with a smaller center hole produced symmetrical patterns in previous tests.

Next, all external wires and cables were checked to make certain that the magnetic fields existing around these components when they carried current would have little if any influence on

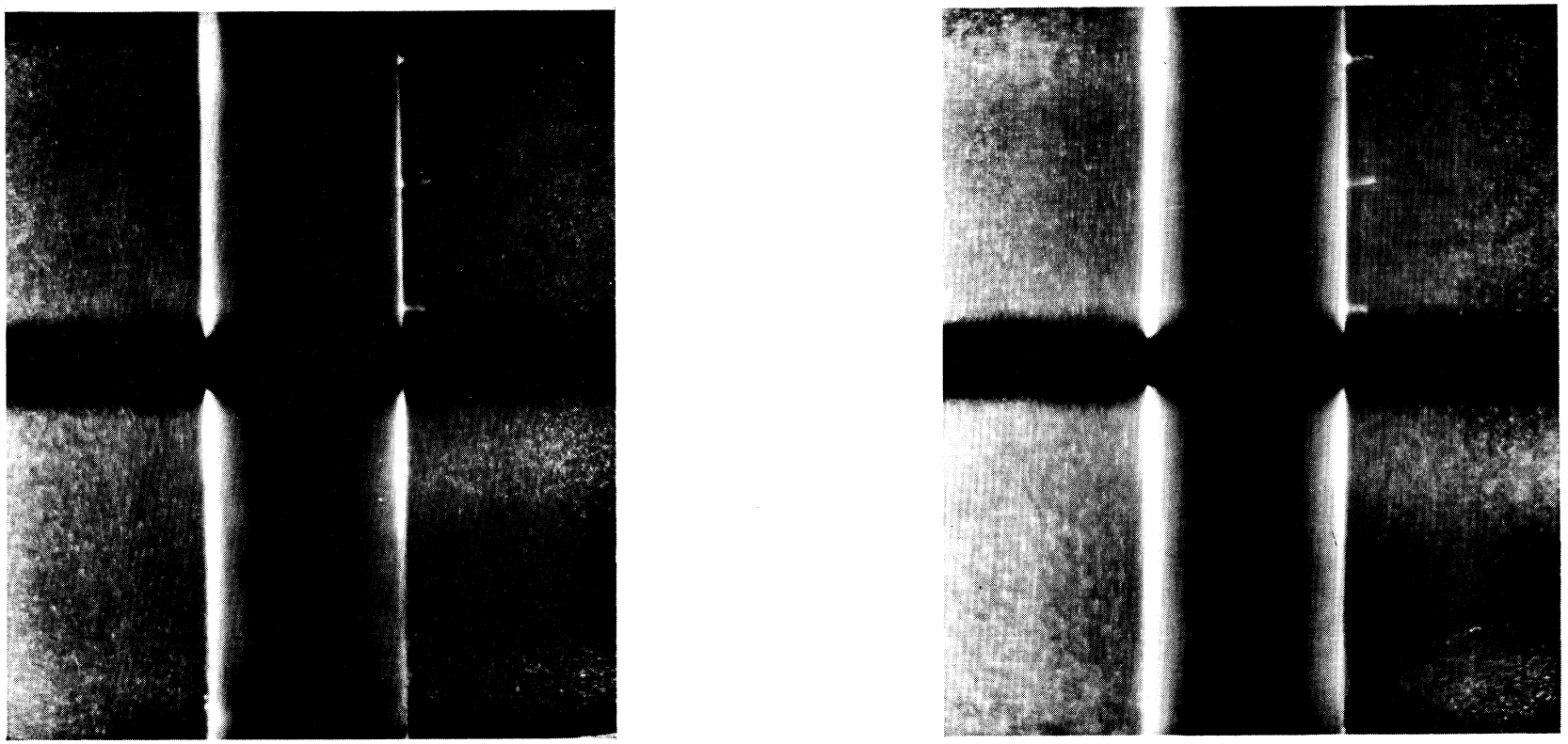

(a) (b)

Figure 25. Fluid Patterns After 15 Minutes of Current Flow with the Unit Horizontal, the Rod Current Turned off, and Fluid Currents of 15 and 30 Amps Respectively.

fluid motion. It was concluded that these components could not significantly contribute to the result in question.

Although electrochemical effects had some influence, as indicated previously, they could not be held solely responsible.

The presence of the thermocouples should have a negligible affect on the fluid patterns, but to verify such an attitude, all thermocouples were removed from the unit. Later findings indicated that the removal of these wires caused no noticable changes to occur.

Finally, the question of how truly horizontal the lighted plane was came under consideration. Levelling had been defined with reference to exterior surfaces, so it was possible that this lighted region was not exactly horizontal. No means were available to verify this condition with the present structure, so it appeared that the best course open was to physically alter the existing position of the unit and see if any changes occurred. Shims were placed under one of the pillow blocks thereby tilting the lighted plane about 1 degree from its previous position. One test was conducted with a fluid current of 30 amps and a rod current of 300 amps, both in the same direction. A sequence of pictures was taken during the 15 minute run and these are shown in Figures 26a to 26f. These were compared with the set that produced Figure 24b since test conditions were nearly identical. Some slight changes in patterns were noted but how conclusive such evidence becomes is open to conjecture. It must be admitted that the susceptibility of the fluid patterns to change with minor adjustments of the test unit is offered as a posibility, but a positive explanation remains unanswered.

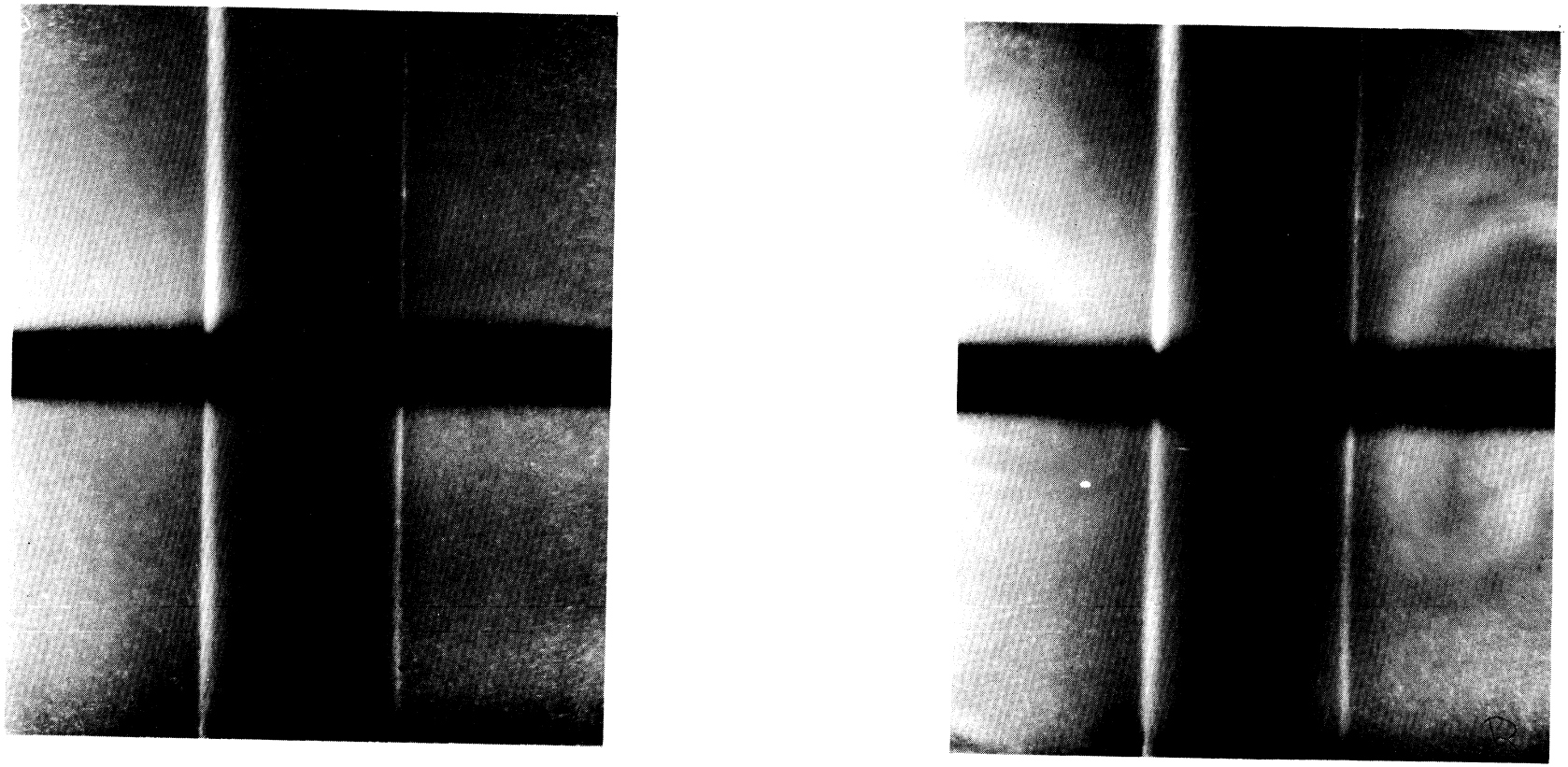

30 Seconds (a) (b) 1.5 Minutes

Figure 26. Sequence of Fluid Patterns After Various Time Intervals of Current Flow with the Unit Horizontal and Shimmed at one End, and a Fluid Current of 30 Amps.

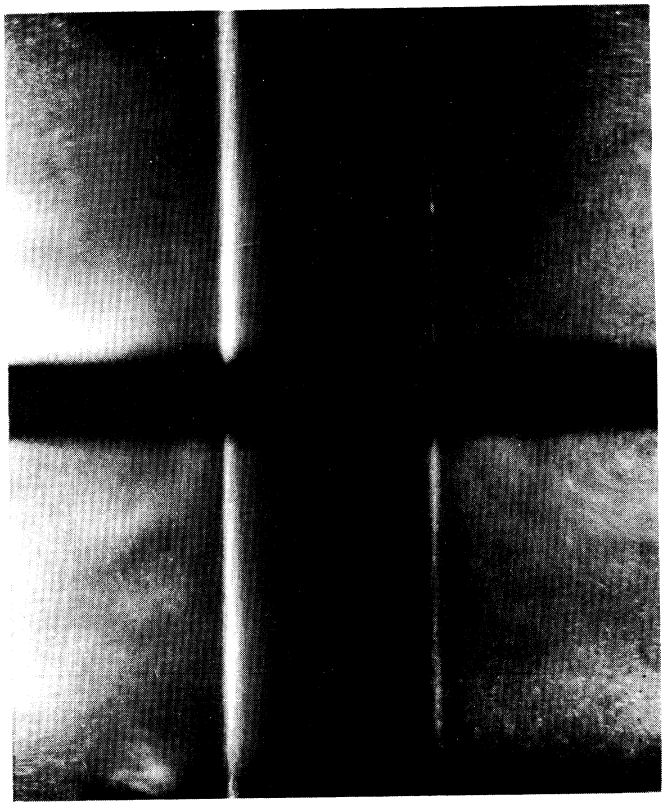

2.5 Minutes

(c)

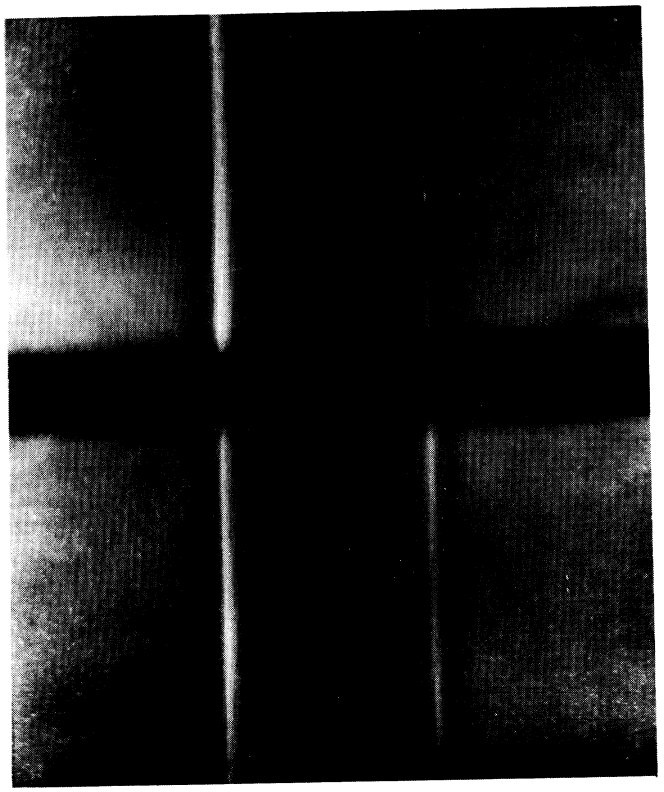

4 Minutes

(d)

Figure 26. Sequence of Fluid Patterns After Various Time Intervals of Current Flow with the Unit Horizontal and Shimmed at one End, and a Fluid Current of 30 Amps.

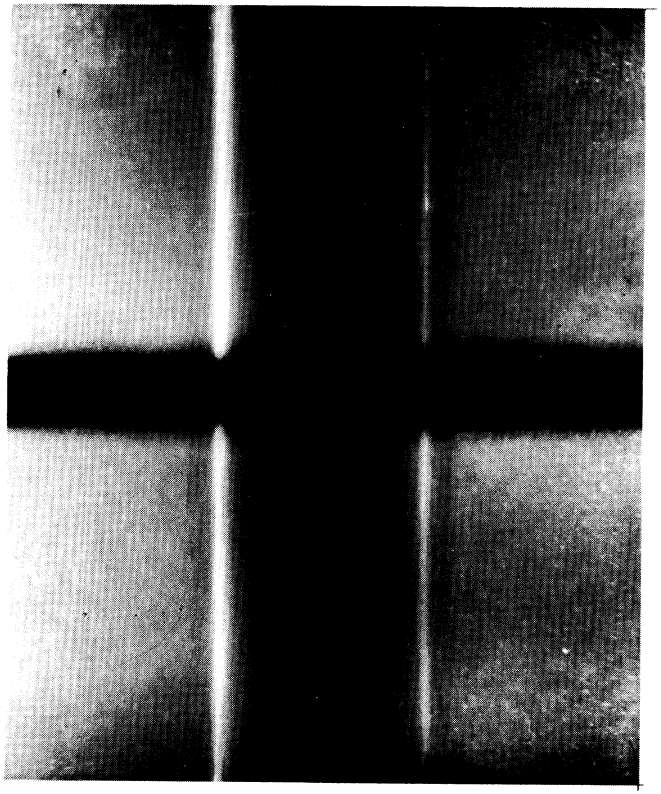

6 Minutes

(e)

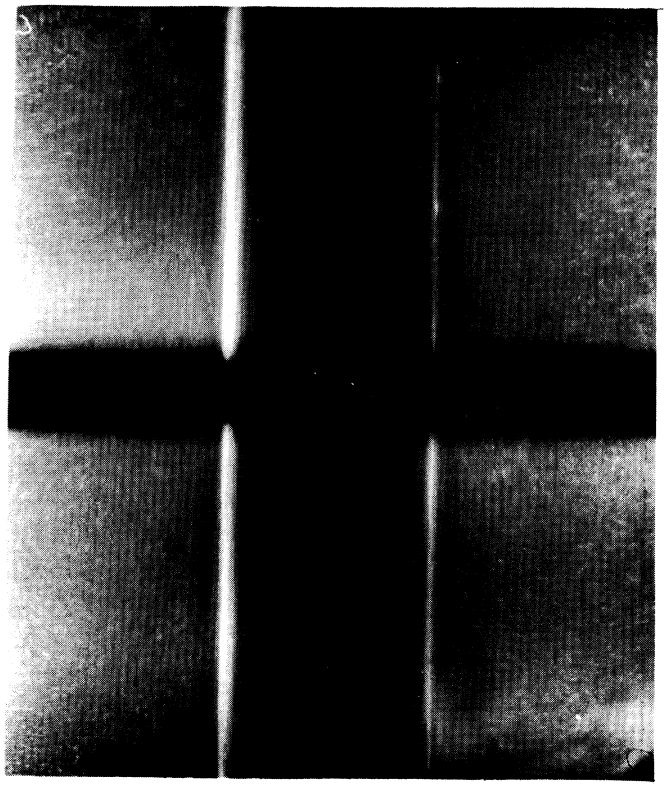

12 Minutes

(f)

Figure 26. Sequence of Fluid Patterns After Various Time Intervals of Current Flow with the Unit Horizontal and Shimmed at one End, and a Fluid Current of 30 Amps.

A final test was conducted with the unit vertical, a fluid current of 25 amps, and a rod current of 300 amps. The purpose of this test was to determine the severity of convective effects with a unit of almost constant cross-sectional area. Figures 27a to 27d show the sequence of results. Although it is difficult to judge from these pictures, the degree of motion in the top quadrants was still decidely greater then in the lower quadrants.

30 Seconds

(a)

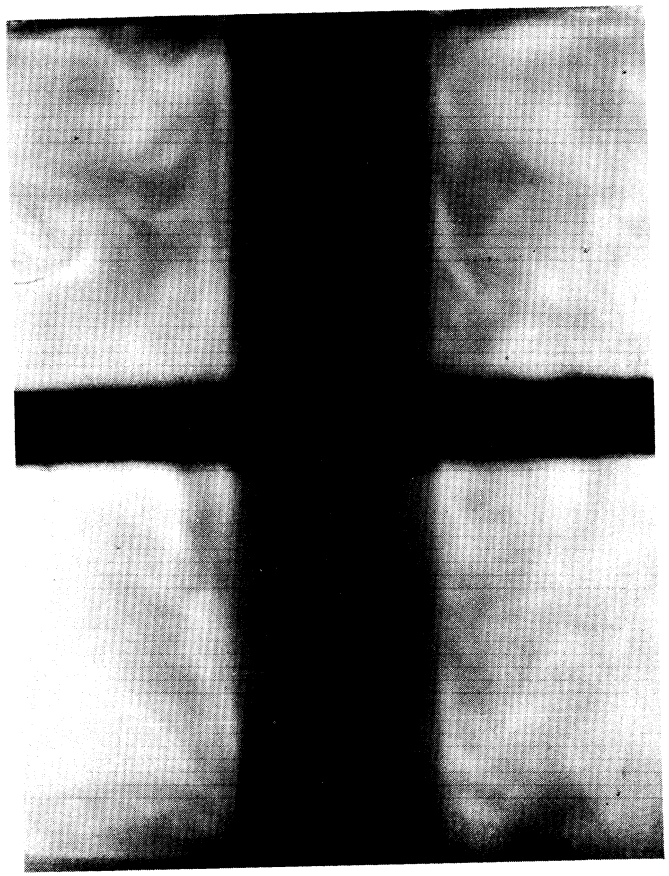

5 Minutes

(b)

Figure 27. Sequence of Fluid Patterns After Various Time Intervals of Current Flow with the Unit Vertical and a Fluid Current of 25 Amps.

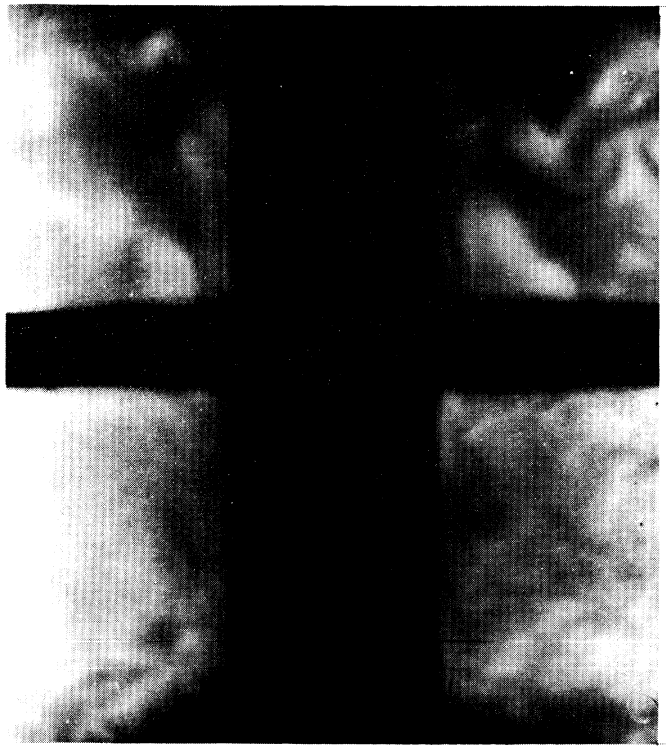

9 Minutes

(c)

15 Minutes

(d)

Figure 27. Sequence of Fluid Patterns After Various Time Intervals of Current Flow with the Unit Vertical and a Fluid Current of 25 Amps.

III. COMPARISON OF ANALYTICAL AND EXPERIMENTAL RESULTS

3.1 Explanatory Remarks

During the later stages of the experimental work, it was learned that Uberoi and Chow[29] had completed an analytical solution for MHD flows between concentric tubes. It is the intent of these authors to submit this work for publication in the near future and they have consented to allow their findings to be used and discussed in this thesis. As in Uberoi's[24] previous work, the concept of small wall perturbations has been utilized for both inner and outer tubes. The particular case wherein the inner tube would be straight walled while the outer tube wall was slightly perturbed finds some similarity with the unit employed in the experimental work of section 2.8. Therefore, it seemed that a comparison of predicted and measured velocities might prove interesting. Numerous differences, both physically and in regard to assumptions, prevailed between the analytical and experimental works, consequently, it was not intended that the experimental study be viewed as an accurate means of checking the analysis.

3.2 Variations Between the Analysis and Experiment

In addition to physical differences between the analytical model and the experimental one, certain assumptions employed in the analysis were not satisfied during the experimental work. Before proceeding with any quantitative comparisons, a listing of assumptions with pertinent comments should prove helpful.

1. End effects are ignored in the analysis by assuming tubes of infinite length. This condition was not duplicated with the experimental model.

2. Fluid properties are assumed constant in the analysis. Certainly the fluid density was not constant during experimentation as evidenced by the convective effects.

3. The analytical model considered an outer tube whose wall varied in the form of a cosine wave about a mean radius, thus, the wall was periodic in the z direction. The experimental model involved a straight wall that changed an abrupt 90° at the separator plate.

4. Both models cause curvature of the current lines but differ as to the geometry which produced this curvature.

5. The ratio of maximum wall amplitude to mean radius was assumed to be $\ll 1$ in the analysis. Considering similar parameters in the experimental model, this ratio was 0.034.

6. Analytical solutions were based upon steady state conditions. It would appear that the velocity approached a steady state condition during the 15 minute time interval used during experimentation.

7. The analysis employed the assumptions that convection of the magnetic field and the convective terms in the equations of motion were negligible. These assumptions are discussed further in the Appendix.

In view of statements 1 and 3 above, it becomes apparent that the design of the experimental model was not completed with the

intention of providing an accurate quantitative check with existing theory.

3.3 Procedure for Obtaining Velocity Measurements

The photographs in Figures 24a to 24e were selected for comparison with theoretical predictions since they resulted from the test unit that most closely matched the analytical model. Conditions approaching steady state motion seemed to exist when these pictures were obtained and they involved a reasonable range of fluid currents which served as the independent variable. To indicate any differences that would result if the concept of small wall perturbations were abandoned, it was decided to include the results that occurred when the hole in the separator plate was 7 1/2 inches. Figures 18f, 21d, and 22d were selected since they were the last picture per set and most closely approached a steady state condition. Fluid currents pertinent to these three pictures were 10, 5, and 2 1/2 amps respectively. Thus 8 photographs were used to obtain velocity measurements, 5 for a hole size of 10 7/16 inch and 3 for a 7 1/2 inch hole.

Since the 4 quadrants in each of the 8 pictures were not always symmetrical a judgement had to be instituted regarding which quadrant most probably reflected the motion due principally to electromagnetic effects. An additional consideration involved the photograph sharpness and clarity where one of several quadrants would seem to be acceptable.

For Figures 18f, 21d, and 22d, the upper right quadrant was chosen, while for Figures 24a to 24e the lower left quadrant was used.

Besides consideration of picture contrast, each of these regions typified the pattern form predicted analytically, so it seemed they most closely represented a true electromagnetic effect.

A 2x2 inch mounted slide was prepared from each area of interest. These were then individually projected on a blank sheet of paper by using a standard 35 millimeter slide projector. From each slide, numerous particle traces were then reproduced on the sheet of paper. One sheet contained all of the clearly visible traces of the 3 slides pertaining to the 7 1/2 inch hole while a second sheet was devoted to those relating to the 10 7/16 inch hole. To account for visual distortions caused by curvature of the test unit and by the fluid itself, a grid system of known dimensions was produced on a piece of clear plastic. This was placed inside the test unit to correspond with one of the quadrants and upon filling the unit with the copper sulphate solution, a photograph was obtained. Figure 28 shows the result. This grid area was also reproduced in the form of a 2x2 inch slide and when projected and traced upon the sheets containing the indications of particle motion, an accurate dimensional scale, both radially and axially, resulted. All tracing was accomplished with the same focal setting of the projector, thus, the magnified images were all related to the same scale factor.

To show the degree of detail that was prevalent, an enlargement of one of the quadrants that was converted into a slide is shown in Figure 29. By comparing this figure with the 8 photographs that contain all 4 quadrants (Figures 18f, 21d, 22d, and 24a to 24e), one can immediately see that the true detail of particle traces was much

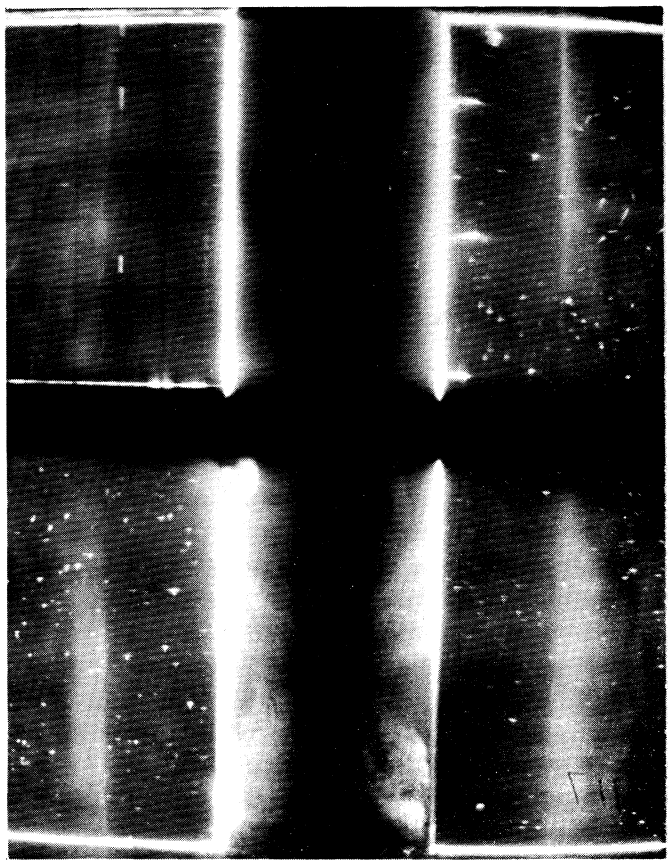

Figure 28. Grid Pattern for Correction of Measurements.

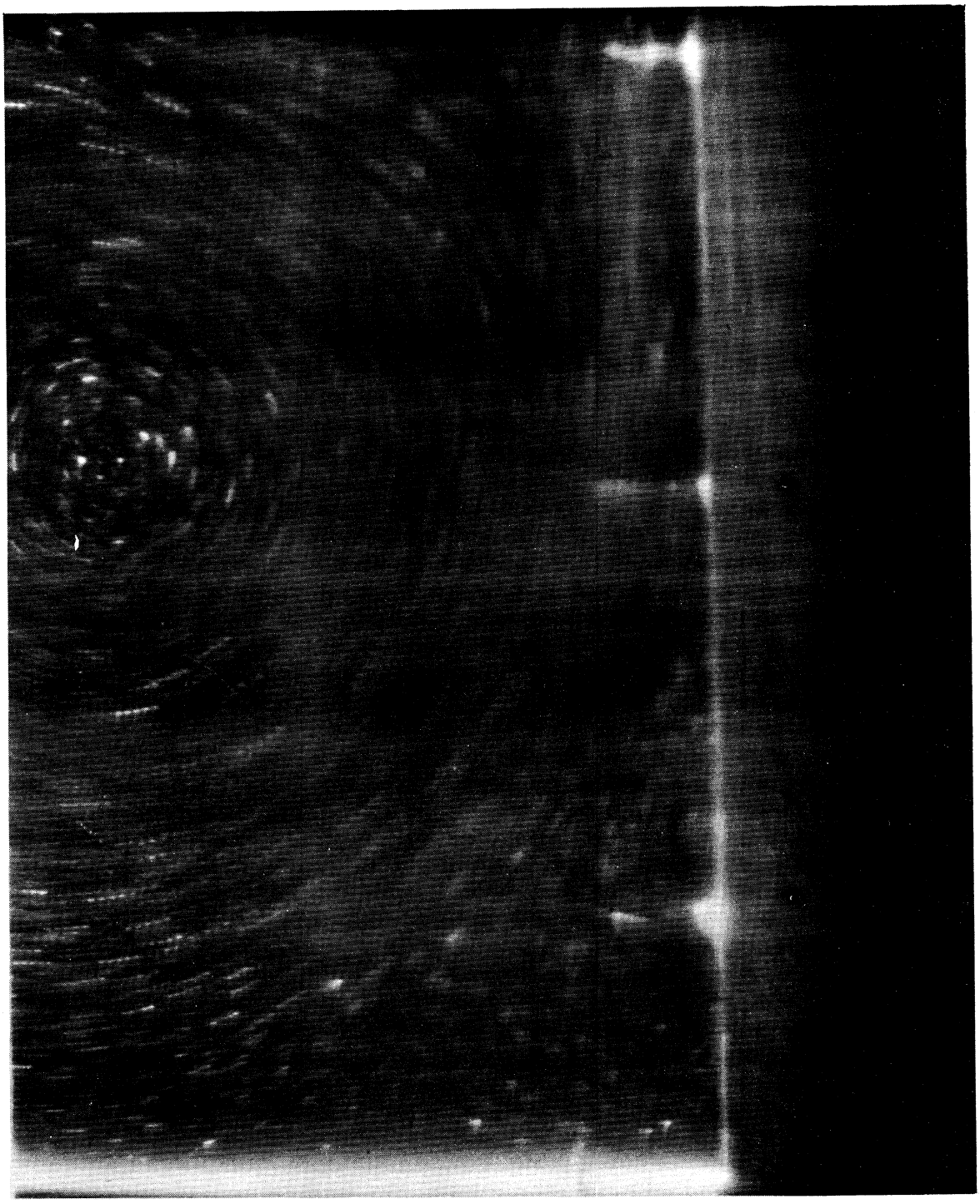

Figure 29. Enlargement of one Quandrant of Figure 18f.

sharper than might be judged from the smaller pictures. Reproduction of photographs for the final form of this thesis plus the care in development of the prints both tend to diminish the clarity that existed on the slides.

Once all tracing was completed, the traces were studied to select coordinate points of interest. Obviously, one could not expect a trace from all 8 slides to fall on one exact point since this would call for a particle to be at that spot when the individual pictures were taken. However, several regions did exist where the largest true deviation of any trace, from the coordinate point of interest, was 3/16 inch. In addition, other traces in that area indicated that the measurements which were made were quite descriptive of the average velocities at the chosen coordinate point.

3.4 Predicted Versus Measured Results

Figures 30a to 30c show the comparison of velocities at three different coordinate points, the true radial and axial components of these points being given. The solid line resulted from a plot of points obtained analytically. Since the Appendix includes the full mathematical presentation, further interest in the analysis itself should be directed to the Appendix. It should be noted that total velocities, rather than radial and axial components, have been plotted.

The experimental values for the large hole, symbolized by an x, are consistently lower than those predicted analytically. In view of the differences between the analytical model and the experimental one, the fact that exact agreement did not result should not be surprising. Comparing the actual and predicted values shows that a very

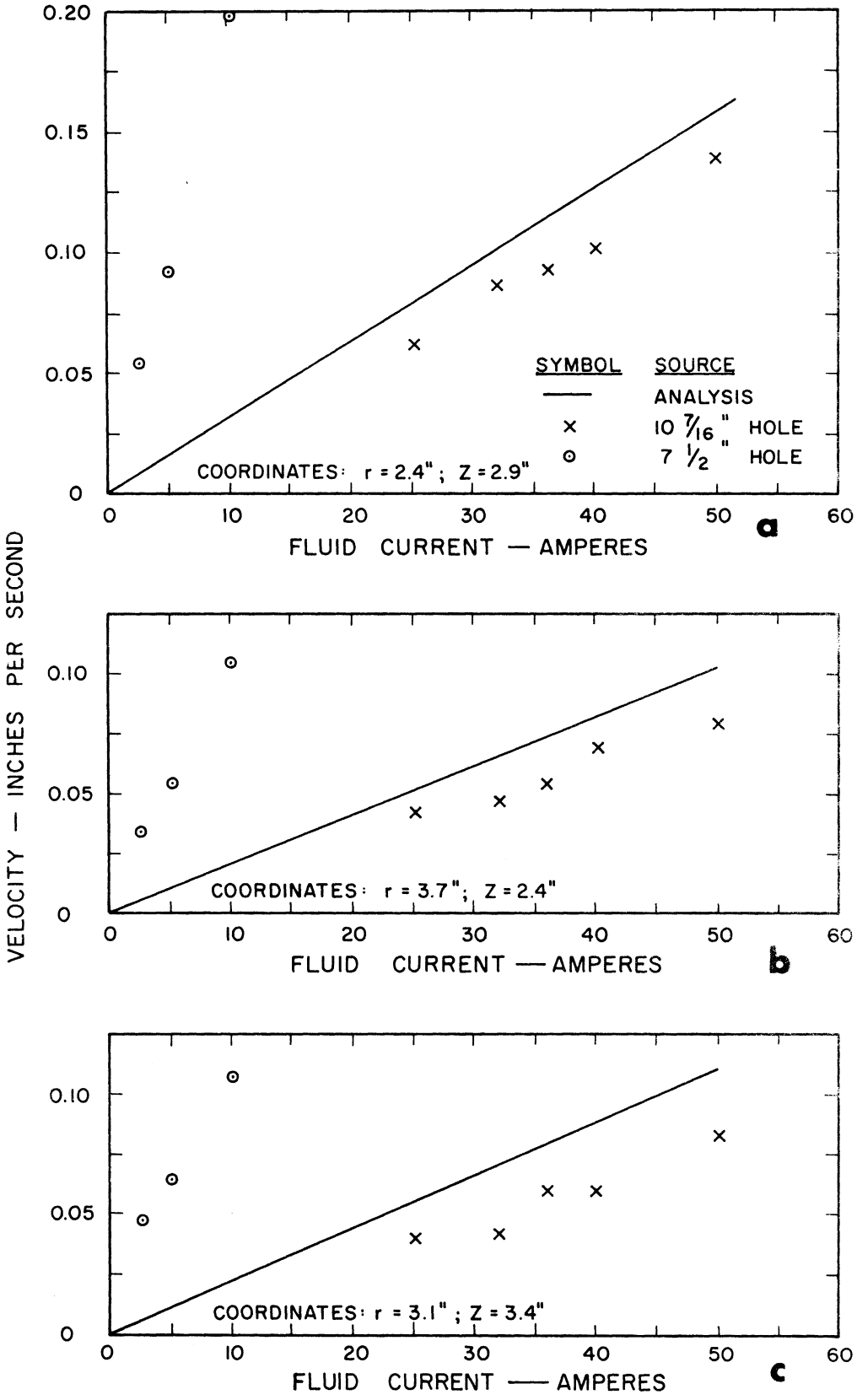

Figure 30. Analytical Versus Experimental Values of Velocity Versus Fluid Current for Three Different Coordinate Points.

good agreement results from an order of magnitude viewpoint. This would indicate that the theoretical predictions seem quite reasonable. Just what factors cause the experimental values to be lower than those predicted cannot be defined with certainty due to the differences that existed between the two models.

As would be expected the velocities resulting from the 7 1/2 hole fall well above those for the 10 7/16 hole. This can be readily explained since the current density, for a given fluid current, would be much larger at the smaller hole and electromagnetic effects increase with current density. The reason why fluid current rather than current density was used as the independent variable in these plots was due to uncertainty as to how best define current density when the smaller hole was being considered since a "mean" radius here could not be realistically employed.

Figures 31a and 31b compare the predicted and measured values of the coordinates of the stagnation point that occurs at the center of the circulatory motion. Analytically, the value of these points is unaffected by fluid current and is discussed in some detail in the Appendix. Although the measured values of each coordinate show a reasonable consistency, they indicate that the point of stagnation falls closer to the area of current convergence and at a greater radial distance than predicted analytically. Again this must be attributed to discrepancies between the models employed. One contributing factor would be the difference in physical structure of the units. To illustrate this Figures 32a and 32b show drawings of three dimensional field maps produced by graphical trial-and-error methods.

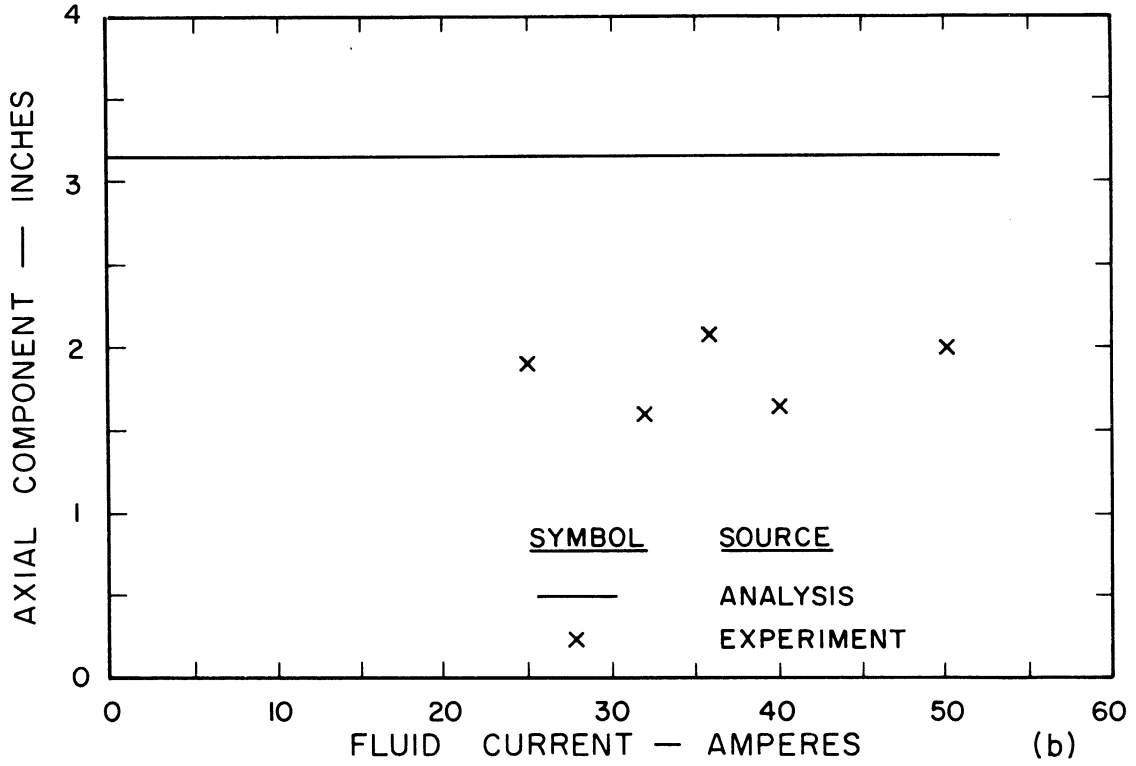

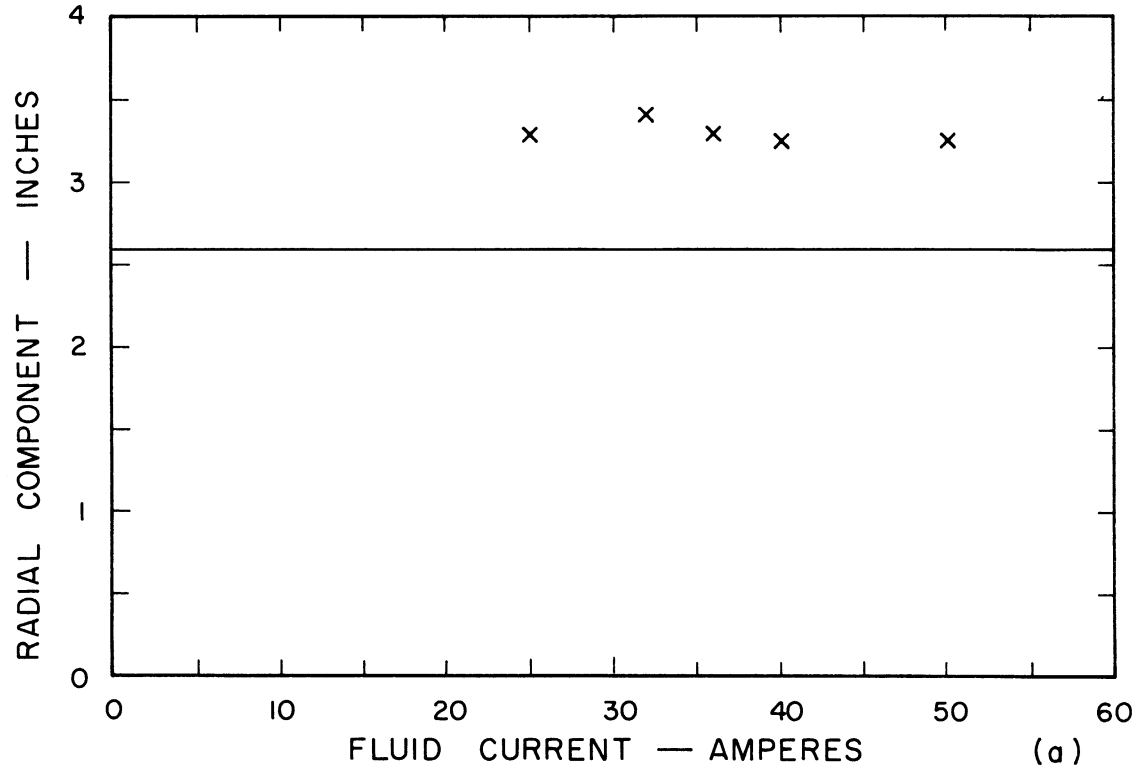

Figure 31. Analytical Versus Experimental Values of the Stagnation Point Coordinates.

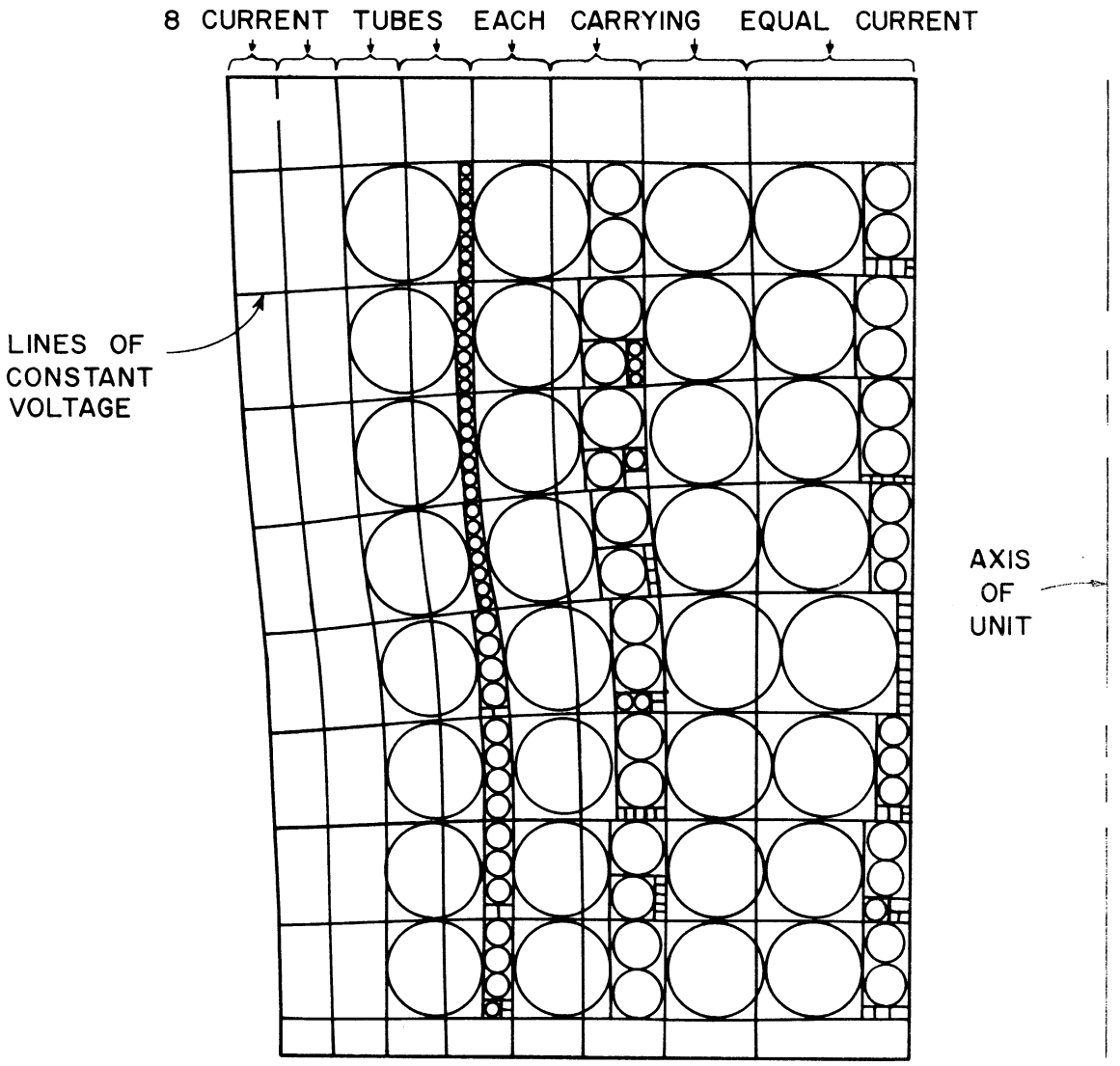

Figure 32a. Three Dimensional Field Map for the Geometric Shape of the Analytical Model.

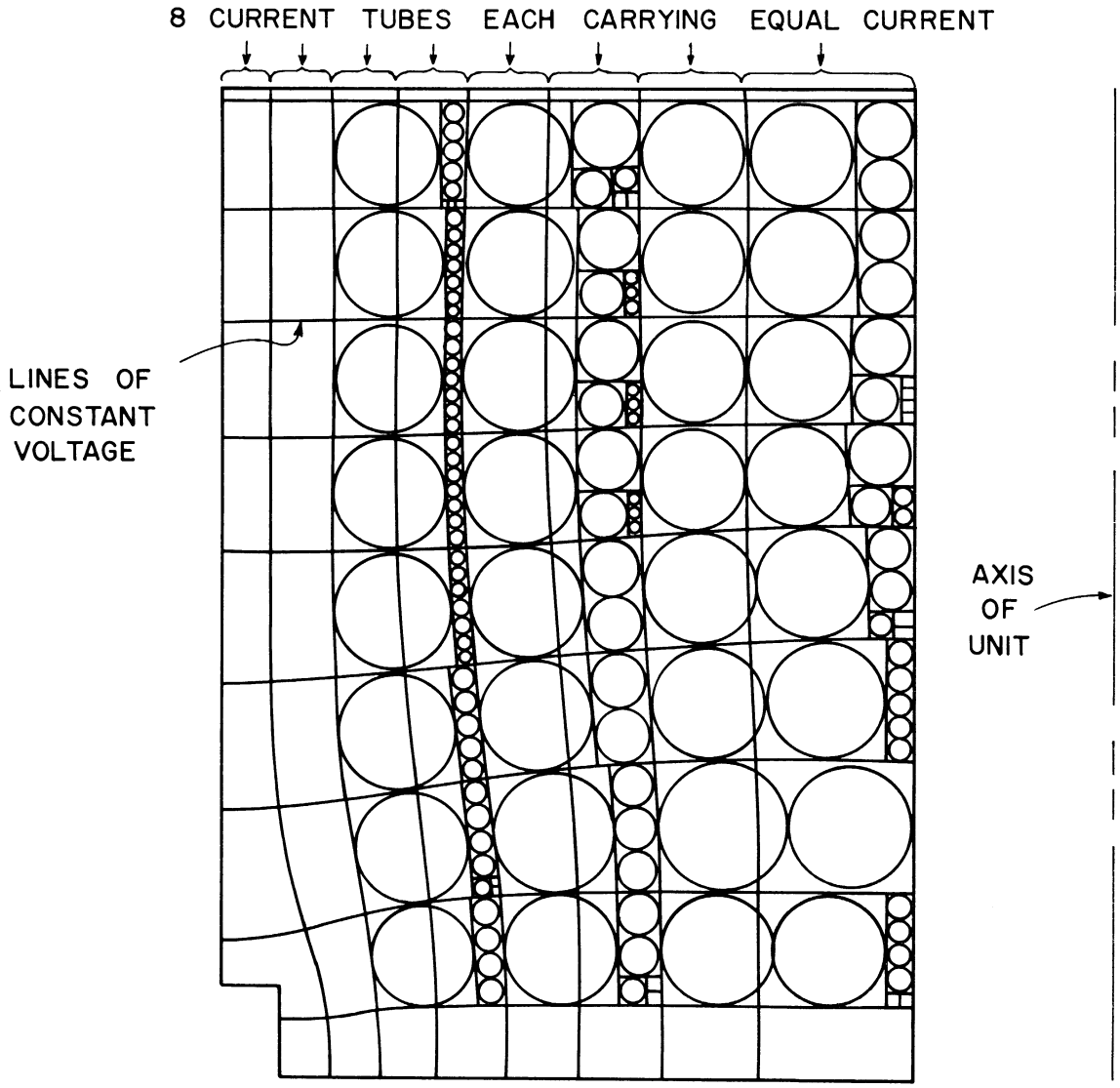

Figure 32b. Three Dimensional Field Map for the Geometric Shape of the Experimental Model.

References 30 to 35 may be consulted to provide the underlying theory of the construction techniques employed in such graphical constructions. Due to symmetry of the models employed, only one quadrant has been shown since this is sufficient for the pruposes here. Equipotential lines, current tubes, and construction details are included on these figures. It should be noted that neither of these is a perfect map. To attain such an end, the remainders of each current and voltage tube should be identical from one curvilinear square to the next and the spacing of equipotential lines should show uniform voltage increments. However, the limited accuracy of these two maps still provides the result sought which was to indicate visually why the physical structures of the models would cause some deviations between analytical predictions and experimental measurements. The use of fluid mappers, discussed in references 30 to 35, would probably lead to still better maps compared to those produced by graphical methods.

Each current tube in either Figure 32a or 32b carries 1/8 of the total current flowing through the fluid as indicated on the figures. The differences between these two maps is most pronounced in the region of the lower left hand corner.

As a means of further indicating why different results should be expected with these two models, Figures 32c and 32d were constructed. These are reproductions of Figures 32a and 32b with construction details eliminated and with force vectors, drawn to scale, shown at selected points. The magnitudes of these forces were determined solely on the basis of electromagnetic effects by considering a small element located at the center of selected curvilinear squares. By assuming that current

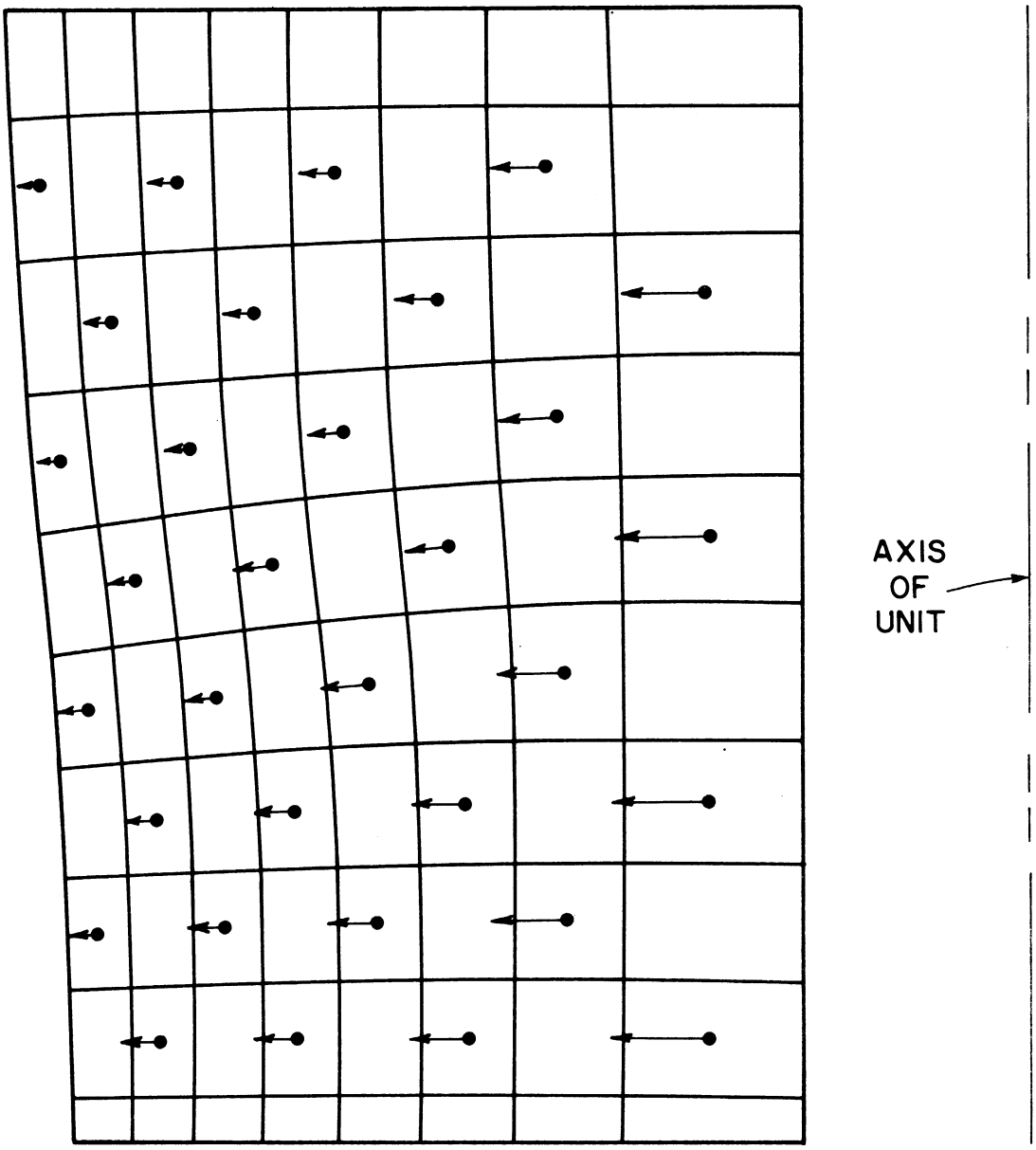

Figure 32c. Field of Force Vectors, Due to Electromagnetic Effects, Positioned on the Field Map for the Analytical Model.

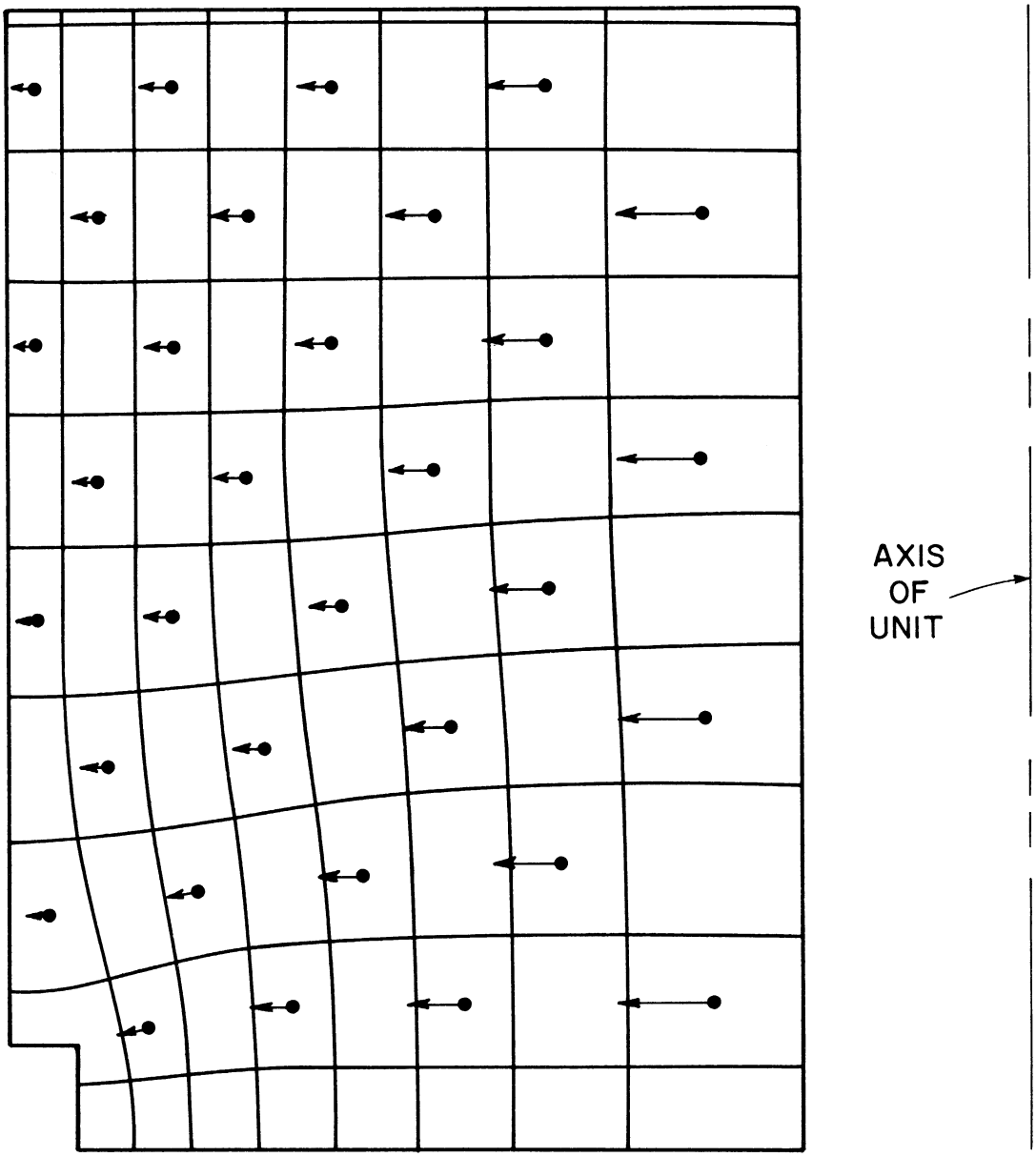

Figure 32d. Field of Force Vectors, Due to Electromagnetic Effects, Positioned on the Field Map for the Experimental Model.

density was directly proportional to area, the current flowing through each elemental volume was determined. The magnitude of magnetic flux density at each element was considered to be inversely proportional to the radial distance between the centerline of the unit and the centerline of the elemental volume under consideration. Based upon these assumptions, the relative magnitude of each force was calculated as in section 2.3. The direction of each force was plotted perpendicular to the closest line of current.

Figure 33 more clearly demonstrates the differences between the field maps of the two models. From this plot and by considering the differences in the force plots on Figures 32c and 32d, the variation between the predicted and measured values of the stagnation point coordinates may be explained. If intuition can be trusted, the differences in the directions of the forces near the region of the lower left hand corner of these plotted fields would lead one to expect that the stagnation point for the experimental model would tend to be closer to the lower left hand corner than it would be for the analytical model. This is the result indicated on Figure 31.

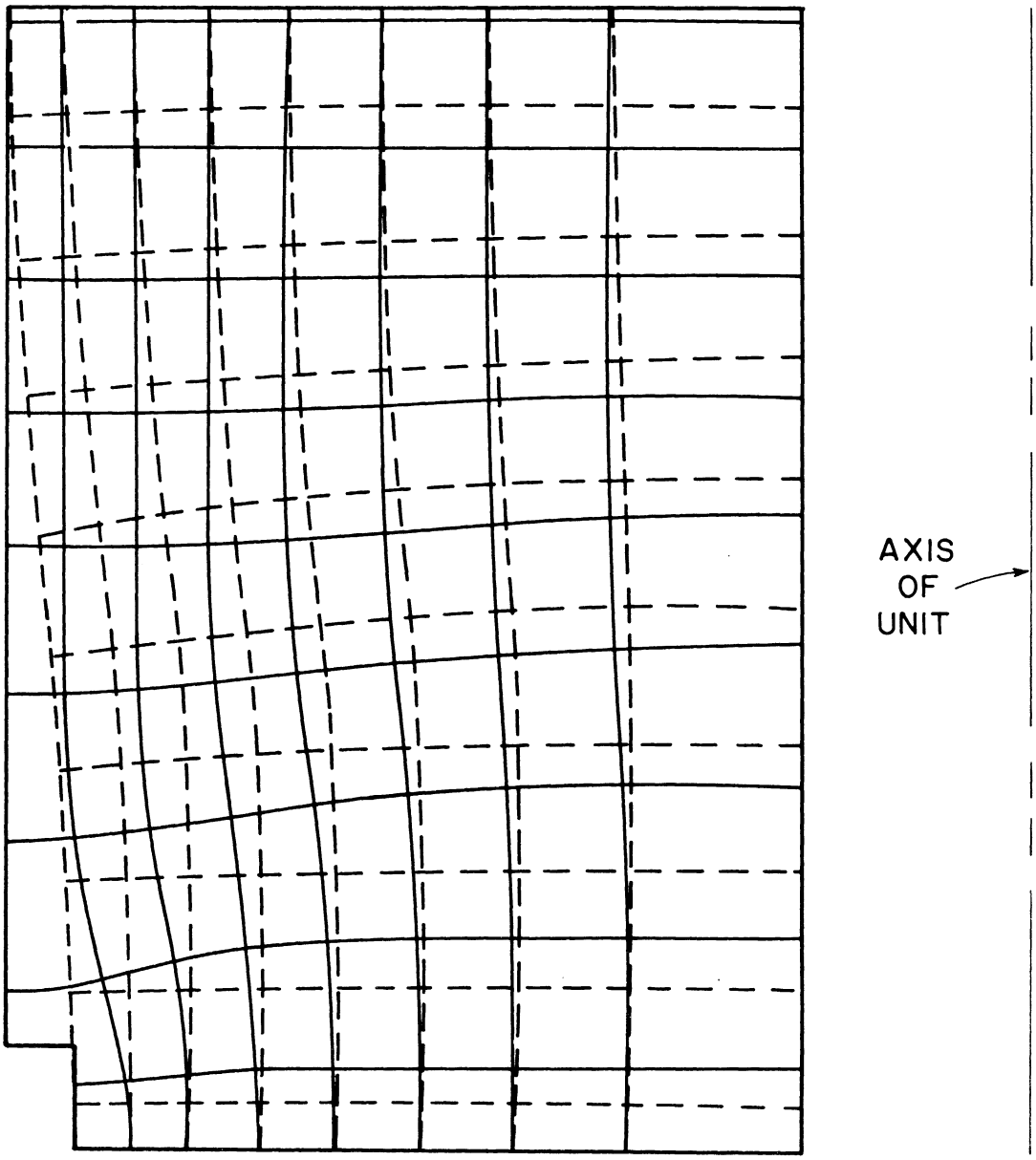

Figure 33. Field Maps for the Analytical and Experimental Models Superimposed to Indicate the Difference.

IV. CONCLUSIONS

The purpose of this study was to experimentally investigate the motion induced in an originally static fluid by the creation of electromagnetic forces. Since a transparent fluid was required for photographic needs, a common salt solution was selected. Certain model alterations were found necessary as the program progressed and are now considered individually.

4.1 Induced Motion Due to Fluid Current Only

For models wherein the induced motion caused by electromagnetic effects depends solely upon the passage of current through the fluid the following conclusions are drawn.

1. Water based fluids do not satisfy the assumption of constant properties when subjected to non-uniform current densities.

2. Convective motion due to thermal buoyancy completely predominates the fluid motion and masks out any electromagnetic effects. This occurs regardless of the physical position of the unit.

4.2 Motion Induced Between Concentric Tubes

When the primary magnetic field intensity is caused by a source located within a central tube and current is passed through a fluid contained between this central tube and an outer one, the following conclusions are drawn.

1. For fields of moderate intensity, convective motion, caused by non-uniform current densities in the fluid, predominates the resultant flow pattern when the axis of the unit lies parallel to the field of gravity.

2. The components of motion as observed in the lighted plane appear to be due primarily to electromagnetic effects when the axis of the unit was placed perpendicular to the field of gravity.

4.3 Test Fluid and Photographic Technique

Solutions of copper sulphate, and probably other salt solutions, provide certain desirable characteristics for the goals being sought in a study such as the one conducted. From the results, several conclusions can be drawn.

1. When certain limiting current densities are exceeded, adverse electrochemical reactions occur at the electrodes and influence the flow pattern.

2. Strong consideration should be given to such current densities in designing models for use with salt solutions.

3. Copper sulphate solutions are highly susceptible to density variations in the presence of non-uniform current densities.

4. The use of aluminum powder suspended in a solution of copper sulphate and illuminated by external sources, provides an excellent means of observing or photographing internal pathlines of fluid motion. In addition, measurement of internal fluid velocity can be obtained.

4.4 Theoretical and Experimental Comparisons of MHD Flow Between Concentric Tubes

Although the experimental model and test conditions do not satisfy certain factors involved in an analytical solution of a similar problem, the following conclusions seem reasonable.

1. The type of motion predicted analytically was qualitatively verified by experiment.

2. Measured values of velocity tend to be lower than those predicted analytically, but the quantitative predictions appear reasonable.

4.5 Suggestions for Further Study

1. Modifications in an arrangement such as used in this study could be made to increase the field strength created by the central rod in order to increase the magnitude of electromagnetic effects. For example, the central rod could be replaced by a heavy tubular conductor which was cooled by water flowing through this tube. This would allow much larger currents to be employed in this central unit without causing excessive heating.

2. The problem of non-symmetry of flow patterns when the unit was horizontal should be investigated in greater detail.

3. Development of a test model which would eliminate the possibility of end effects, and more closely agrees with the analytical model in physical structure could be considered as one outgrowth of this study.

4. The entire problem of convection due to thermal buoyancy caused by non-uniform heat generation appears open for study.

5. Another possible method for studying the fluid circulation would be to construct specialized fluid mappers of the "pinhole" type from which the circulation pattern could be deduced. Such mappers have never been constructed for the physical situation comparable to the geometry involved in this thesis so any efforts devoted towards this goal would be a trial. There is no guarantee that success would be inevitable.

A P P E N D I X

Development of the Equations for Radial and Axial Velocities and Their Application.

The authors of the solution for a class of MHD flows between concentric tubes have been mentioned previously. Since this work is yet unpublished, it might be of aid to develop the major results of their entire solution here. All assumptions involved in this analysis have been discussed previously and are repeated here when they aid in the continuity of this presentation. The following sketch includes the pertinent physical parameters.

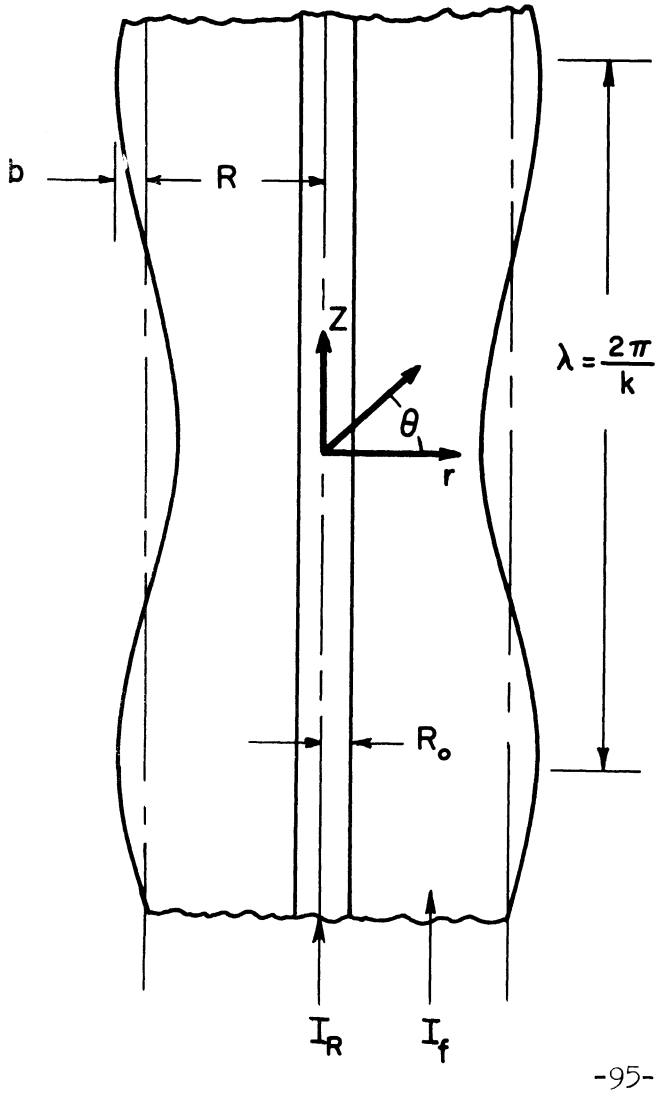

where:

R = mean radius of outer tube

R_o = radius of inner tube

b = maximum amplitude of outer wall perturbation

λ = wave length

k = wave number

I_R = current in center tube

I_f = current in fluid between the tubes

$b/R \ll 1$

By neglecting displacement currents, the pertinent electromagnetic equations take the forms:

$$\text{curl } \vec{H} = \vec{J} \tag{A-1}$$

$$\text{curl } \vec{E} = -\frac{\partial \vec{B}}{\partial t} \tag{A-2}$$

$$\vec{B} = \mu_e \vec{H} \tag{A-3}$$

$$\vec{J} = \sigma\left(\vec{E} + \vec{U} \times \vec{B}\right) \tag{A-4}$$

The equation for the intensity of the magnetic field may then be written as:

$$\frac{\partial \vec{H}}{\partial t} = \text{curl}\left(\vec{U} \times \vec{H}\right) - \frac{1}{\sigma \mu_e} \text{curl curl } \vec{H} \tag{A-5}$$

where σ and μ_e are assumed constant.

If U_o, H_o, and L_o are the characteristic velocity, magnetic intensity, and scale for a given situation, then the ratio of the two terms on the right-hand side of Equation (A-5) is given by:

$$R_m = U_o L_o / (\sigma \mu_e)^{-1}$$

where R_m is called the magnetic Reynolds number. For cases where R_m is small, as occurs in most laboratory situations, convection of the magnetic field may be neglected and useful information may still result. By introducing this approximation the above equations become:

$$\text{curl } \vec{H} = \vec{J} \tag{A-6}$$

$$\text{curl}\ \vec{E} = -\frac{\partial \vec{B}}{\partial t} \tag{A-7}$$

$$\vec{B} = \mu_e \vec{H} \tag{A-8}$$

$$\vec{J} = \sigma \vec{E} \tag{A-9}$$

$$\frac{\partial \vec{H}}{\partial t} = -\frac{1}{\sigma \mu_e}\ \text{curl curl}\ \vec{H} \tag{A-10}$$

In this approximation, electric current and magnetic field intensity do not depend upon the motion.

The equation of motion for an incompressible viscous fluid may be expressed in the form:

$$\rho\left(\frac{D\vec{U}}{Dt}\right) = -\text{grad}\ p - \mu\ \text{curl curl}\ \vec{U} + \vec{J} \times \vec{B} \tag{A-11}$$

where $\vec{J} \times \vec{B}$ is the electromagnetic body force.

Considering the steady state case and assuming the convective terms in the left-hand side of Equation (A-11) are negligible, (A-11) becomes:

$$-\text{grad}\ p - \mu\ \text{curl curl}\ \vec{U} + \vec{J} \times \vec{B} = 0 \tag{A-12}$$

or:

$$-\mu\ \text{curl curl curl}\ \vec{U} + \text{curl}\left(\vec{J} \times \vec{B}\right) = 0 \tag{A-13}$$

The condition for static equilibrium is that

$$\text{curl } \vec{J} \times \vec{B} = -\mu_e \frac{\partial}{\partial z}\left(\frac{H^2}{r}\right) \tag{A-14}$$

should vanish which happens only if the tubes both have straight walls.

For axisymmetric flow and considering steady state,

$$\vec{H} = \vec{i}_\theta H_{(r,z)} \tag{A-15}$$

$$U_r = -\frac{\partial \Psi_{(r,z)}}{\partial z} \tag{A-16}$$

$$U_z = \frac{1}{r}\frac{\partial}{\partial r}\left(r\Psi_{(r,z)}\right) \tag{A-17}$$

where $r\Psi$ is the stream function.

Now due to axisymmetric flow,

$$\text{curl } \vec{U} = -\left(\frac{\partial}{\partial r}\left[\frac{1}{r}\frac{\partial}{\partial r}(r\Psi)\right] + \frac{\partial^2 \Psi}{\partial r^2}\right) \tag{A-18}$$

The current density in the inner tube is:

$$J_R = \frac{I_R}{\pi R_o^2} \tag{A-19}$$

For the current density in the fluid, J, this is approximated by:

$$J = \frac{I_f}{\pi\left(R^2 - R_o^2\right)} \tag{A-20}$$

since $b/R \ll 1$.

The total magnetic field intensity becomes:

$$H = \frac{Jr}{2} + \frac{(J_R - J) R_o^2}{2r} + \bar{h} \qquad \text{(A-21)}$$

where $\bar{h}$ is the perturbation of the magnetic field due to the small wall perturbation.

Considering solutions of the type:

$$\bar{h} = h_{(r)} e^{ikz} \qquad \text{(A-22)}$$

$$\Psi = \psi_{(r)} e^{ikz} \qquad \text{(A-23)}$$

the solution for $\bar{h}$ may be found from:

$$\mathcal{L}\, h_{(x)} = 0 \qquad \text{where} \qquad x = kr$$

$$\text{and} \qquad \mathcal{L} \equiv \left(\frac{d^2}{dx^2} + \frac{1}{x}\frac{d}{dx} - \left[\frac{1}{x^2} + 1 \right] \right)$$

subject to appropriate boundary conditions. For the special case, where the outer tube contains a small perturbation periodic in z while the inner tube has a straight wall, Equation (A-13) reduces to:

$$\mathcal{L}^2 \psi_{(x)} = - \frac{i \mu_e k}{\mu k^3} \left[J + (J_R - J) \frac{R_o^2}{x^2} \right] \left[\alpha I_1(x) + \gamma K_1(x) \right] \qquad \text{(A-24)}$$

when Equations (A-14), (A-16), (A-17), (A-18), and (A-21) are introduced into (A-13).

The solution pertinent here is as follows:

$$\psi(x) = -\frac{i\mu_e b R_o^2 J^2}{16\mu k}\left\{\frac{2x^2}{(kR_o)^2}\left[\alpha I_1(x)+\gamma K_1(x)\right]-4\left(\frac{J_R}{J}-1\right)\left[\alpha I_*(x)+\gamma K_*(x)\right]\right. \\ \left. + C_1 x I_0(x)+C_2 I_1(x)+C_3 x K_0(x)+C_4 K_1(x)\right\} \quad \text{(A-25)}$$

where:

$$\alpha = -K_1(kR_o) \Big/ I_1(kR)\,K_1(kR_o) - I_1(kR_o)\,K_1(kR) \quad \text{(A-26)}$$

$$\gamma = I_1(kR_o) \Big/ I_1(kR)K_1(kR_o) - I_1(kR_o)K_1(kR) \quad \text{(A-27)}$$

i $= \sqrt{-1}$

μ_e = magnetic permeability

J = current density in the fluid based upon the annular area between R and R_o

μ = fluid viscosity

x = kr = non-dimensionalized radius

J_R = current density in the center tube based upon the area defined by R_o

I_n and K_n = modified Bessel Functions of order n

$$I_*(x) = I_1(x)\int^x \frac{I_0^2(\delta)}{I_1^2(\delta)}\,\frac{d\delta}{\delta} \quad \text{(A-28)}$$

$$K_*(x) = K_1(x)\int^x \frac{K_0^2(\delta)}{K_1^2(\delta)}\,\frac{d\delta}{\delta} \quad \text{(A-29)}$$

δ = dummy variable of integration

C_1, C_2, C_3, C_4, are constants to be determined from the boundary conditions and current densities. It should be noted that expressions for U_r and U_z were not developed in the original work. The equation for $\psi_{(x)}$ is subject to the following boundary conditions:

$$\psi\,(kR) = \psi\,(kR_o) = \psi'\,(kR) = \psi'\,(kR_o) = 0$$

since both U_r and U_z vanish at $r = R$ and $r = R_o$. The assumption that $b/R \ll 1$ allows an approximate solution to be obtained by satisfying two boundary conditions at the mean radius R rather than the outer wall itself. The first step is then to define the constants C_1 through C_4. Applying the 4 boundary conditions leads to the following set of simultaneous equations:

$$C_1 kR I_0(kR) + C_2 I_1(kR) + C_3 kR K_0(kR) + C_4 K_1(kR) = -2\frac{(kR)^2}{(kR_o)^2}\left\{\alpha I_1(kR) + \gamma K_1(kR)\right\} + 4\left(\frac{J_R}{J} - 1\right)\left\{\alpha I_*(kR) + \gamma K_*(kR)\right\} \tag{A-30}$$

$$C_1\left[I_0(kR) + kR I_1(kR)\right] + C_2\left[I_0(kR) - \frac{I_1(kR)}{kR}\right] + C_3\left[K_0(kR) - kR K_1(kR)\right] - C_4\left[K_0(kR) + \frac{K_1(kR)}{kR}\right] = +4\left(\frac{J_R}{J} - 1\right)\left[\alpha I_*'(kR) + \gamma K_*'(kR)\right] - 2\frac{kR}{(kR_o)^2}\left\{\alpha\left[I_1(kR) + kR I_0(kR)\right] + \gamma\left[K_1(kR) - kR K_0(kR)\right]\right\} \tag{A-31}$$

Two other equations result by substituting R_o for R in (A-30) and (A-31) thereby producing four simultaneous equations with the four unknown constants such as C_1. $I_*'(k)$ and $K_*'(x)$ are the derivatives of $I_*(x)$ and $K_*(x)$.

The following pertinent expressions are taken from the original solution of the problem:

$$I_*(x) \approx I_1(x)\left[\ln x - \frac{2}{x^2} + \frac{x^2}{96} - \frac{x^4}{1536}\right] \tag{A-32}$$

$$I_*'(x) = \frac{I_0^2(x)}{x\, I_1(x)} + I_*(x)\left[\frac{I_0(x)}{I_1(x)} + \frac{1}{x}\right] \tag{A-33}$$

$$K_*(x) \approx K_1(x)\left[\ln x + \frac{.975}{x} - \frac{.354}{x^2} + \frac{.096}{x^3} - \frac{.0114}{x^4}\right] \tag{A-34}$$

$$K_*'(x) = \frac{K_0^2(x)}{x\, K_1(x)} - K_*(x)\left[\frac{K_0(x)}{K_1(x)} + \frac{1}{x}\right] \tag{A-35}$$

The important physical dimensions of the experimental model that are of interest are as follows:

R_o = 1.25 inch	λ = 12.56 inch
R = 5.407 inch	k = .50 1/inch
b = .188 inch	b/R = .034

Certain constants dependent only on the physical dimensions were found next. The fixed values for kR and kR_o were 2.703 and .625 respectively, so the use of equations (A-26), (A-27), and (A-32) through (A-35) led to the determination of said constants. It should be noted that in those equations containing the parameter x, kR and kR_o are substituted for x.

TABLE A.1

Constants Resulting From Model Geometry

$\alpha = -.3333$	$I_*(kR_o) = -1.832$	$I'_*(kR_o) = 2.70$
$\gamma = .0882$	$K_*(kR_o) = .6228$	$K'_*(kR_o) = -.645$
$I_*(kR) = 2.291$	$I'_*(kR) = 3.882$	
$K_*(kR) = .0755$	$K'_*(kR) = -.0775$	

Before the constants C_1 through C_4 can be defined, values must be selected for fluid and rod currents. Since the rod current was fixed at 300 amperes, the expressions that follow define these two current densities.

$$\text{Current density in rod} = J_R = \frac{I_R}{\pi R_o^2} = \frac{300}{\pi(1.25)^2} = 61.15 \ \frac{\text{amps}}{\text{inch}^2}$$

$$\text{Current density in fluid} = J = \frac{I_f}{\pi(R^2 - R_o^2)} = \frac{I_f}{\pi(5.407^2 - 1.25^2)} = .01265\, I_f \ \frac{\text{amps}}{\text{inch}^2}$$

The actual fluid currents employed when the test model contained the large hole in the separator plate are utilized in the table that follows. In addition, the entire right hand side of equations (A-30), (A-31) and the two additional equations resulting when R_o is substituted for R are employed. For simplicity, the right hand sides of these four equations are expressed as $A(kR)$, $A(kR_o)$, $A'(kR)$, and $A'(kR_o)$ respectively. It can be seen that $A(kR)$ and the others are functions of the current densities. By solving these expressions for the different current densities the following tabulated values resulted.

TABLE A.2

Constants Resulting from Model Geometry and Current Densities

I_f	J	$\frac{J_R}{J} - 1$	A(kR)	$A(kR_o)$	A'(kR)	$A'(kR_o)$
25	.3163	192.3	-545	512	-938	-732
32	.4048	150.1	-417	400	-719	-571
36	.4554	133.3	-366	355	-632	-507
40	.506	119.8	-325	319	-561	-456
50	.6326	95.6	-252	255	-436	-364

The four simultaneous equations originating from (A-30) and (A-31) were then produced in the following forms by appropriate substitutions in the left hand side of those equations:

$$10.385\ C_1 + 3.016\ C_2 + .1333\ C_3 + .0577\ C_4 = A(kR)$$

$$.688\ C_1 + .328\ C_2 + .468\ C_3 + 1.239\ C_4 = A(kR_o)$$

$$12.00\ C_1 + 2.73\ C_2 - .107\ C_3 - .0737\ C_4 = A'(kR)$$

$$1.305\ C_1 + .575\ C_2 - .0264\ C_3 - 2.73\ C_4 = A'(kR_o)$$

It now becomes apparent that the unknown constants in the above expressions are a function of current densities. Thus, every change in the ratio J_R/J requires the calculation of a new set of constants. These were determined for the five values of this ratio employed in the experiment and the following table shows the results.

TABLE A.3

Constants for Equation (A-25) as a Function of the Ratio of Current Densities

I_f	$(\frac{J_R}{J} - 1)$	C_1	C_2	C_3	C_4
25	192.3	-118.3	201.5	466.1	249.6
32	150.1	- 90	151.7	364.5	194.7
36	133.3	- 78.7	132.1	323.3	172.9
40	119.8	- 69.6	116.1	291.4	155.3
50	95.6	- 53.3	87.4	233.2	123.9

By substituting equation (A-25) into (A-23) and utilizing the real part of the resultant equation, the form of Ψ to be used in equations (A-16) and (A-17) is obtained. Performing the necessary differentiation indicated in (A-16) and (A-17) leads to the following general forms for the velocity components.

$$U_r = -\frac{\mu_e b R_o^2 J^2}{16\mu}\cos(y)\left\{\begin{array}{l}(C_2 - 1.71x^2)I_1(x) + (C_4 + .452x^2)K_1(x) + C_1 x I_0(x) \\ + C_3 x K_0(x) + 1.333\left(\frac{J_R}{J} - 1\right)I_*(x) - .353\left(\frac{J_R}{J} - 1\right)K_*(x)\end{array}\right\} \quad \text{(A-36)}$$

$$U_z = \frac{\mu_e b R_o^2 J^2}{16\mu}\sin(y)\left\{\begin{array}{l}(C_1 - 3.41)x I_1(x) + (C_2 + 2C_1 - 1.71x^2)I_0(x) \\ + (.9 - C_3)x K_1(x) + (2C_3 - C_4 - .45x^2)K_0(x) \\ + 1.333\left(\frac{J_R}{J} - 1\right)\left(I_*'(x) + \frac{I_*(x)}{x}\right) \\ - .353\left(\frac{J_R}{J} - 1\right)\left(K_*'(x) + \frac{K_*(x)}{x}\right)\end{array}\right\} \quad \text{(A-37)}$$

where $y = kz$, a non-dimensional axial component. It may be noted that in both equations of velocity components, the terms included in brackets are non-dimensional.

To numerically evaluate the coefficient of equations (A-36) and (A-37), the following values, either measured or selected, were used:

$\mu_e = 4\pi \times 10^{-7}$ henrys/meter $= 4\pi \times 10^{-7} \quad \frac{\text{Kg meter}}{\text{amp}^2 \text{ sec}^2}$

$k = .500$ 1/inch

$b = .188$ inch

$R_o^2 = 1.56$ inch^2

$J^2 =$ amp^2/inch^4

$\mu = 17.2 \times 10^{-6}$ lbf sec / ft^2

The value for μ was calculated by using values for the viscosity of water at 100°F which was considered as a reasonable value for the experimental tests. This had been checked periodically with a sensitive thermometer, the indicated reading being the bulk temperature. From references 27 and 28, the value of μ was obtained. Utilizing information from reference 26, which tabulated values of specific viscosity of copper sulphate for certain molar solutions, an appropriate correction was made of the viscosity for water. The numerical result is shown above.

Performing the necessary operations and making appropriate dimensional conversions led to the following:

$$\frac{\mu_e \, b R_o^2 J^2}{16 \, \mu} = .0433 J^2 \quad \frac{\text{inch}}{\text{sec.}}$$

Therefore, the final forms for U_r and U_z became:

$$U_r = -.0433 J^2 \cos y \quad \left(\text{non-dimensional quantity} \right) \qquad \text{(A-38)}$$

$$U_z = .0433J^2 \sin y \left(\text{non-dimensional quantity}\right) \quad \text{(A-39)}$$

From this point it simply became a matter of selecting the radial and axial components of a coordinate point of interest, employing the current densities of immediate concern, and carrying out the necessary arithmetical operation. An electric desk calculator was employed to provide accuracy to the 4th decimal place as it was found that slide rule results were too inaccurate.

Recalling that $x = kr$ and $y = kz$ the following sketch defines the coordinate system used:

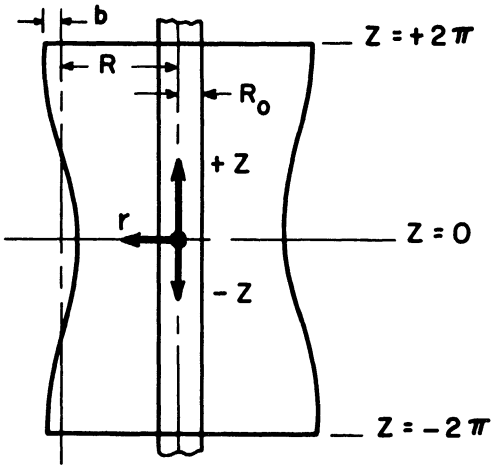

The actual values of coordinate points employed corresponded to those at which velocity measurements were obtained experimentally. These were as follows:

Point No. 1------ r = 3.1 inch, z = 3.36 inch

Point No. 2------ r = 3.7 inch, z = 2.36 inch

Point No. 3------ r = 2.38 inch, z = 2.90 inch

Equations (A-38) and (A-39) were used to produce the velocity components at each of the three points for each of the 5 values of fluid current employed. This necessitated the use of the values of $\left(\frac{J_R}{J} - 1\right)$ and the four constants presented in Table A.3. The total velocity was then obtained from:

$$U = (U_r^2 + U_z^2)^{1/2}$$

These values for U were then plotted against fluid current to produce the solid lines shown in Figures 30a to 30c.

In regard to the stagnation points, the radial velocity component vanishes when $y = \pm \pi/2$ as the cosine function vanishes at that point. Physically this would occur midway between the origin and the ends of one wavelength of tube section, that is when $z = \pm \pi$.

Within any one wavelength of tube section, the axial component of velocity cannot vanish due to y dependency since the sine function does not go to zero. Consequently, this component must vanish due to r dependency. The large quantity of terms in the bracket of equation (A-37), that is the non-dimensional quantity, was analyzed for different values of r until it was found to vanish. The particular value of r that caused this then defined the radial component of the stagnation point. This procedure was followed using the appropriate forms of (A-37) for the five different fluid currents. It was found that this component apparently was independent of current densities. The results for the analytical values of stagnation point components were then drawn as solid lines on Figures 31a and 31b.

BIBLIOGRAPHY

1. Northrup, E. F., "Some Newly Observed Manifestations of Forces in the Interior of an Electric Conductor," Physical Review, Vol. 24, (1907), p. 474.

2. Williams, E. J., "The Induction of Electromotive Forces in a Moving Liquid by a Magnetic Field, and its Application to an Investigation of the Flow of Liquids," Proc. Phys. Soc., London, Vol. 42, (1929), p. 466.

3. Williams, E. J., "The Motion of a Liquid in an Enclosed Space," Proc. Phys. Soc., London, Vol. 42, (1929), p. 479.

4. Hartmann, J., "Hg-Dynamics I," Kgl. Danske Vid. Selskab, Math-Fys. Medd., Vol. 15, No. 6, Copenhagen, (1937).

5. Hartmann, J. and Lazarus, F., "Hg-Dynamics II," Kgl. Danske Vid. Selskab, Math-Fys. Medd., Vol. 15, No. 7, Copenhagen, (1937).

6. Murgatroyd, W., "Experiments on Magneto-Hydrodynamic Channel Flow," London Phil. Mag., Vol. 44, 7th series, No. 358, (1953), p. 1348.

7. Alpher, R. A., Hurwitz, H., Johnson, R. H., and White, D. R., "Some Studies of Free-Surface Mercury Magnetohydrodynamics," Rev. of Mod. Phys., Vol. 32, No. 4, (Oct. 1960), p. 758.

8. Rossow, V. J., "Theoretical and Experimental Study of the Interaction of Free-Surface Waves on Liquid Metals with Transverse Magnetic Fields," NASA TR R-161, Washington, (1963).

9. Alfven, H., "Existence of Electromagnetic-Hydrodynamic Waves," Nature, Vol. 150, (1942), p. 405.

10. Lundquist, S., "Experimental Investigations of Magnetohydrodynamic Waves," Phys. Review, Series 2, Vol. 76, (1949), p. 1805.

11. Lehnert, B., "On the Behavior of an Electrically Conductive Liquid in a Magnetic Field," Ark for Fysik, 5-6, (1952), p. 69.

12. Lehnert, B., "Magneto-Hydrodynamic Waves in Liquid Sodium," Phys. Review, Series 2, Vol. 94, (1954), p. 815.

13. Lehnert, B., and Little, N. C., "Experiments on the Effect of Inhomogeneity and Obliquity of a Magnetic Field in Inhibiting Convection," Tellus, Vol. 9, (1957), p. 97.

14. Nakagawa, Y., "Experiments on the Instability of a Layer of Mercury Heated from Below and Subject to the Simultaneous Action of a Magnetic Field and Rotation II," Proc. Roy. Soc., London, Series A, Vol. 249, (1959), p. 138.

15. Lehnert, B., "An Instability of Laminar Flow of Mercury Caused by an External Magnetic Field," Proc. Roy. Soc., London, Series A, Vol. 233, (1955), p. 299.

16. Lehnert, B. and Sjogren, G., "Stability of a Hollow Mercury Jet," Rev. of Mod. Phys., Vol. 32, No. 4, (Oct. 1960), p. 813.

17. Dattner, A., Lehnert, B., and Lundquist, S., "Liquid Conductor Model of Instabilities in a Pinched Discharge," Proc. 2nd Int. Conf. on Peaseful Uses of Atomic Energy, Geneva, Vol. 31, (1958), p. 325.

18. Colgate, S. A., Furth, H. P., and Halliday, F. O., "Hydromagnetic Equilibrium Experiments with Liquid and Solid Sodium," Rev. Mod. Phys., Vol. 32, No. 4, (1960), p. 744.

19. Rossow, V. J., Jones, W. P., and Huerta, R. H., "On the Induced Flow of an Electrically Conducting Liquid in a Rectangular Duct by Electric and Magnetic Fields of Finite Extent," NASA TN D-347, Washington, (1961).

20. Okhremenko, N. M., "Electromagnetic Phenomena in Flat-Type Induction Pumps for Molten Metal," Translated from Elektrichestvo (Electricity), No. 3, (March, 1960), p. 48 - 54, Translated by Primary Sources, New York.

21. Lundquist, S., "Studies in Magneto-Hydrodynamics," Ark. for Fys., 5-6, (1952-1953), p. 297.

22. Bullard, Sir Edward, under the leadership of, "A Discussion on Magneto-Hydrodynamics," Proc. Roy. Soc., London, Series A, 233, (1955-1956), No. 1194.

23. Frenkiel, F. N. and Sears, W. R., edited by, "Magneto-Fluid Dynamics," Rev. of Mod. Phys., Vol. 32, No. 4, (Oct., 1960).

24. Uberoi, M. S., "Magneto-Hydrodynamics at Small Magnetic Reynolds Numbers," Jour. of the Phys. of Fluids, Vol. 5, No. 4, (April, 1962), p. 401.

25. Kreith, F., Principles of Heat Transfer, International Textbook Co., (1959), p. 537.

26, Lange, N. A., edited by, Handbook of Chemistry, 3rd Edition, Handbook Publishers Inc., (1939), p. 1169, 1359.

27. Schlichting, H., Boundary Layer Theory, McGraw Hill Book Co., (1960), p. 8.

28. Olsen, R. M., Essentials of Engineering Fluid Mechanics, International Textbook Co., (1962), p. 19.

29. Oral communications with M. S. Uberoi, formerly Professor of Aeronautical and Astronautical Engineering, University of Michigan, Ann Arbor, Michigan, currently Chairman, Department of Aerospace Sciences, University of Colorado, Boulder, Colorado, and C. Y. Chow, currently a graduate student, Department of Aeronautical and Astronautical Engineering, University of Michigan, Ann Arbor, Michigan, May through August, 1963.

30. Moore, A. D., "Fields from Fluid Flow Mappers," Jour. of Appl. Phys., Vol. 20, (1949), p. 790.

31. Moore, A. D., "Mapping Techniques Applied to Fluid Mapper Patterns," AIEE Trans., Vol. 71, (1952), Part 1, p. 1.

32. Moore, A. D., "Fluid Mappers as Visual Analogs for Potential Fields," Annals of the New York Academy of Sciences, Vol. 60, Art. 6, (1955), p. 948.

33. Moore, A. D., Fluid Mapper Patterns, Overbeck Book Company, Ann Arbor, Michigan, (1956).

34. Moore, A. D., Fluid Mapper Manual, Industry Program, College of Engineering, University of Michigan, Ann Arbor, Michigan, (1961).

35. Moore, A. D., "Ribbon Generators, with Magnetohydrodynamic Generator and Other Implications," Power Apparatus and Systems, AIEE, (1961).